Technical Report ECOM-0138-12-T

Reports Control Symbol
OSD-1366
November 1970

ITERATIVE SYNTHESIS OF TEM-MODE DISTRIBUTED NETWORKS

C.E.L. Technical Report No. 199

Contract No. DAAB07-68-C-0138

DA Project No. 1 HO 62102 A042 01 02

Prepared by

S. Mahdi

COOLEY ELECTRONICS LABORATORY
Department of Electrical Engineering
The University of Michigan
Ann Arbor, Michigan

for

U.S. Army Electronics Command, Fort Monmouth, N.J.

ABSTRACT

A procedure is described for synthesizing transmission networks which are interconnections of uniform line sections. An iterative, digital computer algorithm is developed which achieves a dominant pole synthesis. The line lengths and the characteristic impedances are controlled individually, which gives design flexibility not found in synthesis procedures based on Richards' transformation. Thus, the characteristic impedances may be restricted by upper and lower bounds when there is no restriction on the line lengths. The procedure is detailed for a TEM mode structure of alternating open stubs and connecting lines. The method uses a Newton-Raphson iterative scheme to adjust the characteristic impedances and lengths of the transmission lines for a prescribed set of dominant transmission poles. By controlling the stub line lengths, the dominant pole positions, the principal transmission zeros, and bounded characteristic impedances can be achieved simultaneously.

The occurrence of nondominant poles has been analytically investigated. Frequencies at which each transmission line element is a quarterwave long or an odd multiple thereof divide the s-plane imaginary axis into halfwave frequency bands. In every semi-infinite s-plane strip, which these frequency bands subtend parallel to the imaginary frequency axis, one and only one nondominant pole is present. A numerical technique has been outlined which locates these poles.

A nonlinear programming problem has been formulated, and a method for its solution presented, which aligns $j\omega$-axis transmission zeros opposite the nondominant transmission poles in or near the stopband. This approximate cancellation of these poles extends the frequency range over which the network characteristics can be controlled.

FOREWORD

This report is directed to the engineering problem of designing networks for a prescribed frequency domain characteristic using distributed circuit elements. The specific elements considered are sections of uniform, lossless transmission lines, but the methods presented are applicable to a broader class of elements including RC transmission lines and a mixture of lumped capacities and distributed lines. The frequency domain specification used is the complex frequency (s-plane) location of the poles and zeros of the desired network function. The report treats the problem of selecting the distributed circuit element parameters (characteristic impedances and electrical lengths for lossless lines) to achieve a specified set of dominant poles and zeros while simultaneously restricting the impedance levels to practical ranges.

The distributed elements considered in this report are sections of lossless, uniform transmission lines which are adequately described by the TEM propagation mode. Practical realization of such elements is achieved with coaxial, strip, and microstrip transmission line sections. Generally, the assumption of only the TEM mode is not valid at element junctions, but the principal effect of the junctions can be taken into account by a modification of the element lengths. This is illustrated for the specific example presented in Chapter 5.

The use of a pole-zero specification presumes that the circuit designer has solved an appropriate approximation problem before trying to realize the circuit with distributed elements. For the standard filter types (lowpass, bandpass, etc.,) the required poles and zeros can be determined from a number of tabulations which are available.[1]

In Chapter 4, this report gives a specific method for designing a low-pass distributed filter consisting of open circuited stub lines alternating with connecting lines and terminated at both ends by fixed resistors. Chapter 5 illustrates the method by carrying through a 9-pole design and experimentally verifying the design in stripline form. Appendix II gives the FORTRAN IV program required to carry out such a typical design.

A practical concern in the design of distributed circuits is the unavoidable resonances which occur because of the multiple resonant properties of each distributed element. These resonances give rise to poles and zeros of the network response which are not directly specified and which may disturb the desired response. The question of locating the nondominant poles and zeros is treated in Chapter 6.

---

[1] L. Weinberg, Network Analysis and Synthesis, McGraw-Hill, New York, 1962, pp. 600-631.

R. Saul and E. Ulbrich, "On the Design of Filters by Synthesis," IRE Trans. on Circuit Theory, Vol. CT-5, No. 4, Dec. 1958, pp. 284-327.

There, a method for finding the pole and zero locations is developed; Appendixes III and IV give FORTRAN IV programs which carry out this process for the particular filter form of Chapter 4.

Chapter 7 presents one method of utilizing some of the available degrees of freedom in the distributed network to minimize the effect of non-dominant poles on the performance of a lowpass filter. This should be considered as a fruitful first step toward the optimization of a filter design; it appears that much more can be done in the future.

Finally, Chapter 8, makes a start on the interesting theoretical question of the existence of solutions of the problem: Given line impedances, and load impedances, what line lengths are required to realize a specified set of dominant poles?

Table of Contents

	Page
Abstract	iii
Foreword	v
List of Illustrations	xii
List of Appendices	xvii
List of Symbols	xviii
Chapter 1: Introduction	1
Chapter 2: Literature Survey	4
2.1 Filter with Cascade Elements	5
2.2 Filters with Parallel-Coupled Lines	12
2.3 Filters with Stubs and Richards' Transformation	17
Chapter 3: Mathematical Derivations	20
3.1 General Circuit Parameter Matrix	20
3.2 A System of Nonlinear Equations	25
Chapter 4: Realization of Prescribed Poles and Zeros	29
4.1 Generation of the System of Nonlinear Equations	29
4.2 Newton-Raphson Method	32
4.3 Approximate Solution	35
4.4 Refinement of the Solution by Newton-Raphson Method	40
4.5 Realization of Characteristic Impedances Within a Prescribed Bound	40
4.6 The Realization of Transmission Zeros	44
Chapter 5: Design of a Nine-Element Transmission Line Network	47
5.1 Determination of Dominant Poles and Zeros	48
5.2 Realization of Zeros and Poles	50
5.3 Modified Design	58
5.4 Construction	60

Table of Contents (Cont.)

		Page
Chapter 6:	Nondominant Poles	64
6.1	General Consideration	
6.2	Transmission Poles and the Zeros of Modified GCP	69
6.2.1	$j\omega$-Axis Zeros of $G_1 A_m + G_2 D_m$	71
6.2.2	$j\omega$-Axis Zeros of $G_1 G_2 B_m + C_m$	72
6.2.3	$j\omega$-Axis Zeros of $G_1 A_m + G_2 D_m$ and $G_1 G_2 B_m + C_m$ Are Their Only Zeros	72
6.3	No Repetition Interval is Free of Zeros of A_m, B_m, C_m, D_m	74
6.4	Exactly One Zero of Each GCP in Each Repetition Interval	83
6.5	Numerical Evaluation of Transmission Poles	91
6.5.1	Derivatives of the Zeros of (6.58) with Respect to K	93
6.5.2	Determination of ω_{AD} or ω_{BC}	95
6.5.3	Transmission Poles	96
6.6	An Example	97
6.7	Sensitivity of the Zeros of A_m, B_m, C_m and D_m with the Variation of Line Lengths	101
Chapter 7:	Optimization	105
7.1	Mathematical Formulation	105
7.2	Solution	108
7.3	Calculation of Derivatives	112
7.4	Example	116
Chapter 8:	Existence Consideration for the Solution of the Two-Element Transmission Line Networks	123
8.1	Variation of the Input Admittance of a Resistance-Terminated Transmission Line	126
8.2	Variation of the Admittance of an Open Shunt Stub in Shunt with a Resistor	130
8.3	Condition for Existence of Solution	132
8.4	Example	134
Chapter 9:	Summary	138

Table of Contents (Cont.)

	Page
Appendices	140
Bibliography	170
Distribution List	176

List of Illustrations

Figure	Title	Page
2.1	The periodic nature of the frequency response of transmission line filters illustrated by the Butterworth attenuation of a half-wave filter	6
2.2	A bandpass filter containing admittance inverters J_i $(i = 1, 2, \ldots, n)$	6
2.3	A bandpass filter containing impedance inverters K_i $(i = 1, \ldots, n+1)$	8
2.4	Broad-band impedance-inversion networks	8
2.5	Direct coupled-resonator filters (a) in strip transmission line (b) in waveguide	9
2.6	Quarterwave stepped impedance transformer	9
2.7	Halfwave filter	11
2.8	Equivalent circuit of an impedance step	11
2.9	Shielded parallel coupled stripline	13
2.10	Parallel coupled strip transmission line filters (a) with open-circuited sections (b) with short circuited sections	13
2.11	Effect of folding a $\lambda_0/2$ resonator to make a $\lambda_0/4$ resonator	15
2.12	Interdigital filter with shortcircuited lines at the end	15
2.13	Capacitively loaded interdigital filter with ungrounded end resonators	16
2.14	A comb-line bandpass filter	16

List of Illustrations (Cont.)

Figure	Title	Page
3.1	General structure of the transmission line networks considered in this study	21
4.1	(a) A transmission line terminated by the impedance $z_{in}^{j-1} = \frac{E + jF}{G + jH}$ (b) An impedance $z_{in}^{j-1} = \frac{E + jF}{G + jH}$ shunted by an open stub	31
4.2	Input impedance z_{in} looking into the port 1 - 1' is determined recursively	31
4.3	Approximate lumped equivalent of the distributed network in Fig. 4.2 under the assumptions (4.18) and (4.19)	38
4.4	A nine-element transmission line network	38
4.5	The lumped network having 9th order Butterworth transmission poles	38
4.6	Variation of line lengths necessary to maintain Butterworth poles (n = 9) as the ratio of $z_{\text{Connecting Line}}$ to z_{Stub} is decreased	43
5.1	The calculated and measured attenuation of the designed nine-element transmission line filter	54
5.2	The synthesis procedure outlined in Sections 4.3 through 4.6 summarized	59
5.3	The physical dimensions of the nine-element filter	63
6.1	A doubly-terminated lossless 2-port	65
6.2	(a) Typical curves of modified general circuit parameters A_m, B_m, C_m and D_m (b) Indicates the sections of $j\omega$-axis where the zeros of $G_1A_m + G_2D_m$ and $G_1G_2B_m + C_m$ occur for the curves in (a)	73

List of Illustrations (Cont.)

Figure	Title	Page
6.3	Repetition intervals and principal interval of a transmission line of length ℓ	75
6.4	Two lossless transmission line 2-ports joined by a connecting line	75
6.5	$-x(\omega)$ in Eq. 6.26 and $\tan \frac{\ell \omega}{v}$ for one repetition interval of the connecting line in Fig. 6.4	80
6.6	Two lossless transmission line 2-ports having an open shunt stub at their junction	80
6.7	(a) A lossless 2-port satisfying the theorem I in Section 6.4 (b) A connecting line terminated by the lossless 2-port in (a) (c) An open shunt stub in parallel with the 2-port in (a)	84
6.8	$-x'(\omega)$ in (6.56) for the part $I_1 - I_2$ of a repetition interval of the 2-port in Fig. 6.7 (a)	88
6.9	Graphical representations of $x'(\omega) + \tan \omega\ell/v = 0$ illustrating the three distinct relative positions of $-x'(\omega)$ and $\tan \omega\ell/v$	89
6.10	Zeros ω_A, ω_B, ω_C, ω_D of modified general circuit parameters of either a stub or a connecting line of length ℓ in one of its repetition intervals, verifying the occurrence of exactly one zero of each general circuit parameter in such an interval	92
6.11	A repetition interval and the associated repetition strip	92
6.12	Typical graphs of $G_1 A_m(\omega) + G_2 D_m(\omega)$ and $G_1 G_2 B_m(\omega) + C_m(\omega)$	98
6.13	A five-element transmission line network	98

List of Illustrations (Cont.)

Figure	Title	Page
6.14	The zeros of $G_1A_m + G_2D_m$ and $G_1G_2B_m + C_m$ are identified by ω_{AD} and ω_{BC} respectively and the nondominant poles of the 5-element network in Fig. 6.13 are identified by NP's, together with the repetition interval of each line	100
6.15	The computed attenuation of the 5-element network in Fig. 6.13	102
7.1	A 2-element transmission line network	117
7.2	Attenuation of a 2-element distributed filter	122
8.1	A doubly terminated 2-element transmission line network	125
8.2	A 2-port network shown bisected into two 2-ports	125
8.3	The locus of the extremity of $e^{2s\tau_c}$ for $0 \leqq \tau_c \leqq \pi/2y$	128
8.4	(a) Vectors $e^{2s\tau_c} + a$ and $e^{2s\tau_c} - a$ with $0 < a < e^{\pi x/y}$ and their associated angles β and α (b) Typical representation of y_c with $0 < a < e^{\pi x/y}$	128
8.5	(a) Vectors $e^{2s\tau_c} + a$ and $e^{2s\tau_c} - a$ with $0 < e^{\pi x/y} < a < 1$ and their associated angles β and α (b) Typical representation of y_c with $e^{\pi x/y} < a$	129
8.6	(a) Vectors $e^{2s\tau_c} - a$ and $e^{2s\tau_c} + a$ with $0 < -a < e^{\pi x/y}$ (b) Typical representation of y_c with $0 < -a < e^{\pi x/y}$ for $0 \leqq \tau_c \leqq \pi/2y$	131

List of Illustrations (Cont.)

Figure	Title	Page
8.7	Typical representation of y_c with $0 < e^{\pi x/y} < -a$ for $0 \leqq \tau_c \leqq \pi/2y$	131
8.8	(a) Vectors $e^{2s\tau_s} + 1$ and $e^{2s\tau_s} - 1$ and the locus of $e^{2s\tau_s}$ for $0 \leqq \tau_s \leqq \pi/2y$ (b) Typical representation of y_s for $0 \leqq \tau_s \leqq \pi/2y$	133
8.9	Plots of $-y_c$ for $0 \leqq \tau_c \leqq \pi/2y$, and y_s for $0 \leqq \tau_s \leqq \pi/2y$	137
I.1	(a) A lossless 2-port having n-1 transmission line elements in cascade (b) The network in (a) augmented	141
II.1	The block diagram of the program	146
III.1	The flow-sheet of the program RTAPR	157
IV.1	The flow-sheet of the program RTLOC	163

List of Appendices

		Page
Appendix I:	Proof of The Expressions Given in Eqs. 3.4 Through 3.7	140
Appendix II:	A Program to Solve The System of Eqs. 3.17 And To Decrease $z_{\text{Connecting Line}}/z_{\text{Stub}}$ Automatically	145
Appendix III:	A Program For The Numerical Evaluation of ω_{AD} and ω_{BC}	156
Appendix IV:	A Program For The Numerical Evaluation of Transmission Poles	162

List of Symbols

Symbol	Equation Where The Symbol Is First Used	Remarks
a	(8. 5)	Reflection coefficient
a_i	(3. 4)	Coefficients in a cosine series
a_i'	(I. 1)	
A	(3. 1)	General circuit parameter
A_m	(6. 2)	Modified general circuit parameter
A_{m_1}	(6. 16)	
A_{m_2}	(6. 16)	
A_m'	(I. 1)	
$A^b_{m_N}$	(6. 46)	
$A^c_{m_N}$	(6. 50)	
A_t	(3. 3)	General circuit parameter of a lossless network
A_T	(3. 10)	General circuit parameter of a doubly terminated lossless network
A_T'	(3. 10)	
b_i	(3. 4)	Coefficients in a sine series
b_i'	(I. 1)	
B	(3. 1)	General circuit parameter
B_m	(6. 2)	Modified general circuit parameter

List of Symbols (Cont.)

Symbol	Equation Where The Symbol Is First Used	Remarks
B_{m_1}	(6. 16)	
B_{m_2}	(6. 16)	
B'_m	(I. 1)	
$B^b_{m_N}$	(6. 47)	
$B^c_{m_N}$	(6. 51)	
B_t	(3. 3)	General circuit parameter of a lossless network
B_T	(3. 10)	General circuit parameter of a doubly terminated lossless network
B'_T	(3. 10)	
c_i	(3. 4)	Coefficient in a sine series
c'_i	(I. 1)	
C	(4. 16)	Capacitance
C	(3. 1)	General circuit parameter
C_j	(4. 19)	Capacitance of j^{th} element
C_m	(6. 2)	Modified general circuit parameter
C_{m_1}	(6. 16)	
C_{m_2}	(6. 16)	
C'_m	(I. 1)	

List of Symbols (Cont.)

Symbol	Equation Where The Symbol Is First Used	Remarks
$C^{b}_{m_N}$	(6.48)	
$C^{c}_{m_N}$	(6.52)	
C_t	(3.3)	General circuit parameter of a lossless network
C_T	(3.10)	General circuit parameter of a doubly terminated lossless network
C'_T	(3.10)	
d_i	(3.4)	Coefficients in a cosine series
d'_i	(I.1)	
D	(3.1)	General circuit parameter
D_m	(6.2)	Modified general circuit parameter
D_{m_1}	(6.16)	
D_{m_2}	(6.16)	
D'_m	(I.1)	
$D^{b}_{m_N}$	(6.49)	
$D^{c}_{m_N}$	(6.53)	
D_t	(3.3)	General circuit parameter of a lossless network
D_T	(3.10)	General circuit parameter of a doubly terminated lossless network

List of Symbols (Cont.)

Symbol	Equation Where The Symbol Is First Used	Remarks
D'_T	(3. 10)	
E	(4. 1)	Used to define the impedance $(E + jF)/(G + jH)$
f_o		Quarterwave frequency in hertz
f_i	(3. 16)	Functions $i = 1, \ldots, n$
$f_i^{(j)}$	(4. 9)	Functions f_i evaluated at $x_i^{(j)}$
$f_{lx_k}^{(j)}$	(4. 10)	Derivates of f_i with respect to x_k evaluated at $x_i^{(j)}$
F	(4. 1)	Used to define the impedance $(E + jF)/(G + jH)$
G	(4. 1)	Used to define the impedance $(E + jF)/(G + jH)$
G_1	(3. 10)	Resistive termination of a network
G_2	(3. 10)	Resistive termination of a network
H	(4. 1)	Used to define the impedance $(E + jF)/(G + jH)$
J	(7. 1)	Number of nondominant poles under consideration for optimization
k	(3. 9)	Integer
k_j	(7. 1)	Positive weights
K	(6. 9)	
K_o		Odd integer

List of Symbols (Cont.)

Symbol	Equation Where The Symbol Is First Used	Remarks
ℓ	(3. 1)	Length of a transmission line element
ℓ_i	(3. 3)	Length of i^{th} transmission line element ($i = 1, \ldots, n$)
ℓ_s	(4. 26)	Length of a stub
L	(4. 14)	Inductance
L_j	(4. 18)	Inductance of j^{th} element
m	(5. 6)	
M	(5. 6)	
n		Number of transmission line elements, number of dominant transmission poles
R_c	(8. 3)	Resistive termination
R_s	(8. 4)	Resistive termination
s		Complex frequency
s_i	(3. 15)	Prescribed transmission poles ($i = 1, \ldots, n$)
s_{ke}	(5. 6)	
s_{kd}	(5. 6)	
T_n	(5. 1)	Chebychev polynomial of the first kind of order n
v	(3. 1)	Velocity of propagation
$x_1, \ldots, x_n$	(4. 5)	Dummy variables that define the functions f_i

List of Symbols (Cont.)

Symbol	Equation Where The Symbol Is First Used	Remarks
$x'_1, \ldots, x'_n$	(4. 27)	Dummy variables that define the functions f_i
$x_i^{(j)}$	(4. 6)	x_i at the conclusion of j^{th} iteration
$x(s)$	(6. 22)	Reactance function
$x'(s)$	(6. 54)	Reactance function
z	(3. 1)	Characteristic impedance
z_i	(3. 3)	Characteristic impedance of i^{th} transmission line
z_{12}	(3. 11)	Transfer impedance
z_{in}	(4. 3)	Input impedance
z_{in}^j	(4. 1)	
z_j^i	(7. 13)	
z_{M_j}	(7. 3)	Upper bound on the j^{th} characteristic impedance
z_{m_j}	(7. 3)	Lower bound on the j^{th} characteristic impedance
z'_j	(7. 32)	
z_c	(8. 3)	Characteristic impedance of a connecting line
z_s	(8. 4)	Characteristic impedance of a stub
α_j	(7. 34)	Real part of j^{th} nondominant pole
γ_j	(7. 34)	Imaginary part of j^{th} nondominant pole

List of Symbols (Cont.)

Symbol	Equation Where The Symbol Is First Used	Remarks
ω		Real frequency in rdn/sec
ω_a	(5.1)	Start of stopband
ω_c	(5.1)	Cut-off frequency
ω_A		Zero of A_m
ω_B		Zero of B_m
ω_C		Zero of C_m
ω_D		Zero of D_m
ω_r		Zero of $\cos(\omega \ell / r)$ nearest to the origin
ω_{AD}	(6.61)	Zero of $G_1 A_m + G_2 D_m$
ω_{BC}	(6.66)	Zero of $G_1 G_2 B_m + C_m$
λ		$\lambda = \tanh(s/4f_o)$
$\lambda_i^{(j)}$	(4.7)	
Φ	(3.1)	$\Phi = s\ell/v$
Φ_i	(3.3)	$\Phi_i = s\ell_i/v$
θ_i^n	(3.4)	$i = 1, \ldots, 2^{n-1}$
$\{\theta_i^j\}$		A set containing elements θ_i^j, $i = 1, \ldots, 2^{j-1}$
ξ	(3.12)	Any transmission pole

Symbol	Equation Where The Symbol Is First Used	Remarks
σ	(6.68)	
ζ	(6.71)	Zero of $x(\omega) + \tan(\ell\omega/v)$
μ_j	(7.1)	Imaginary part of j^{th} nondominant pole
μ'_j	(7.39)	
μ_j^i	(7.19)	
ν_j	(7.1)	j^{th} nondominant transmission zero
ν_j^i	(7.19)	
δ	(7.21)	
$\Delta\tau_k^i$	(7.16)	$\Delta\tau_k^i = \tau_k^{i+1} - \tau_k^i$
τ_i	(7.2)	$\tau_i = \ell_i/v$
τ_k^i	(7.13)	τ_k at the conclusion of i^{th} iteration
τ_p	(7.40)	
τ_c	(8.3)	Delay of a connecting line
τ_s	(8.4)	Delay of a stub
τ_m	(8.6)	

List of Symbols (Cont.)

Superscript Symbols	Subscript Symbols
i	a
(j)	c
'	i
	j
	k
	k_d
	k_e
	m
	p
	s

Chapter 1

Introduction

Network functions that characterize a lossless transmission line section can be expressed in terms of a single function $\tanh\left(\frac{s}{4f_0}\right)$, where $s = \sigma + j\omega$ is the complex frequency, and f_0 is the frequency, in hertz, at which the length of the transmission line element is a quarter wavelength. Using the transformation $\lambda = \Sigma + j\Omega = \tanh\left(\frac{s}{4f_0}\right)$ Richards [1] showed that distributed circuits composed of lumped resistors and equal length transmission line elements can be treated exactly as lumped networks in the new variable λ. Thus all the power of conventional lumped parameter synthesis techniques is made available to the designers of distributed parameter networks.

Richards' transformation has been successfully employed for the analytical design of distributed networks by Ozaki and Ishii [2], Horton and Wenzel [3], Wenzel [4], and many others. While this transformation has been a powerful tool for the analytic design of distributed structures, techniques based on it have certain weaknesses. Foremost among these is the requirement that all the transmission line elements have commensurate lengths. One half of the available degrees of freedom are thus fixed for analytic convenience, and all of the design control rests in the characteristic impedances of the

transmission line elements. This can lead to practical difficulty since the range of feasible characteristic impedance is much less than the element value range available with lumped inductances and capacitances.

A microwave network structure with no restriction on line lengths has been considered by Kinariwala [5]. He has derived necessary and sufficient condition for a function to be the input impedance of a circuit made up of sections of unequal length transmission lines in cascade and terminated in a lumped resistor. He also gives a procedure for the synthesis of such a cascaded structure from an input impedance satisfying the given conditions. The approximation problem for such a cascade network is still unsolved, as are the synthesis and approximation methods for a more general structure.

Although analytic design methods for distributed networks without the a priori restriction of commensurable line lengths are yet to be found, the high-speed computational capability of a large digital computer makes feasible the iterative design of such structures.

The purpose of this investigation is to study iterative synthesis of distributed parameter networks to realize a prescribed set of dominant transmission poles and zeros. The synthesis technique has been delineated with reference to the particular uniform transmission line structure which operates in TEM mode and consists of open shunt stubs alternating with connecting lines. For this structure the lower

and upper bounds of the characteristic impedances are specified for the transmission line elements with no restriction on their lengths. The methods developed are also applicable to other microwave structures, such as, series shorted stubs or shunt lumped capacitances alternating with connecting lines.

Chapter 2

Literature Survey

The literature on distributed networks useful as filters is vast. This survey outlines the principal developments in microwave structures operating in TEM-mode, and does not claim to be complete.

The microwave filter design techniques may be classified into two broad categories: approximate procedures, and exact methods, based on Richards' transformation [1]. In the former approach, an appropriate, exact lumped prototype is modified in such a way that it can evolve into a distributed network, when sections of the modified lumped design are replaced by their approximate functional equivalents in distributed elements such as resonant cavities or irises, quarterwave transformers or other impedance inverting configurations, strip lines, parallel coupled lines. This equivalence between a lumped section and its counterpart in the distributed domain is, in general, achieved by comparing them at an important frequency, for example, the frequency at band center. In the exact methods, a distributed filter is directly synthesized starting with an appropriate network function. Even with these methods, however, the mathematical model describing transmission line elements neglects higher order modes and does not take into account the fringing at the junctions of elements.

Approximate methods are numerically less cumbersome than the methods based on Richards' transformation, which, however, have the advantage of being theoretically exact. Since microwave structures designed according to either technique consist of commensurate elements, their responses are periodic (Fig. 2.1) in the real frequency domain, the principal period lying between $-f_0$ and f_0, where f_0 is the frequency at which the length of each element is one quarter-wave long. In practice, at high enough frequencies, the effect of higher order modes will be considerable and the actual response will deviate from being periodic.

2.1 Filter with Cascade Elements

A lumped bandpass filter may consist of shunt parallel-resonant branches alternating with series-resonant branches in series. To obtain a microwave bandpass structure, Fano and Lawson [6] and Mumford [7] transformed such a bandpass lumped network into a configuration where shunt anti-resonant branches are separated from each other by admittance inverters (Fig. 2.2). The function of the impedance inverters are twofold. They separate the resonators; and convert a series resonant branch into a shunt resonator thus allowing the modified network to have only one kind of resonator. A quarterwave coupled microwave bandpass filter [6], [7] was thus obtained when admittance inverters were realized by quarterwave transformers and the shunt resonant branches by waveguide cavity resonators. A

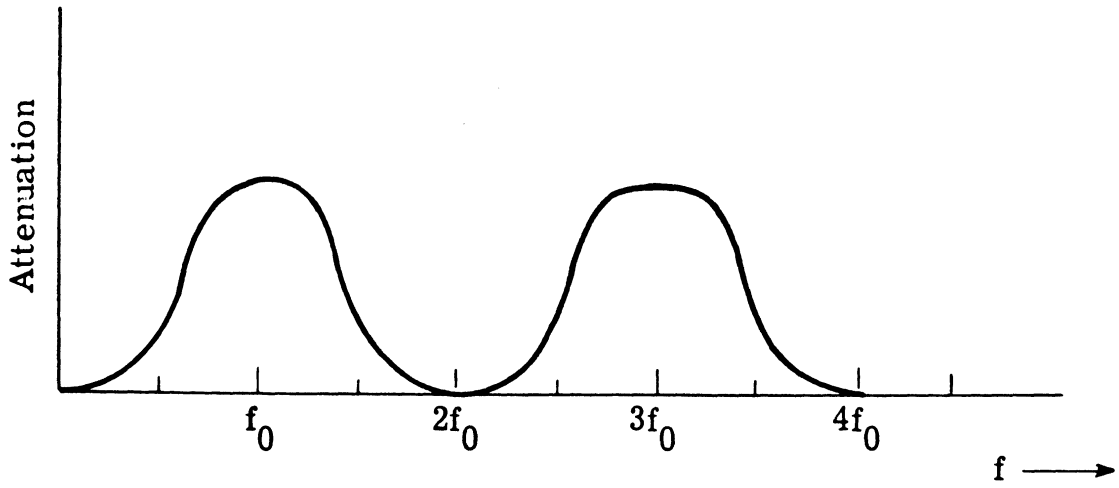

Fig. 2.1. The periodic nature of the frequency response of transmission line filters illustrated by the Butterworth attenuation of a half-wave filter

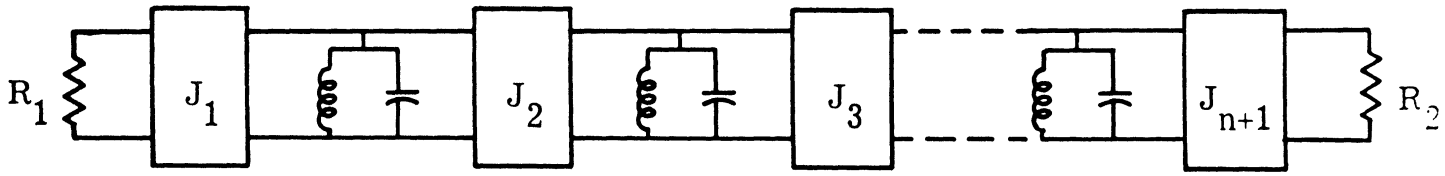

Fig. 2.2. A bandpass filter containing admittance inverters J_i $(i = 1, 2, \ldots, n)$

quarterwave long transmission line section is an exact inverter at only a single frequency; thus quarterwave transformer coupled filter designs are useful only for narrowband (10 percent).

A somewhat similar but more general approach was taken by Cohn [8] in designing direct-coupled resonator filters. With the interposition of impedance or admittance inverters, a bandpass structure obtained from a lowpass prototype is modified into a network which has either only series resonant branches alternating with impedance inverters (Fig. 2.3) or only shunt anti-resonant branches alternating with admittance inverters (Fig. 2.2). Instead of quarterwave transformers, suitable combinations (Fig. 2.4) of microwave circuit elements are used as inverting networks. Cohn thus realizes direct coupled filters which are either capacitively coupled, realizable in stripline resonators (Fig. 2.5) placed end to end, or inductively coupled, realizable in waveguide cavity resonators (Fig. 2.5) separated by inductive irises. The impedance or admittance inverting networks used by Cohn have better properties than a single quarterwave line; thus the design procedure is useful for filters having bandwidths of the order of 30 percent.

Quarterwave stepped impedance transformers (Fig. 2.6) are widely used as impedance matching networks. Design equations for stepped impedance transformers having up to four cascade quarterwave sections were first derived by Collin [9]. An exact synthesis

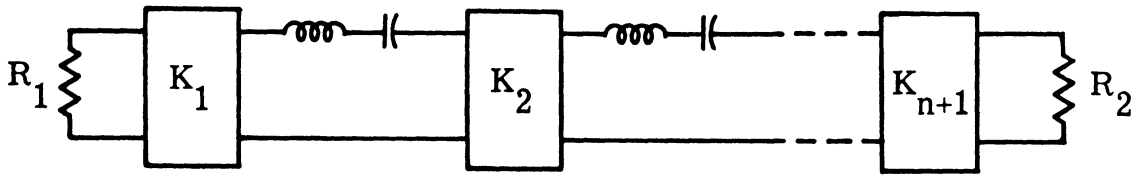

Fig. 2.3. A bandpass filter containing impedance inverters K_i $(i = 1, \ldots, n+1)$

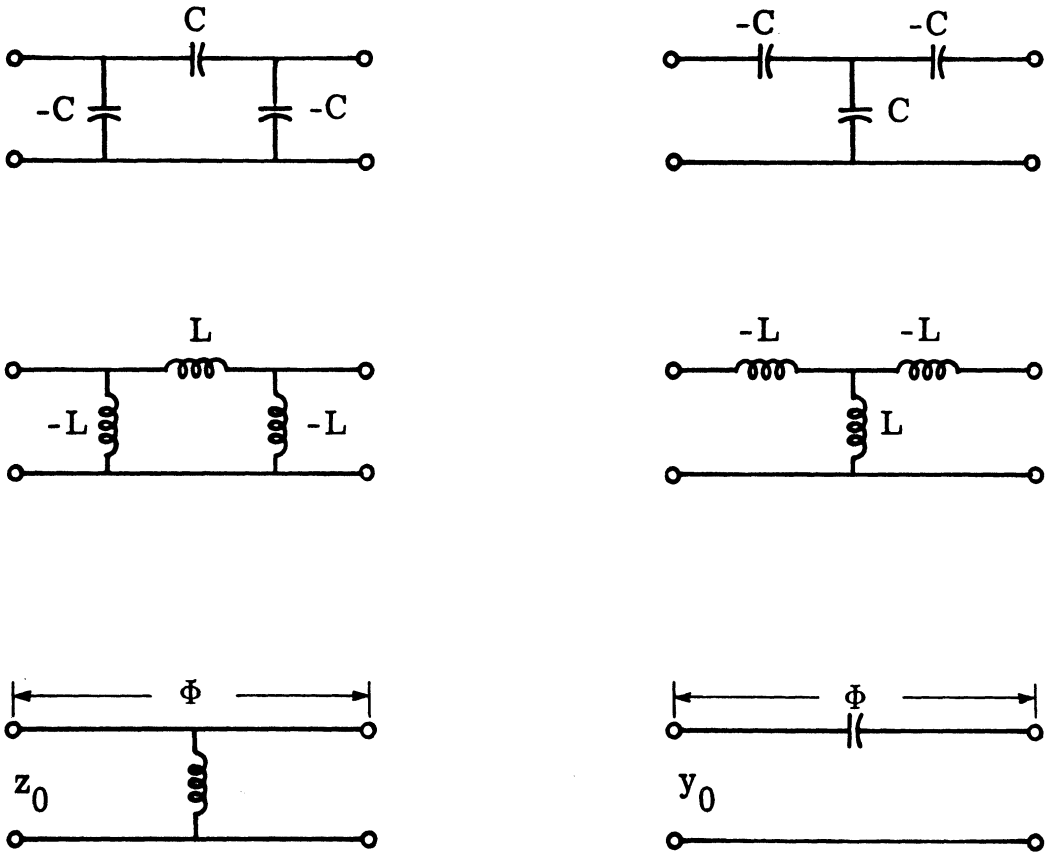

Fig. 2.4. Broad-band impedance-inversion networks

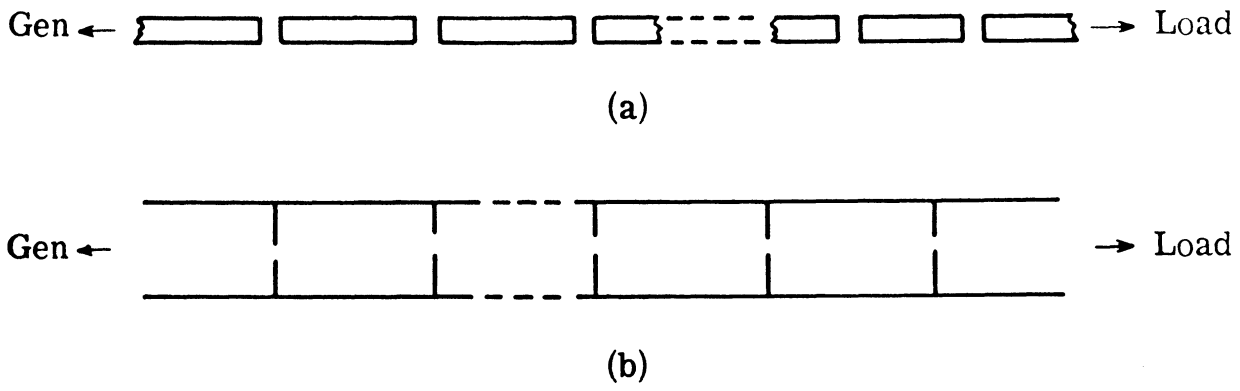

Fig. 2.5. Direct coupled-resonator filters
(a) in strip transmission line
(b) in waveguide

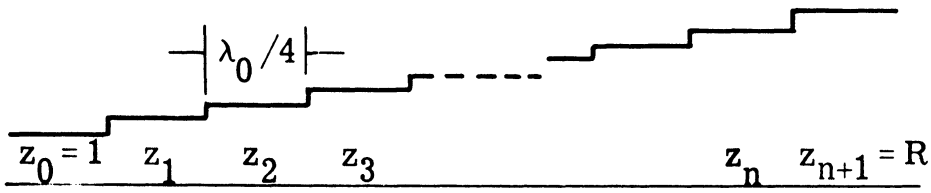

Fig. 2.6. Quarterwave stepped impedance transformer

of stepped impedance transformers consisting of any number of elements has been given by Riblet [10]. Halfwave filters (Fig. 2.7) that find their main application as lowpass or bandpass filters are an extension of quarterwave transformers. Structurally, halfwave filters differ from quarterwave transformers in one important aspect, namely, whereas the impedance of each quarterwave section increases or decreases monotonically along the length of the transformer, the impedances of halfwave sections oscillate about a mean value. Halfwave filters can be synthesized directly from an appropriate insertion loss function [11]. They can also be derived from a quarterwave transformer which is used as a prototype [12, 15]. Young [12] has shown that if, in a quarterwave transformer every other step of reflection coefficient Γ is replaced by its equivalent (Fig. 2.8) consisting of a step of reflection coefficient $-\Gamma$ flanked on either side by a 90 degree long line, the quarterwave transformer expands into a halfwave filter.

Young [12, 13] has used a quarterwave transformer as a prototype for designing the direct-coupled resonator filters [8]. Both are examples of transmission lines loaded at intervals. Young [12, 13] has shown that the impedance steps in a quarterwave transformer can be replaced by inductive obstacles (or capacitive gaps) having the same reflection coefficients as those of the impedance steps. This design is also approximate since the equivalence of an obstacle and an

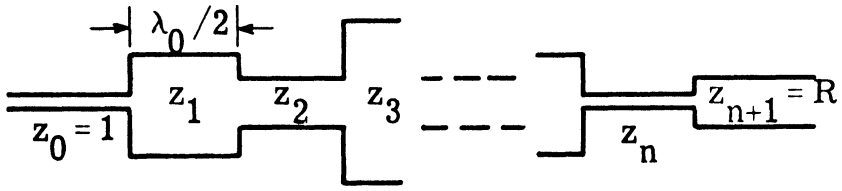

Fig. 2.7. Halfwave filter

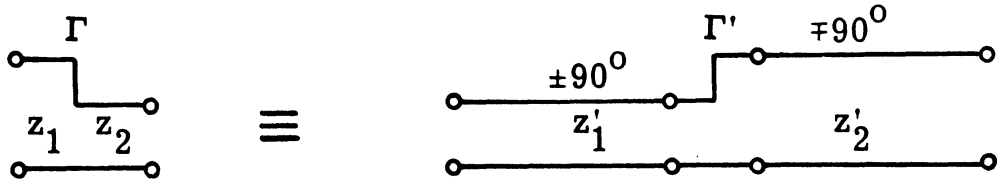

Fig. 2.8. Equivalent circuit of an impedance step
Impedance ratio: $z'_1/z'_2 = z_2/z_1$
Reflection coefficient: $\Gamma' = -\Gamma$

impedance step is exact only at a single frequency. Tables of element values for the design of quarterwave transformers have been given by Young [14] and for the design of halfwave filters by Levy [11].

2.2 Filters with Parallel-Coupled Lines

Filters have been designed using parallel coupled transmission lines [17-23]. Mathematical expressions that describe the network of two transmission lines (Fig. 2.9) coupled along their sides have been derived by E. M. T. Jones and Bolljahn [16]. This design differs from the usual end coupled strip configuration in that successive halfwave long strips are parallel coupled along a distance of a quarter wavelength (Fig. 2.10). In contrast to direct coupled structure where the dimension of the gap between adjacent halfwave resonators becomes critical for relatively wide bandwidth, coupling the strips along their sides permits wider and less critical gaps. However, coupling is no longer capacitive since the overlapping lengths are one-quarter-wave long at band center and phase varies along them. Design formulas that are theoretically exact only in the limit of zero bandwidth, but give tolerably good results for bandwidths of up to about 30 percent have been derived by Cohn [17]. Formulas derived by Matthaei [18] for the design of parallel coupled stripline filters avoid narrowband assumptions, but are also approximate. They give good accuracy from narrow bandwidths to bandwidths of about 2 to 1. Exact design methods

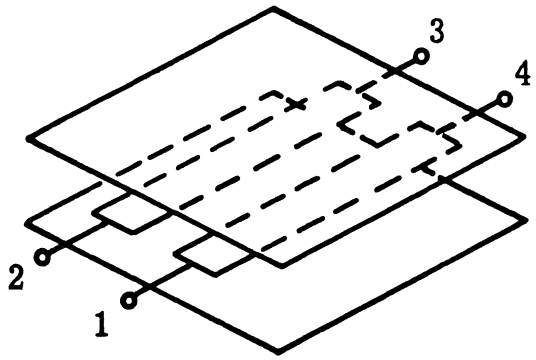

Fig. 2.9. Shielded parallel coupled stripline

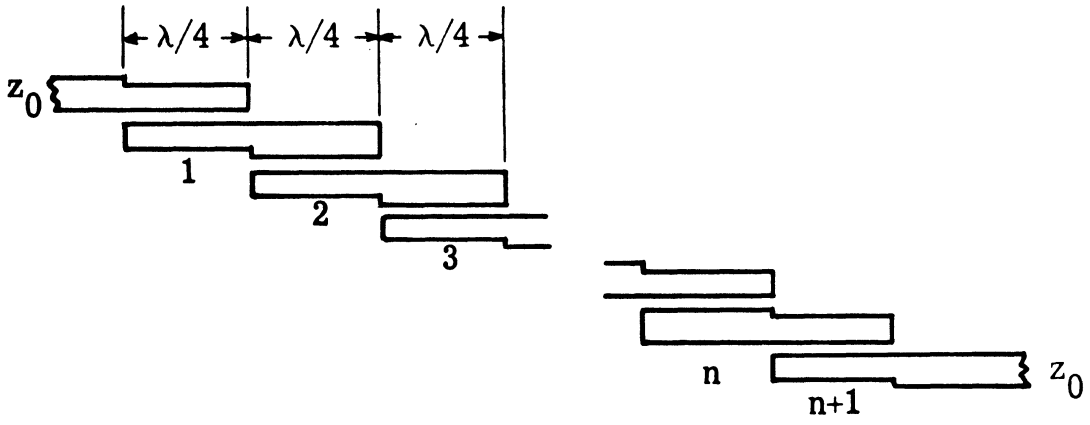

(a)

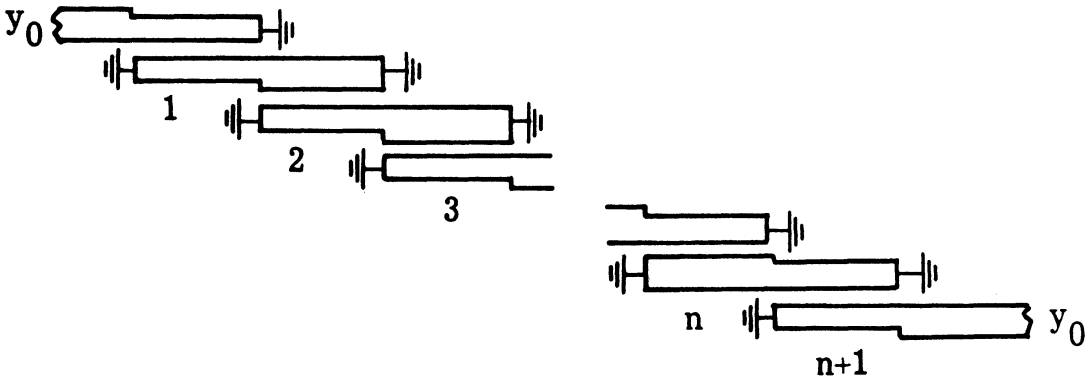

(b)

Fig. 2.10. Parallel coupled strip transmission line filters
(a) with open-circuited sections
(b) with short circuited sections [17, 18]

for these filter structures, based on Richards' transformation have been presented by Ozaki and Ishii [19] and others [4, 24].

Matthaei [20] has shown that for a halfwave long resonator, with both ends grounded, the voltage or current distribution along it does not undergo any change when the resonator is folded in the middle to make a quarterwave long resonator one end of which is grounded and the other open (Fig. 2.11). Matthaei [20] thus converts a parallel coupled resonator filter into an interdigital filter (Fig. 2.12). Such filters consist of quarterwave resonators that are parallel coupled, with alternate ends of the resonators grounded and the opposite ends open circuited. An exact design theory for interdigital filters and related structures is given by Wenzel [21].

The digital resonators of an interdigital filter which are each a quarterwave long at band center can be made shorter, thus making the filter more compact, when loading capacitances are added at the open circuited ends of the resonators (Fig. 2.13), as has been shown by Robinson [22]. The capacitive loading also moves the first spurious response further away from the center frequency of the principal passband.

Similar in many ways to the capacitively loaded interdigital filter is the comb-line bandpass filter (Fig. 2.14) developed by Matthaei [23]. The resonators in these types of filters consist of TEM mode transmission line elements that are short circuited at one end and have

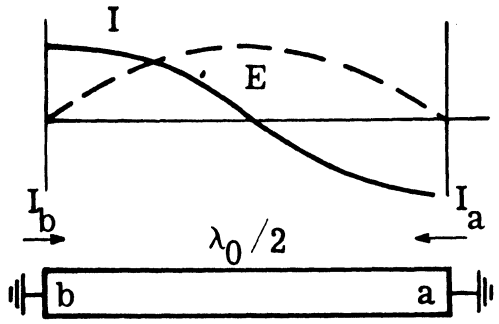

(a)

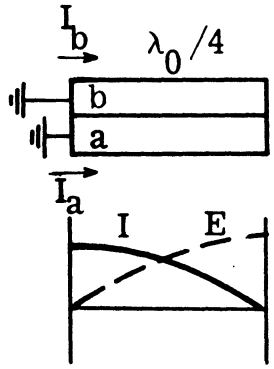

(b)

Fig. 2.11. Effect of folding a $\lambda_0/2$ resonator to make a $\lambda_0/4$ resonator

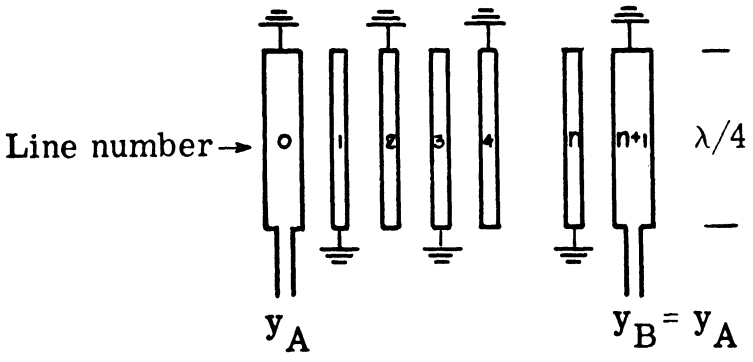

Fig. 2.12. Interdigital filter with shortcircuited lines at the end

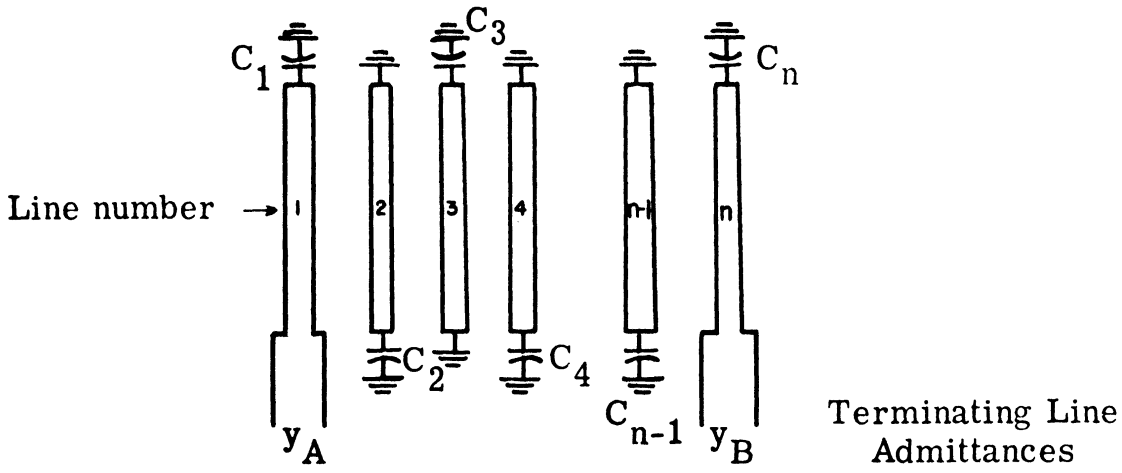

Fig. 2.13. Capacitively loaded interdigital filter with ungrounded end resonators. Typically, each line is less than $\lambda/4$ long

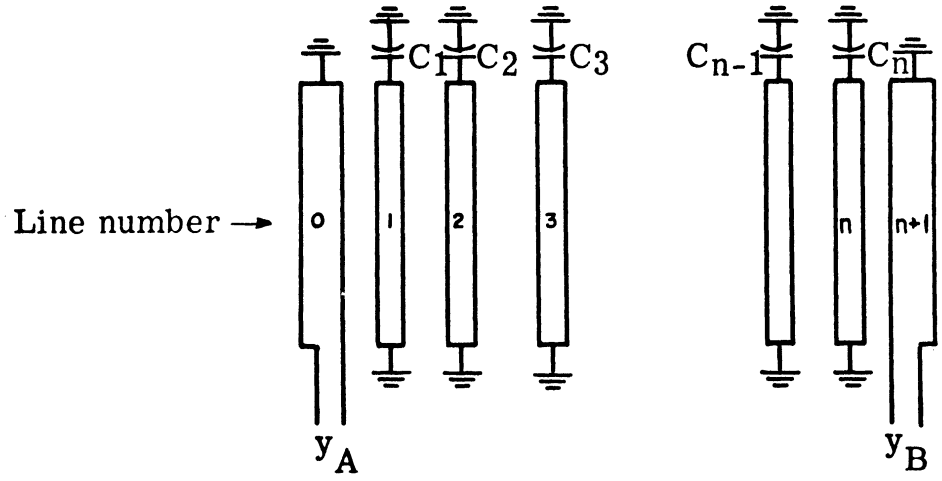

Fig. 2.14. A comb-line bandpass filter [23]

a lumped capacitance between the other end of each resonator element and the ground. The capacitive loadings are essential for the function of the filter, since magnetic and electric coupling effects would cancel each other when the resonators are all open circuited at one end and grounded at the opposite end. The resonator elements are typically one-eighth of a wavelength long at the center frequency of the primary passband. Thus, a filter of this type is compact and has its first spurious band center around four times the frequency of the center of the primary passband.

2.3 Filters with Stubs and Richards' Transformation

Filters that make use of stubs are designed by techniques based on Richards' transformation [1]. Richards has shown that with the transformation $\lambda = \tanh s/4f_0$, s-plane distributed networks consisting of lumped resistors and commensurate transmission line elements that are a quarterwave long at the frequency f_0, can be treated exactly as a lumped network in the new variable λ. A shorted or open stub is thus transformed into a λ-plane inductor or capacitor respectively. A one quarterwave long connecting section of transmission line, henceforth referred to as a unit element, does not have an s-plane single lumped counterpart; it produces transmission zeros of order $1/2$ at ± 1 in the λ-plane. Richards [1, 30] has derived the conditions for removing a unit element from an input impedance or admittance

function. In the absence of a transmission zero associated with the input impedance, at $\lambda = \pm 1$, the removal of a unit element produces a phase rotation and does not result in the reduction of degree of the input impedance [29].

Ikeno [31] has given a synthesis procedure for the structure consisting of stubs and connecting line alternating. The same structure has been considered, from a different point of view, by Kuroda [34], who derived and made use of what are now known as Kuroda's identities. A detailed discussion of these identities may be found in [4]. The procedure developed by Ikeno and Kuroda, aided by Kuroda's identity, has been further extended by Ozaki and Ishii [2], Wenzel [4], Ozaki and Ishii [19], Grayzel [29] and many others [24, 25, 27, 28, 31-39].

In the distributed structures that result from a straightforward synthesis of transmission functions that have been developed for s-plane lumped networks and therefore do not possess transmission zeros at ± 1, unit elements do not occur naturally; they must be incorporated into the structure as a means of relaxing the constraints on fabrication. Such unit elements produce only phase rotation and do not contribute to improving the magnitude of the response. In this sense, they are redundant. Transmission functions for the design of "optimum" filters where the connecting unit elements also contribute to the filter response have been derived by Horton and Wenzel [3] for both

Butterworth and Chebychev response in the passband. Synthesis of filters which realize such transfer functions are also presented.

Original and independent Japanese contributions to the design of such "optimum" filters and other microwave structures are reported to be considerable. In a seminar on the design of distributed networks given at The University of Michigan, Professor Fujisawa cited works in this area by Japanese researchers [31-39].

Chapter 3

Mathematical Derivations

The physical structure of the transmission line networks under investigation in this study is depicted in Fig. 3.1. Analytic expressions for the elements of the general circuit parameter matrix of the lossless part of this network are obtained in Sec. 3.1. Other network functions are derivable from the general circuit parameter matrix. The characteristic impedances and the lengths of the transmission line elements in the circuit of Fig. 3.1 with a prescribed set of dominant transmission poles are related by a system of nonlinear equations presented in Sec. 3.2.

3.1 General Circuit Parameter Matrix

The network configuration, shown in Fig. 3.1, consists of n transmission line elements. In this structure open shunt stubs, numbered 1, 3, 5,..., n, alternate with connecting lines, numbered 2, 4,..., n - 1. The i^{th} element is assumed to be completely described by two parameters: its characteristic impedance z_i and its length ℓ_i.[1]

The general circuit parameter matrices for an open stub and a connecting line are respectively given by

[1] This assumption neglects fringing effects and higher order modes.

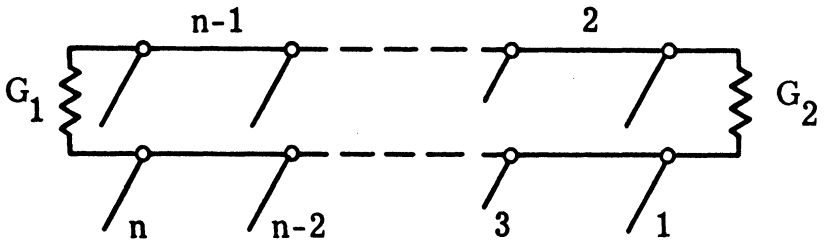

Fig. 3.1. General structure of the transmission line networks considered in this study. The length ℓ_j and the characteristic impedance z_j characterize the jth transmission line

$$\begin{bmatrix} A & B \\ C & D \end{bmatrix} = \begin{bmatrix} 1 & 0 \\ \frac{1}{z}\tanh\Phi & 1 \end{bmatrix} = \frac{1}{z\cosh\Phi}\begin{bmatrix} z\cosh\Phi & 0 \\ \sinh\Phi & z\cosh\Phi \end{bmatrix} \tag{3.1}$$

and

$$\begin{bmatrix} A & B \\ C & D \end{bmatrix} = \frac{1}{z}\begin{bmatrix} z\cosh\Phi & z^2\sinh\Phi \\ \sinh\Phi & z\cosh\Phi \end{bmatrix} \tag{3.2}$$

where

z = characteristic impedance of the element,

ℓ = length of the element,

v = velocity of propagation,

$\Phi = \frac{s\ell}{v}$.

The general circuit parameter matrix,

$$\begin{bmatrix} A_t & B_t \\ C_t & D_t \end{bmatrix},$$

for the lossless part of the network in Fig. 3.1 is the product of individual matrices characterizing each element and therefore can be written as

$$\begin{bmatrix} A_t & B_t \\ C_t & D_t \end{bmatrix} = \left\{ \frac{1}{z_n \cosh \Phi_n} \begin{bmatrix} z_n \cosh \Phi_n & 0 \\ \sinh \Phi_n & z_n \cosh \Phi_n \end{bmatrix} \right.$$

$$\frac{1}{z_{n-1}} \begin{bmatrix} z_{n-1} \cosh \Phi_{n-1} & z_{n-1}^2 \sinh \Phi_{n-1} \\ \sinh \Phi_{n-1} & z_{n-1} \cosh \Phi_{n-1} \end{bmatrix} \cdot \tag{3.3}$$

$$\cdots \frac{1}{z_2} \begin{bmatrix} z_2 \cosh \Phi_2 & z_2^2 \sinh \Phi_2 \\ \sinh \Phi_2 & z_2 \cosh \Phi_2 \end{bmatrix}$$

$$\left. \frac{1}{z_1 \cosh \Phi_1} \begin{bmatrix} z_1 \cosh \Phi_1 & 0 \\ \sinh \Phi_1 & z_1 \cosh \Phi_1 \end{bmatrix} \right\} ,$$

where $\Phi_i = s\ell_i / v$, $i = 1, 2, \ldots, n$.

Let $\{\theta^j\}$ be the set of all the different sums that can be formed out of $(\ell_1/v \pm \ell_2/v \pm \ldots \pm \ell_j/v)$ retaining all the terms, $(+\ell_1/v$, $\pm \ell_2/v, \ldots, \pm \ell_j/v)$, but choosing either of the two signs associated with each term. There are 2^{j-1} terms in the set $\{\theta^j\}$. Let each term be designated

$$\theta_i^j \ , \quad i = 1, 2, 3, \ldots, 2^{j-1} \ .$$

It has been shown in Appendix I that the elements of the left hand matrix in (3.3) can be expressed as

$$A_t = \frac{1}{\prod_{i=1}^{n} z_i \prod_{i=1,\ 3,\ \ldots}^{n} \cosh \Phi_i} \cdot \sum_{i=1}^{2^{n-1}} a_i \cosh (\theta_i^n s) \qquad (3.4)$$

$$B_t = \frac{1}{\prod_{i=1}^{n} z_i \prod_{i=1,\ 3,\ \ldots}^{n} \cosh \Phi_i} \cdot \sum_{i=1}^{2^{n-1}} b_i \sinh (\theta_i^n s) \qquad (3.5)$$

$$C_t = \frac{1}{\prod_{i=1}^{n} z_i \prod_{i=1,\ 3,\ \ldots}^{n} \cosh \Phi_i} \cdot \sum_{i=1}^{2^{n-1}} c_i \sinh (\theta_i^n s) \qquad (3.6)$$

$$D_t = \frac{1}{\prod_{i=1}^{n} z_i \prod_{i=1,\ 3,\ \ldots}^{n} \cosh \Phi_i} \cdot \sum_{i=1}^{2^{n-1}} d_i \cosh (\theta_i^n s) \quad . \qquad (3.7)$$

Equations 3.4 through 3.7 demonstrate that A_t, B_t, C_t and D_t all have the same poles given by

$$\prod_{i=1,\ 3,\ \ldots}^{n} \cosh \frac{s\ell_i}{v} = 0 \qquad (3.8)$$

i. e. ,

$$s = \pm j \frac{2k - 1}{2} \frac{\pi}{\ell_i / v} \quad , \qquad \begin{matrix} i = 1, 3, 5, \ldots, n \\ k = 1, 2, 3, 4, \ldots \end{matrix} \tag{3.9}$$

Thus poles of A_t, B_t, C_t and D_t occur at those frequencies at which the length of each stub is one quarterwave long or an odd multiple thereof. The zeros of A_t, B_t, C_t and D_t are not as straightforward to determine as the poles. The positions of these zeros are investigated in Chapter 6.

3.2 A System of Nonlinear Equations

The characteristic impedances and the lengths of the transmission line elements that realize a prescribed set of transmission poles are the solution of a system of nonlinear equations. In this section, this system of nonlinear equations is derived.

The general circuit parameter matrix for the whole circuit in Fig. 3.1 is the product of individual matrices representing each circuit element, which may be written

$$\begin{bmatrix} 1 & 0 \\ G_1 & 1 \end{bmatrix} \left\{ \frac{1}{\cosh \frac{s\ell_n}{v}} \begin{bmatrix} \cosh \frac{s\ell_n}{v} & 0 \\ \frac{1}{z_n} \sinh \frac{s\ell_n}{v} & \cosh \frac{s\ell_n}{v} \end{bmatrix} \right\}$$

$$\begin{bmatrix} \cosh \frac{s\ell_{n-1}}{v} & z_{n-1} \sinh \frac{s\ell_{n-1}}{v} \\ \frac{1}{z_{n-1}} \sinh \frac{s\ell_{n-1}}{v} & \cosh \frac{s\ell_{n-1}}{v} \end{bmatrix} \cdots \begin{bmatrix} \cosh \frac{s\ell_2}{v} & z_2 \sinh \frac{s\ell_2}{v} \\ \frac{1}{z_2} \sinh \frac{s\ell_2}{v} & \cosh \frac{s\ell_2}{v} \end{bmatrix}$$

$$\left\{ \frac{1}{\cosh \frac{s\ell_1}{v}} \begin{bmatrix} \cosh \frac{s\ell_1}{v} & 0 \\ \frac{1}{z_1} \sinh \frac{s\ell_1}{v} & \cosh \frac{s\ell_1}{v} \end{bmatrix} \right\} \begin{bmatrix} 1 & 0 \\ G_2 & 1 \end{bmatrix}$$

$$= \begin{bmatrix} A_T & B_T \\ C_T & D_T \end{bmatrix} = \prod_{i=1,3,\ldots}^{n} \left[\operatorname{sech} \left(\frac{s\ell_i}{v} \right) \right] \begin{bmatrix} A'_T & B'_T \\ C'_T & D'_T \end{bmatrix} . \quad (3.10)$$

Since the transfer impedance is given by

$$z_{12} = \frac{1}{C_T} = \frac{\prod_{i=1,3,\ldots}^{n} \left[\cosh \left(\frac{s\ell_i}{v} \right) \right]}{C'_T} , \quad (3.11)$$

transmission poles are the zeros of C'_T. To emphasize that C'_T is a function of lengths of the line elements, $(\ell_1, \ell_2, \ldots, \ell_n)$, the characteristic impedances of the line elements, $(z_1, z_2, \ldots, z_n)$ and the complex frequency s, it can be written as

$$C'_T(\ell_1, \ldots, \ell_n; z_1, \ldots, z_n; s)$$

If ξ (and its conjugate) is a complex transmission pole of the network in Fig. 3.1, one gets

$$C'_T(\ell_1, \ldots, \ell_n; z_1, \ldots, z_n; \xi) = 0 \ . \tag{3.12}$$

C'_T being a complex-valued function, Eq. 3.12 can be separated into two real equations

$$\mathrm{Re}[C'_T(\ell_1, \ldots, \ell_n; z_1, \ldots, z_n; \xi)] = 0 \ , \tag{3.13}$$

$$\mathrm{Im}[C'_T(\ell_1, \ldots, \ell_n; z_1, \ldots, z_n; \xi)] = 0 \ . \tag{3.14}$$

If ξ is real, C'_T is real, and in that case Eq. 3.12 is a real equation. A complex pole and its conjugate results in two equations and a real pole results in one equation. Realization of n transmission poles at prescribed locations s_i, $i = 1, 2, \ldots, n$ requires that

$$C_T(\ell_1, \ldots, \ell_n; z_1, \ldots, z_n; s_i) = 0 \ ; \ i = 1, 2, \ldots, n \ . \tag{3.15}$$

Following the procedure outlined above the system of Eq. 3.15 may be written in the form

$$f_i(\ell_1, \ldots, \ell_n; z_1, \ldots, z_n) = 0 \; ; \; i = 1, \ldots, n \; . \tag{3.16}$$

The functions f_i are the real and imaginary parts of C'_T at the complex poles and C'_T itself at the real poles. Assuming that the prescribed set of n pole locations are given by

$$s_1, s_2 = s_1^*; s_3, s_4 = s_3^*; \ldots; s_{n-2}, s_{n-1} = s_{n-2}^*; s_n(\text{real}),$$

the system of equations (3.16) can be explicitly expressed as

$$\left.\begin{aligned}
f_1 &= \mathrm{Re}[C'_T(\ell_1, \ldots, \ell_n; z_1, \ldots, z_n; s_1)] = 0 \\
f_2 &= \mathrm{Im}[C'_T(\ell_1, \ldots, \ell_n; z_1, \ldots, z_n; s_1)] = 0 \\
f_3 &= \mathrm{Re}[C'_T(\ell_1, \ldots, \ell_n; z_1, \ldots, z_n; s_3)] = 0 \\
f_4 &= \mathrm{Im}[C'_T(\ell_1, \ldots, \ell_n; z_1, \ldots, z_n; s_3)] = 0 \\
&\;\;\vdots \\
f_{n-2} &= \mathrm{Re}[C'_T(\ell_1, \ldots, \ell_n; z_1, \ldots, z_n; s_{n-2})] = 0 \\
f_{n-1} &= \mathrm{Im}[C'_T(\ell_1, \ldots, \ell_n; z_1, \ldots, z_n; s_{n-2})] = 0 \\
f_n &= C'_T(\ell_1, \ldots, \ell_n; z_1, \ldots, z_n; s_n) = 0
\end{aligned}\right\} \tag{3.17}$$

Chapter 4

Realization of Prescribed Poles and Zeros

In Section 3. 2 a system of equations has been outlined; a solution of these equations specifies a circuit of the type shown in Fig. 3. 1 to realize a prescribed set of dominant poles. In this chapter the generation of this system of equations is outlined in more detail in Section 4. 1. Section 4. 2 discusses a numerical technique for solving this system. Explicit iteration formulas are given. Since the successful convergence of most of the iterative numerical techniques is dependent on the point where the iteration is initiated, a good approximate solution of the system is derived in Section 4. 3. The exact solution that results from the iteration of this approximate solution is not, in general, practically realizable. A method for attaining a practically realizable solution is described in Section 4. 5. The computer program that has been developed to realize a prescribed set of poles is listed in Appendix II, together with a note on its capability and use. Section 4. 6 outlines a method for realizing the prescribed zeros.

4. 1 Generation of the System of Nonlinear Equations

Functional dependence of all the f_i in Eq. 3. 17 on the lengths and characteristic impedances of the line elements could be found

explicitly from the multiplication of the matrices in Eq. 3.10. Such a determination of analytic expressions for the functions f_i in terms of ℓ_i and z_i would be tedious and lengthy. Since the ability to solve this system of equations only requires that it be possible to evaluate the individual functions at given values of ℓ_i and z_i, a digital computer can be programmed to accomplish this, even though explicit analytic expressions are not developed. A computer algorithm for evaluations of the functions f_i is described in this section.

The functions f_i are the real and imaginary parts of C'_T at the prescribed poles. C'_T is calculated conveniently from the input impedance at the port 1-1', as indicated in Fig. 4.2, because $z_{in} = A'_T / C'_T$. Evaluation of z_{in} proceeds in the following way.

The input impedance of a transmission line terminated in an impedance $\frac{E+jF}{G+jH}$ as shown in Fig. 4.1(a), can be manipulated into the form

$$z^j_{in} = z_j \frac{(E+jF)\cosh(s\ell_j/v) + (G+jH)z_j \sinh(s\ell_j/v)}{(G+jH)z_j \cosh(s\ell_j/v) + (E+jF)\sinh(s\ell_j/v)} \quad . \qquad (4.1)$$

The input impedance of a one port shunted by an open stub as depicted in Fig. 4.1(b), is found to be

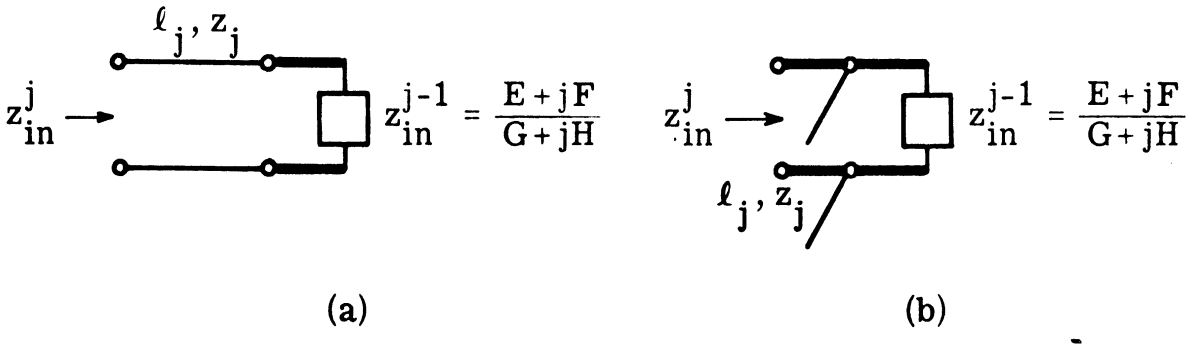

Fig. 4.1. (a) A transmission line terminated by the impedance

$$z_{in}^{j-1} = \frac{E+jF}{G+jH}$$

(b) An impedance $z_{in}^{j-1} = \frac{E+jF}{G+jH}$ shunted by an open stub

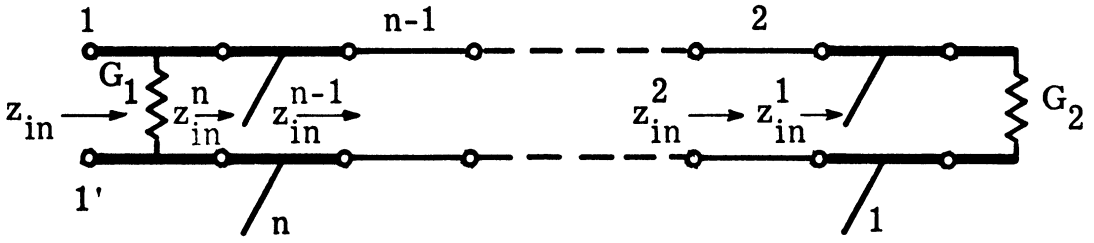

Fig. 4.2. Input impedance z_{in} looking into the port 1 - 1' is determined recursively. Computation starts at G_2, then proceeds toward the left as z_{in}^{j} (j = 1, 2, . . ., n) are found using (4.1) or (4.2) until port 1 - 1' is reached

$$z_{in}^{j} = \frac{(E+jF)z_j \cosh(s\ell_j/v)}{(G+jH)z_j \cosh(s\ell_j/v) + (E+jF)\sinh(s\ell_j/v)} \quad . \tag{4.2}$$

Starting with $E = 1/G_2$, $F = 0$, $G = 1$, $H = 0$, z_{in}^{1}, z_{in}^{2}, ..., z_{in}^{n} are computed recursively by using whichever of the expressions (4.1) or (4.2) is applicable as shown in Fig. 4.2.

Finally

$$z_{in} = \frac{1}{G_1 + \frac{1}{z_{in}^{n}}} \quad . \tag{4.3}$$

Evaluation of C_T' by first finding z_{in} from Eq. 4.3 involves determination of z_{in}^{j} ($j = 1, 2, \ldots, n$) using either Eq. 4.1 or Eq. 4.2. Each of these z_{in}^{j} is expressed by four real numbers. In the computer program developed to solve the system of equations (3.17), which is described in Appendix II, C_T' was found from the denominator of z_{in}. An alternate approach would be to calculate the product of the n matrices in Eq. 3.10, where the representation of each matrix needs eight real numbers.

4.2 Newton-Raphson Method

We are now ready to consider the solution of the system of equations generated in Section 4.1. There are a number of numerical techniques available for the solution of a system of nonlinear equations. Discussions of these methods can be found in [40 through 45].

The Newton-Raphson iterative algorithm has been utilized by the writer to solve the system of equations (3.17); an outline of the method is presented here.

Let the system of equations (3.17) be written as

$$f_i(\ell_1, \ell_2, \ldots, \ell_n; z_1, \ldots, z_n) = 0 \ , \quad i = 1, 2, \ldots, n \ . \tag{4.4}$$

This system possesses 2n variables: n line lengths and an equal number of characteristic impedances.

Let any n of these 2n variables be assigned known values chosen arbitrarily or otherwise. Let the remaining n variables, which are, then, the unknowns in the system, be designated by $x_1, x_2, \ldots, x_n$.

The system of equations (4.4) then becomes

$$f_i(x_1, x_2, \ldots, x_n) = 0 \ , \quad i = 1, 2, \ldots, n \ . \tag{4.5}$$

Adopt now the following notation:

$x_i^{(j)}$ = the value of x_i at the conclusion of the j^{th} iteration, (4.6)

$$x_i^{(j+1)} - x_i^{(j)} = \lambda_i^{(j)} \ , \quad i = 1, 2, \ldots, n \ , \tag{4.7}$$

$$f_i = f_i(x_1, x_2, \ldots, x_n) \ , \quad i = 1, 2, \ldots, n \ , \tag{4.8}$$

$$f_i^{(j)} = f_i(x_1^{(j)}, x_2^{(j)}, \ldots, x_n^{(j)}) \ , \quad i = 1, 2, \ldots, n \ , \tag{4.9}$$

$$f_{ix_k}^{(j)} = \frac{\partial}{\partial x_k}\left[f_i\,(x_1, x_2, \ldots, x_n)\right]\Big|_{(x_1^{(j)}, x_2^{(j)}, \ldots, x_n^{(j)})}, \qquad (4.10)$$

$$i = 1, 2, \ldots, n,$$

$$k = 1, 2, \ldots, n.$$

The corrections $\lambda_i^{(j)}$ $(i = 1, 2, \ldots, n)$ are obtained from $x_i^{(j)}$ $(i = 1, 2, \ldots, n)$ by solving the linear system

$$\sum_{k=1}^{n} \lambda_k^{(j)} f_{ix_k}^{(j)} + f_i^{(j)} = 0, \quad i = 1, 2, \ldots, n, \qquad (4.11)$$

where $\lambda_k^{(j)}$ are the unknowns. With $x_i^{(j)}$ $(i = 1, 2, \ldots, n)$ given, the process of solving the linear system of equations (4.11) to determine $\lambda_k^{(j)}$ defines the $(j + 1)^{th}$ iteration. The corrections $\lambda_i^{(j)}$, thus found, are added to $x_i^{(j)}$ to arrive at the new values, $x_i^{(j+1)} = x_i^{(j)} + \lambda_i^{(j)}$, of the variables. The iteration is then repeated until it converges to the solution of the nonlinear system. The whole process is initiated at $x_i^{(0)}$. Convergence considerations dictate that the point $x_i^{(0)}$ may not be completely arbitrary. The question of convergence of the Newton-Raphson algorithm has been studied in detail by Ostrowski [40], and Isaacson and Keller [44]. They have shown that convergence requires that $x_i^{(0)}$, the point where the iteration is initiated, lie in the close proximity of the solution.

4.3 Approximate Solution

A method of evaluating an approximate solution of the system of equations (3.17) under suitable assumptions regarding the lengths and the characteristic impedances is outlined in this section.

Using the series expansions for $\cosh \frac{s\ell}{v}$ and $\tanh \frac{s\ell}{v}$, the transmission matrixes (Eq. 3.1 and Eq. 3.2) for a connecting line and an open stub can be written in the forms

$$\begin{bmatrix} 1 + \frac{\ell^2}{v^2}\frac{s^2}{2!} + \dots & z\left(\frac{\ell}{v}s + \frac{\ell^3}{v^3}\frac{s^3}{3!} + \dots\right) \\ \frac{1}{z}\left(\frac{\ell}{v}s + \frac{\ell^3}{v^3}\frac{s^3}{3!} + \dots\right) & 1 + \frac{\ell^2}{v^2}\frac{s^2}{2!} + \dots \end{bmatrix}, \qquad (4.12)$$

and

$$\begin{bmatrix} 1 & 0 \\ \frac{1}{z}\left(\frac{\ell}{v}s - \frac{\ell^3}{v^3}\frac{s^3}{3} + \dots\right) & 1 \end{bmatrix}. \qquad (4.13)$$

If for the connecting line it is assumed that

$$\left.\begin{aligned} z &\to \infty \\ \frac{\ell}{v} &\to 0 \\ z\frac{\ell}{v} &\to L \end{aligned}\right\}, \qquad (4.14)$$

and

the matrix (Eq. 4.12) in the finite frequency-plane approaches the limiting value

$$\begin{bmatrix} 1 & sL \\ 0 & 1 \end{bmatrix} \quad . \tag{4.15}$$

Similarly, if the open stub satisfies the conditions

$$\left.\begin{aligned} z &\to 0 \\ \frac{\ell}{v} &\to 0 \\ \frac{\ell/v}{z} &\to C \end{aligned}\right\} \quad , \tag{4.16}$$

the matrix (Eq. 4.13) in the limit becomes

$$\begin{bmatrix} 1 & 0 \\ Cs & 1 \end{bmatrix} \quad . \tag{4.17}$$

Therefore, in Fig. 4.2, if all the connecting lines satisfy conditions similar to (4.14), i.e.,

$$\left.\begin{aligned} z_j &\to \infty \\ \ell_j/v &\to 0 \\ z_j\ell_j/v &= L_j \end{aligned}\right\} \quad , \tag{4.18}$$

$$j = 2, 4, 6, \ldots$$

and all the open stubs satisfy conditions similar to Eq. 4.16, i.e.,

$$\left.\begin{aligned} z_j &\to 0 \\ \ell_j/v &\to 0 \\ \frac{\ell_j/v}{z_j} &= C_j \end{aligned}\right\} \quad , \qquad (4.19)$$

$$j = 1, 3, 5, \ldots$$

the general circuit matrix for the lossless portion of the distributed structure in Fig. 4.2 becomes

$$\begin{bmatrix} 1 & 0 \\ C_n s & 1 \end{bmatrix} \begin{bmatrix} 1 & L_{n-1} s \\ 0 & 1 \end{bmatrix} \cdots \begin{bmatrix} 1 & L_2 s \\ 0 & 1 \end{bmatrix} \begin{bmatrix} 1 & 0 \\ C_1 s & 1 \end{bmatrix} . \qquad (4.20)$$

The matrix product (4.20) is the transmission matrix of the lossless part of the lumped network in Fig. 4.3. Assuming that all the connecting lines have very high characteristic impedances, all the shunt stubs have very low characteristic impedances, and all the line lengths are electrically short, the distributed network in Fig. 4.2 is approximately represented by the lumped network in Fig. 4.3. It follows that the poles of this lumped network are very close to the dominant transmission poles of the distributed structure.

To obtain an approximate solution of the system of equations (3.17), the lumped network in Fig. 4.3 is first synthesized for the prescribed set of transmission poles. With the values of

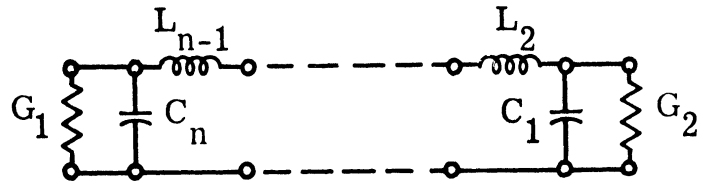

Fig. 4.3. Approximate lumped equivalent of the distributed network in Fig. 4.2 under the assumptions (4.18) and (4.19)

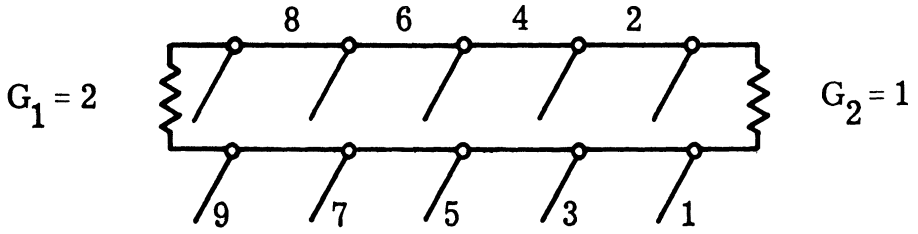

Fig. 4.4. A nine-element transmission line network

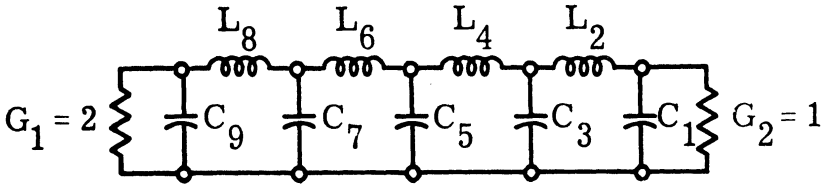

Fig. 4.5. The lumped network having 9th order Butterworth transmission poles. The element values are given in column I of Table I

inductances and capacitances thus determined, the lengths of the transmission line in Fig. 4.2 are found from the relations

$$\ell_j/v = \frac{L_j}{z_j} \quad , \quad j = 2, 4, 6, \ldots \tag{4.21}$$

$$\ell_j/v = C_j z_j \quad , \quad j = 1, 3, 5, \ldots \tag{4.22}$$

using, arbitrarily chosen, high values of characteristic impedances for connecting lines and low values of characteristic impedances for the stubs. For the examples that were worked out by the writer the values of 10 for the impedances of the connecting lines and 0.1 for the impedances of the stubs were used in determining the lengths of the lines. This gave a good approximate solution of the system of equations (3.17) when the terminations were of the order of unity.

As an example, consider the nine-element distributed structure in Fig. 4.4. It is required to find the approximate values of the lengths and the characteristic impedances [i.e., the approximate solution of the system (Eq. 3.17)] that realizes the ninth order Butterworth poles as the dominant transmission poles of this structure. The lumped network that has these prescribed transmission poles (and all the transmission zeros at infinity) is shown in Fig. 4.5.

The element values of the distributed network found by using Eq. 4. 21 and Eq. 4. 22 and the values of the inductances and capacitances for the lumped network are given in columns 1, 2, and 3 of Table I.

4. 4 Refinement of the Solution by Newton-Raphson Method

Once an approximate solution is obtained, this is refined to the desired degree of accuracy by the Newton-Raphson technique. For example, since the characteristic impedances are picked arbitrarily, the system of equations (4.4) is solved for the lengths of the lines. Thus the system of equations (4.5) becomes

$$f_i(\ell_1, \ldots, \ell_n) = 0 \ , \quad i = 1, 2, \ldots, n \ , \tag{4.23}$$

which is solved by the Newton-Raphson method starting from the approximate solution obtained in Section 4. 3. The result of applying this iteration method to the approximate solution of the nine-element distributed network in Fig. 4. 4 is given in column 4 of Table I.

4. 5 Realization of Characteristic Impedances Within a Prescribed Bound

In the initial solution of the system of equations (3.17) outlined in Section 4. 4, the characteristic impedances of the connecting

TABLE I

		Approximate Solution From Eq. 4.21 and Eq. 4.22	Solution Refined By Newton-Raphson Method
$C_1 = 3.0223$	$z_1 = 0.1$	$\ell_1/v = 0.30223$	0.3536814
$L_2 = 0.9579$	$z_2 = 10.0$	$\ell_2/v = 0.09579$	0.09084188
$C_3 = 3.7426$	$z_3 = 0.1$	$\ell_3/v = 0.37426$	0.3598843
$L_4 = 0.8565$	$z_4 = 10.0$	$\ell_4/v = 0.08565$	0.08299981
$C_5 = 2.9734$	$z_5 = 0.1$	$\ell_5/v = 0.29734$	0.2877055
$L_6 = 0.6046$	$z_6 = 10.0$	$\ell_6/v = 0.06046$	0.05878263
$C_7 = 1.7846$	$z_7 = 0.1$	$\ell_7/v = 0.17846$	0.1730608
$L_8 = 0.2735$	$z_8 = 10.0$	$\ell_8/v = 0.02735$	0.0265765
$C_9 = 0.3685$	$z_9 = 0.1$	$\ell_9/v = 0.03685$	0.03653245

The capacitances and the inductances are given respectively in farads and henrys. Characteristic impedances are in ohms and delays ℓ/v are in sec.

lines are impractically high and the characteristic impedances of the stubs are impractically low. However, this difficulty can be overcome. The characteristic impedances of the connecting lines can be gradually lowered and the characteristic impedances of the stubs can be gradually increased, and each time a change in the impedance (or impedances, in case more than one impedance is changed simultaneously) is made, the system (Eq. 3.17) is solved again to find new lengths for the line elements, thus preserving the prescribed dominant poles. The iteration for this new solution is initiated with the old solution as the starting point. The variation of line lengths necessary to maintain the prescribed Butterworth poles for the nine-element filter as the ratio of characteristic impedance of connecting lines to that of the stubs was decreased is graphically presented in Fig. 4.6.

Decreasing the ratio $z_{\text{connecting lines}}/z_{\text{stubs}}$ results, in general, in an increase of the line lengths. When all the connecting lines have characteristic impedance $3.5\ \Omega$ and all the stubs have characteristic impedance $0.3\ \Omega$, the line lengths that realize the Butterworth transmission poles were found to be

$$\begin{aligned} \ell_1/v &= 1.933716 \text{ Sec} & \ell_4/v &= 0.204529 \text{ Sec} \\ \ell_2/v &= 0.1635795 \text{ "} & \ell_5/v &= 0.7253457 \text{ "} \\ \ell_3/v &= 0.8731836 \text{ "} & \ell_6/v &= 0.1454346 \text{ "} \end{aligned} \tag{4.24}$$

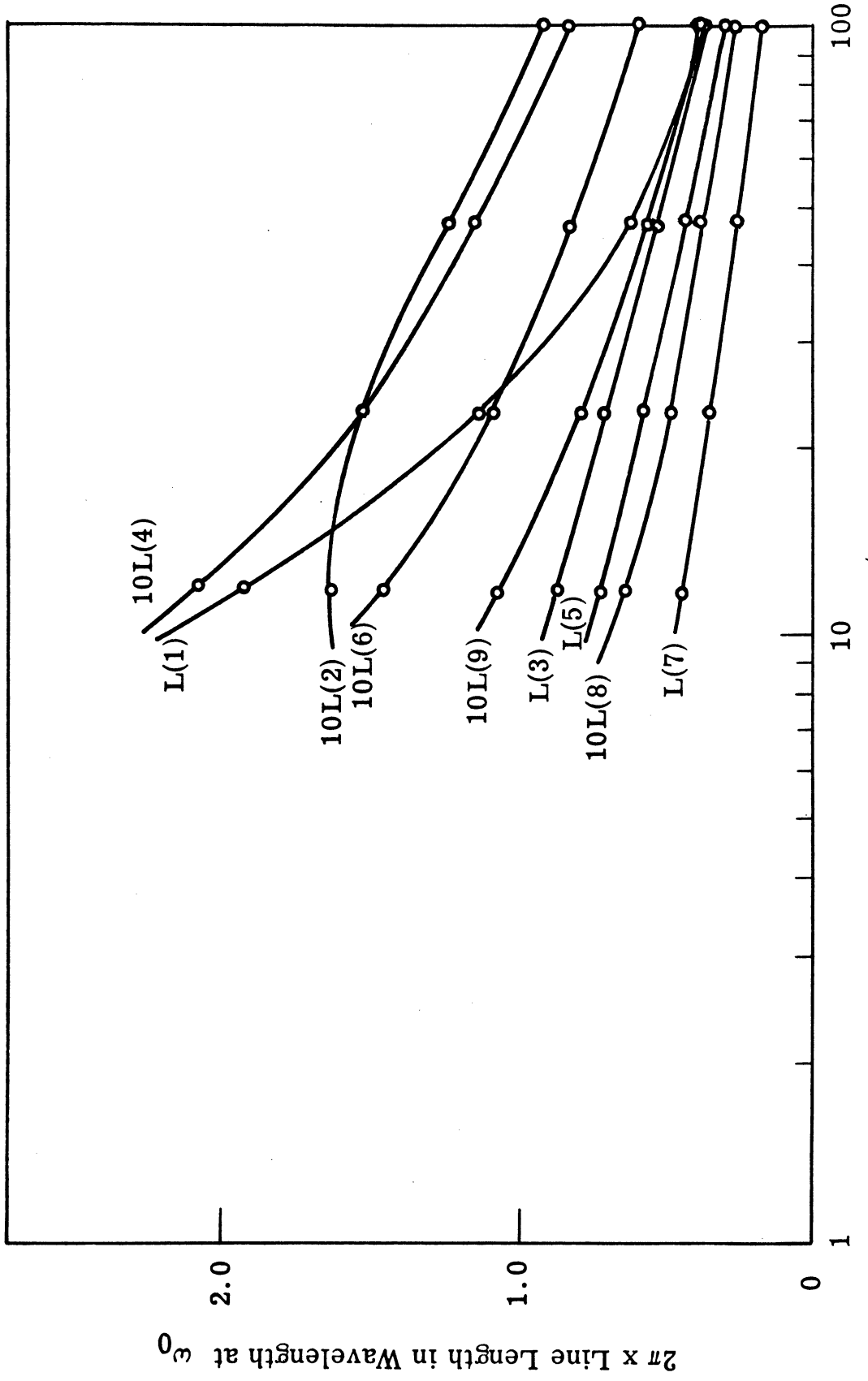

Fig. 4.6. Variation of line lengths necessary to maintain Butterworth poles (n = 9) as the ratio of $z_{\text{connecting line}}$ to z_{stub} is decreased

$$\ell_7/v = 0.4402347 \text{ Sec} \qquad \ell_9/v = 0.1061295 \text{ Sec} \quad . \qquad \text{(4.24 Cont.)}$$
$$\ell_8/v = 0.06485635 \text{ "}$$

The computer program written for changing the characteristic impedances has the capability of automatically bringing down the ratio $z_{\text{connecting line}}/z_{\text{stub}}$ while finding the lengths of the transmission lines needed to maintain the transmission poles at the prescribed positions. A typical run is initiated by specifying the prescribed poles, the approximate solution, and that the line lengths are to be varied.

This program (listed in Appendix II) has been successfully applied to distributed structures having 2, 3, 5, and 9 elements when the transmission poles were prescribed to be the Butterworth poles. In each of these cases, impedances of the connecting lines were each decreased from $10\ \Omega$ to $3.333\ \Omega$ and the impedances of the stubs were each increased from $0.1\ \Omega$ to $0.3\ \Omega$ automatically.

4.6 The Realization of Transmission Zeros

Equation 3.11 shows that for the transmission line structure being studied, the transmission zeros are given by

$$s = \pm \sqrt{-1}\ \frac{2k-1}{2}\ \frac{\pi}{\ell_i/v} \qquad (4.25)$$

$$i = 1, 3, 5, \ldots, n \ ,$$

$$k = 1, 2, 3, \ldots \ .$$

Thus the stubs alone are responsible for creating transmission zeros, their positions on the $j\omega$-axis being controlled by only the lengths of the stubs. Prescribed transmission zeros, generally, determine the lengths required for as many stubs as there are transmission zeros. The lengths of selected stubs can be gradually changed to the desired values to realize the transmission zeros. The resulting perturbations in the specified transmission poles are offset by adjusting any n of the remaining parameters, i. e., the impedances of all the lines and the lengths of the connecting lines, thus preserving the pole positions. The required adjustments are obtained from the solution of Eq. 3. 17 in the following way.

Let ℓ_s be the length of the stub being modified to $\ell_s + \Delta\ell_s$. Let the n parameters selected for adjustment to maintain the poles be designated $x_1, x_2, \ldots, x_n$. Then, from Eq. 3.17, one can write

$$f_i(x_1, x_2, \ldots, x_n; \ell_s) = 0 \ , \quad i = 1, 2, \ldots, n \ . \tag{4.26}$$

With ℓ_s changed to $\ell_s + \Delta\ell_s$, the new solution of Eq. 4. 26 denoted $x'_1, x'_2, \ldots, x'_n$, can be obtained from

$$f_i(x'_1, x'_2, \ldots, x'_n; \ell_s + \Delta\ell_s) = 0 \ , \quad i = 1, 2, \ldots, n \ . \tag{4.27}$$

Thus adjustments required in the n parameters $(x_i, i = 1, \ldots, n)$

to keep the pole locations unchanged in spite of a change in the length of a stub can be determined from Eq. 4. 27.

Chapter 5

Design of a Nine-Element Transmission Line Network

A design technique to achieve a prescribed set of transmission poles for a transmission line network has been illustrated in Section 4.5. In that example the values of a nine-element transmission line network were selected by iteration to realize the ninth order Butterworth poles as its dominant transmission poles with a specified ratio of characteristic impedances. For the transmission line network considered in this study (Fig. 3.1), finite transmission zeros always are present because of the open shunt stubs in the circuit. Increased lengths of stubs that accompany the decrease in the ratio of $z_{\text{connecting line}}/z_{\text{stub}}$ (Fig. 4.6) can bring the transmission zeros close enough to the origin of the s-plane to have considerable influence on the circuit response in the frequency range of interest. Such transmission zeros can be used to an advantage for improving stop band attenuation. However, to preserve the pass-band attenuation in the presence of transmission zeros, the dominant transmission poles must be moved to new locations. The purpose of this chapter is to present an illustrative design example of a nine-element filter where, in addition to achieving a prescribed set of dominant poles, several of the stub lengths are controlled to realize a set of specified transmission zeros.

5.1 Determination of Dominant Poles and Zeros

Consider the physical structure of the nine-element network in Fig. 4.4. If it is assumed that only the first transmission zeros produced by each of the stubs (1), (3), (5) and (7) are significant, eight finite transmission zeros must be considered. Choosing, for example, the passband response to be maximally flat as a design criterion, the square magnitude of the transfer impedance, according to the theory of Inverse Chebychev filters [54], can be written as

$$|z_{12}(j\omega)|^2 = \frac{[\omega^n T_n(\omega_a/\omega)]^2}{[\omega^n T_n(\omega_a/\omega)]^2 + \epsilon^2 [\omega^n T_n(\omega_a/\omega_c)]^2} , \qquad (5.1)$$

where

T_n = Chebychev polynomial of first kind of order n,

n = number of transmission poles in the lumped prototype,

ω_c = cut-off frequency where $|z_{12}|^2 = \frac{1}{1+\epsilon^2}$,

ω_a = start of stop band where $|z_{12}|^2 = \frac{1}{1+\epsilon^2 T_n^2(\omega_a/\omega_c)}$.

From Eq. 5.1, with $n = 9$, $\omega_a = 1.3$, $\omega_c = 1$ and $\epsilon = 1$, the transmission poles were found to be

$$\begin{aligned} s_{1,2} &= -0.112954 \pm j\, 1.002688 \\ s_{3,4} &= -0.374950 \pm j\, 1.016385 \end{aligned} \qquad (5.2)$$

$$
\begin{aligned}
s_{5,6} &= -0.749856 \pm j\,0.984713 \\
s_{7,8} &= -1.257454 \pm j\,0.716270 \\
s_{9} &= -1.565015 \pm j\,0.0
\end{aligned}
\qquad \text{(5.2 Cont.)}
$$

and the eight zeros were

$$\pm j\,1.320055\ ,\ \pm j\,1.501110\ ,\ \pm j\,2.02241\ ,\ \pm j\,3.800946 \qquad (5.3)$$

which were placed to produce equi-ripple response in the stop band of the prototype. It should be noted that because of the nondominant transmission poles and zeros of the distributed system, which are not accounted for in this lumped prototype, Eq. 5.2 represents approximations to the dominant transmission poles desired in the distributed system. Starting with the nine-element filter in Fig. 4.4 characterized by the element values (Eq. 4.24), which were selected for dominant Butterworth pole locations, the present design may be completed in, broadly speaking, two steps:

(i) Control the lengths of the stubs to realize the desired transmission zeros and at the same time, adjust other parameters of the circuit to preserve the Butterworth poles.

(ii) Make, in steps, appropriate changes in the parameters other than the stub lengths responsible for the desired zeros, to gradually move the dominant poles from the

Butterworth locations toward the desired poles until the poles of the network coincide with the desired ones.

5. 2 Realization of Zeros and Poles

The lengths (ℓ/v, to be exact) of the stubs required to produce the desired transmission zeros (Eq. 5. 3) are calculated to be 1. 19 sec, 1. 047 sec, 0. 775 sec, 0. 4135 sec. A designer has some degree of freedom in selecting one particular stub from the several at his disposal to realize a zero. For example, assuming the realization of the zero at $\pm$ j 1. 320055 (desired length 1. 19 sec) under consideration, the length of any one of the stubs (1), (3), (5) or (7) may be modified to 1. 19 sec, thus achieving the desired zero at $\pm$ j 1. 320055. Our procedure was to take each stub in the network realizing the Butterworth poles and a specified $z_{\text{connecting line}}/z_{\text{stub}}$ and examine all the desired lengths to pick the one which was closest to the length of the stub. The length of this stub was then gradually modified to the desired dimension. Thus, to attain the desired transmission zeros given in Eq. 5. 3, the lengths of the stubs (1), (3), (5), (7) were changed from their values 1. 933716, 0. 8731836, 0. 7253457, 0. 4402347 (in Eq. 4. 24) to respectively 1. 19, 1. 047, 0. 775, 0. 4135. While changing the lengths of these stubs appropriate changes could be made in any nine of the remaining variables [nine characteristic impedances, the lengths of the four connecting lines and stub (9)] to preserve

the Butterworth poles. In the computer program listed in Appendix II, any n of the 2n parameters defining the system of Eq. 3.17 can be kept fixed, while the iteration is carried out on the remaining n parameters. In this particular example, while the lengths of the stubs were changed to desired dimensions, iteration was performed on $z_1, \ell_2, z_3, \ell_4, z_5, \ell_6, z_7, \ell_8, z_9$, i.e., these were the variables designated $x_1, x_2, \ldots, x_9$ in Eq. 4.5. The element values that achieve the transmission zeros (Eq. 5.3) and maintains the Butterworth poles were found to be

$$
\begin{aligned}
\ell_1/v &= 1.1900000 \text{ Sec} & Z_1 &= 0.1930863\ \Omega \\
\ell_2/v &= 0.2196553 \text{ "} & Z_2 &= 3.5000000 \text{ "} \\
\ell_3/v &= 1.0470000 \text{ "} & Z_3 &= 0.3901989 \text{ "} \\
\ell_4/v &= 0.1899826 \text{ "} & Z_4 &= 3.5000000 \text{ "} \\
\ell_5/v &= 0.7750000 \text{ "} & Z_5 &= 0.3310432 \text{ "} \\
\ell_6/v &= 0.1429601 \text{ "} & Z_6 &= 3.5000000 \text{ "} \\
\ell_7/v &= 0.4135000 \text{ "} & Z_7 &= 0.2752242 \text{ "} \\
\ell_8/v &= 0.06693098 \text{ "} & Z_8 &= 3.5000000 \text{ "} \\
\ell_9/v &= 0.1060000 \text{ "} & Z_9 &= 0.2968349 \text{ "}
\end{aligned}
\qquad (5.4)
$$

Now consider shifting the poles of the transmission line circuit from the Butterworth positions to the desired locations. Observe that in the system of equations (3.17), the poles also enter as parameters. Therefore, just as the stub lengths were modified to

desired dimensions, the pole location can be gradually moved to the desired positions. Every time a step toward the desired poles is made element values compatible with the new poles are found by solving Eq. 3.17 anew. While this is accomplished, the lengths of the stubs responsible for the desired zeros are not allowed to change. Let n of remaining parameters, which will be treated as iteration variables during one step of the pole movement, be designated $x_1, x_2, \ldots, x_n$. The system of equations (3.17) can be written as

$$f_i(x_1, x_2, \ldots, x_n; s_k) = 0 \qquad (5.5)$$

$$i = 1, 2, \ldots, n$$

$$k = i \quad \text{if } i \text{ odd}$$

$$k = i - 1 \quad \text{if } i \text{ even}.$$

Let

$$s_{ke} \quad , \quad s_{kd}$$

where $k = 1, 3, \ldots, n$ if n odd

and $k = 1, 3, \ldots, n - 1$ if n even

denote respectively the existing and the desired pole locations. Choosing to move along the shortest path while shifting the poles from the existing to the desired location, the poles in an intermediate position are

$$s_k = s_{ke} + \frac{m}{M}(s_{kd} - s_{ke}) \quad , \qquad (5.6)$$

$$k = 1, 3, \ldots$$

where m and M are positive and may be selected as integers ($m \leq M$). The relative magnitudes of m and M depend on the size of the step one wishes to take. When m equals or nearly equals M, the desired pole locations have been achieved. The results of iteration as the poles were being shifted according to Eq. 5.6 are shown in Table II. Finally, the element values given in Part 6 of Table II achieve simultaneously the transmission zeros (Eq. 5.3) and pole locations mentioned in that part of the table. Transmission pole locations realized are within three percent of the desired ones. The attenuation characteristic of the network characterized by the element values in Part 6 of Table II is shown by the dashed curve in Fig. 5.1.

The above example illustrates the design of a distributed network from a lumped design that has eight finite transmission zeros and nine transmission poles. The distributed network which was designed to have Butterworth poles as its dominant transmission poles was used as the starting point and following the realization of transmission zeros, the transmission poles were shifted from the Butterworth locations to the desired locations. An alternate

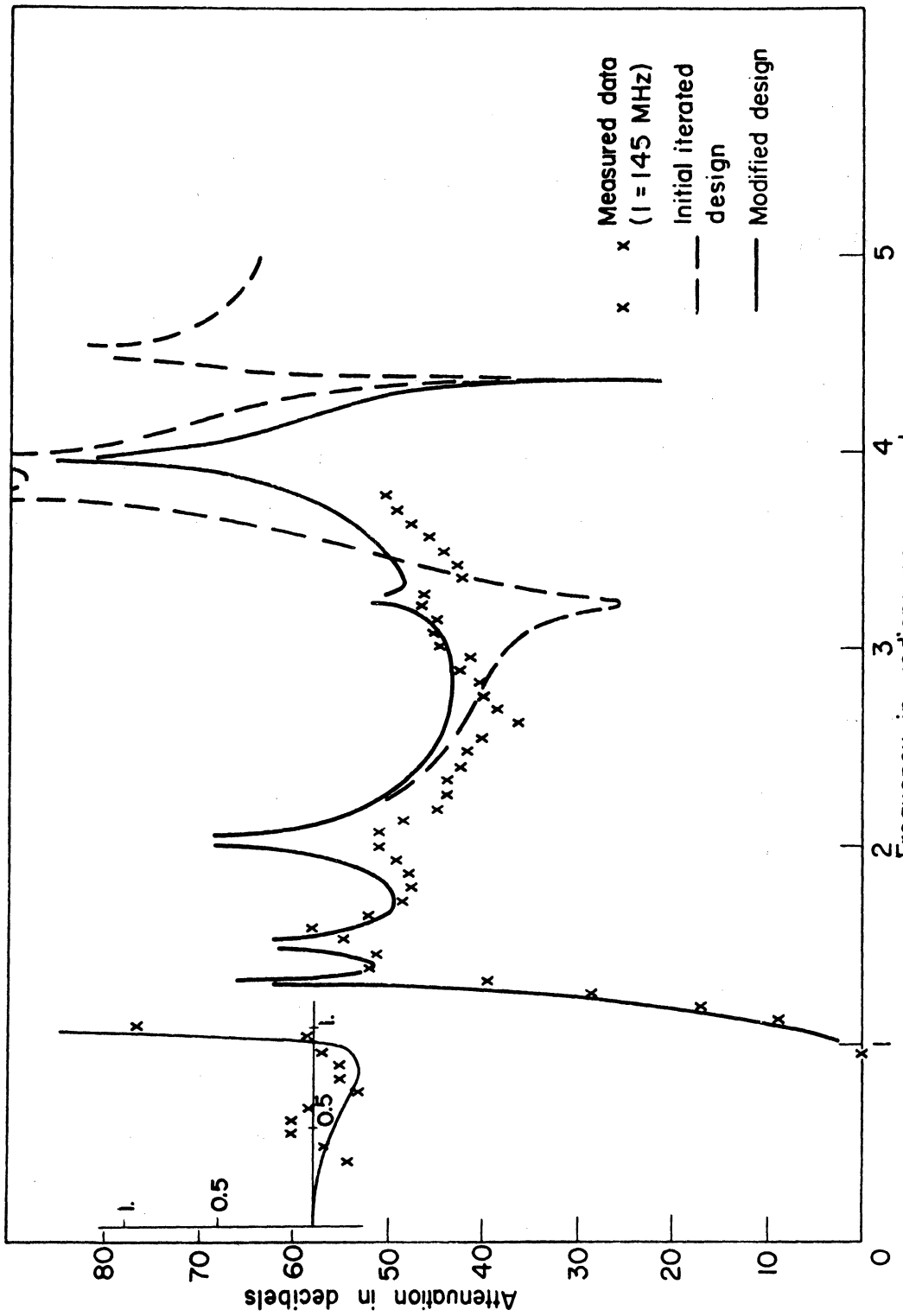

Fig. 5.1. The calculated and measured attenuation of the designed nine-element transmission line filter

TABLE II

Those parameters that were regarded as iteration variables are marked with asterisk.

Part	New Pole Locations	ℓ_i/v And z_i That Achieve The New Poles		i
		ℓ_i/v	z_i	
1	-0.161509 ± j 0.988384	1.19	0.2379369*	1
	-0.474990 ± j 0.896094	0.2046626*	3.5	2
	-0.762807 ± j 0.711173	1.047	0.3960831*	3
	-1.003245 ± j 0.416870	0.186637*	3.5	4
	-1.113003 ± j 0.0	0.775	0.3396033*	5
		0.1389825*	3.5	6
		0.4135	0.2831522*	7
		0.06494685*	3.5	8
		0.106	0.303761*	9
2	-0.149371 ± j 0.991960	1.19	0.3014739*	1
	-0.449980 ± j 0.926169	0.1966559*	3.5	2
	-0.759569 ± j 0.779558	1.047	0.4008054*	3
	-1.066797 ± j 0.491720	0.1836065*	3.5	4
	-1.226006 ± j 0.0	0.775	0.3479070*	5
		0.1353706*	3.5	6
		0.4135	0.2907403*	7
		0.06314698*	3.5	8
		0.106	0.3102937*	9

TABLE II (Cont.)

Part	New Pole Locations	ℓ_i/v And z_i That Achieve The New Poles		i
		ℓ_i/v	z_i	
	-0.137232 ± j 0.995536	1.19	0.3998215*	1
	-0.424970 ± j 0.956241	0.1975815*	3.5	2
	-0.756331 ± j 0.847943	1.047	0.4055608*	3
	-1.130349 ± j 0.566570	0.1813539*	3.5	4
3	-1.339009 ± j 0.0	0.775	0.3552969*	5
		0.1323241*	3.5	6
		0.4135	0.2975375*	7
		0.06160388*	3.5	8
		0.106	0.3161074*	9
	-0.125093 ± j 0.999112	1.19	0.5865872*	1
	-0.399960 ± j 0.986313	0.2152370*	3.5	2
	-0.753094 ± j 0.916328	1.047	0.4105986*	3
	-1.193902 ± j 0.641420	0.1814096*	3.5	4
4	-1.452012 ± j 0.0	0.775	0.3594772*	5
		0.1305629*	3.5	6
		0.4135	0.3020097*	7
		0.06059191	3.5	8
		0.106	0.3200997*	9

TABLE II (Cont.)

Part	New Pole Locations	ℓ_i/v And z_i That Achieve The New Poles		
		ℓ_i/v	z_i	i
5	-0.118417 ± j 1.001079	1.19	0.8554185*	1
	-0.386204 ± j 1.002853	0.250467*	3.5	2
	-0.751313 ± j 0.95394	1.047	0.4096821*	3
	-1.228856 ± j 0.682587	0.1863467*	3.5	4
	-1.514164 ± j 0.0	0.775	0.3545361*	5
		0.1320657*	3.5	6
		0.4135	0.2996928*	7
		0.06099037*	3.5	8
		0.106	0.3187789*	9
6	-0.116232 ± j 1.001723	1.19	1.119369*	1
	-0.381702 ± j 1.008266	0.250467	3.931361*	2
	-0.750730 ± j 0.966249	1.047	0.3983251*	3
	-1.240295 ± j 0.696060	0.1863467	3.643610*	4
	-1.534504 ± j 0.0	0.775	0.3439001*	5
		0.1320657	3.587569*	6
		0.4135	0.2936443*	7
		0.06099037	3.564882*	8
		0.106	0.3144931*	9

approach would be to design the lumped network having the desired transmission poles and all the zeros at infinity. Then, following the procedure outlined in Sections 4. 3, 4. 4 and 4. 5 a distributed network having the desired transmission poles could be synthesized. The lengths of the stubs would then be adjusted for prescribed transmission zeros. The block-diagram in Fig. 5. 2 summarizes the synthesis procedure.

5. 3 Modified Design

The transmission delay caused by the connecting lines combined with the repetitive nature of the transmission zeros produced by the shunt stubs produces transmission poles in addition to the dominant poles which are being controlled. The dip in the attenuation near $\omega = 3.25$ rdn/sec is caused by such a non-dominant pole. It is sometimes possible to approximately nullify the undesirable effect of a non-dominant pole by placing opposite it a transmission zero on the real frequency axis. A general strategy for accomplishing this can be formulated as a nonlinear programming problem. This nonlinear programming problem may then be approximately solved by successive linearization; the linear problem thus obtained at each step being solved by simplex algorithm.[1] For this

[1] See Chapter 7.

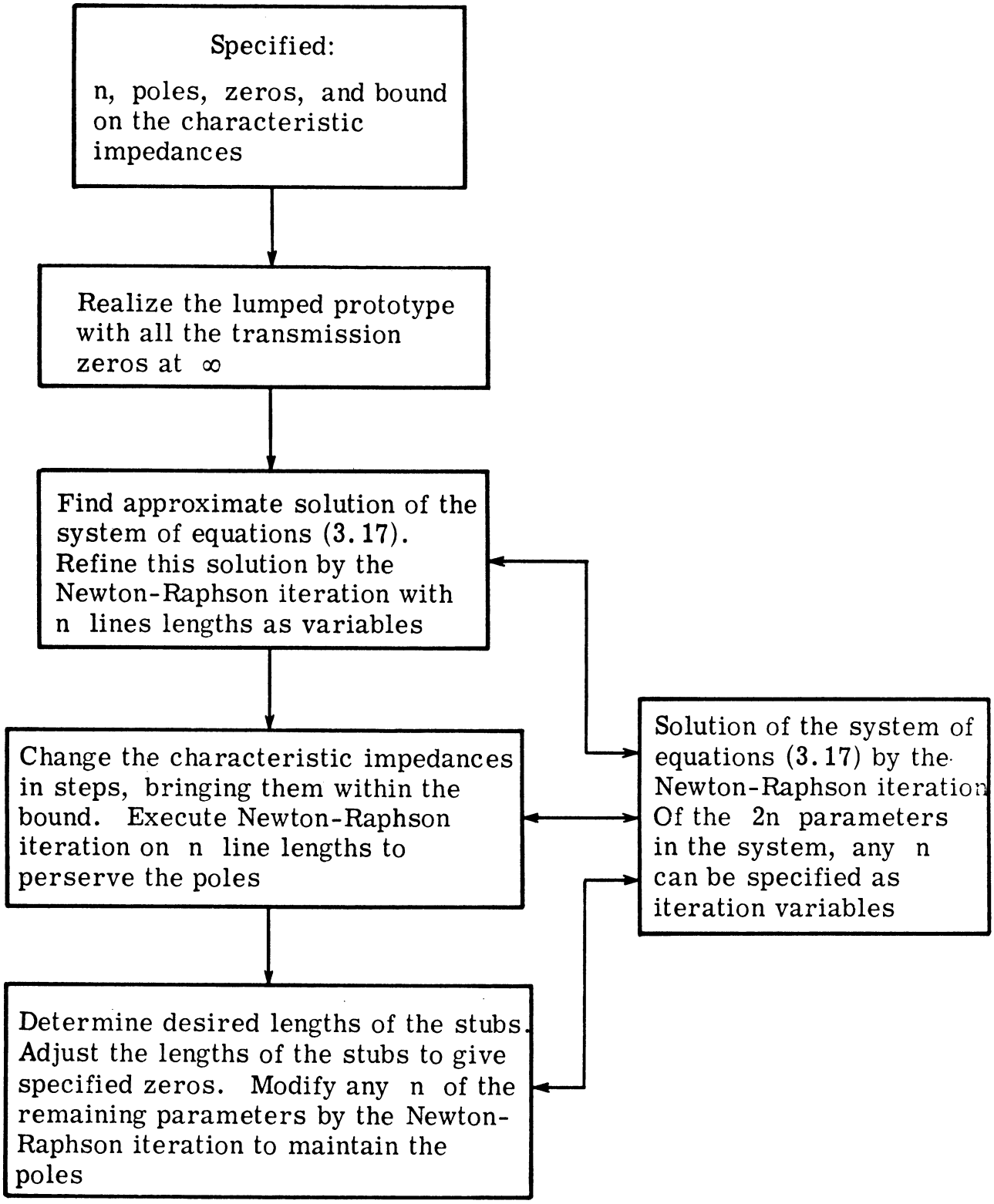

Fig. 5.2. The synthesis procedure outlined in Sections 4.3-4.6 is summarized above

particular example, it is observed that stub (1), in addition to creating a desired transmission zero at j 1.32, places a second transmission zero at j 3.96. This latter zero is very close to the desired transmission zero at j 3.800 produced by stub (7). Stub (7) can, therefore, be utilized elsewhere. When the length of the stub (7) was adjusted to place a transmission zero at j 3.25, the changed element values were found to be

$$
\begin{aligned}
\ell_1/v &= 1.19 \quad \text{Sec} & z_1 &= 0.9373091\ \Omega \\
\ell_2/v &= 0.250467 \quad " & z_2 &= 3.609804\ " \\
\ell_3/v &= 1.047 \quad " & z_3 &= 0.4040285\ " \\
\ell_4/v &= 0.1863467 \quad " & z_4 &= 3.544972\ " \\
\ell_5/v &= 0.775 \quad " & z_5 &= 0.3478956\ " \\
\ell_6/v &= 0.1320657 \quad " & z_6 &= 3.51709\ " \\
\ell_7/v &= 0.4835 \quad " & z_7 &= 0.3755778\ " \\
\ell_8/v &= 0.1 \quad " & z_8 &= 1.976803\ " \\
\ell_9/v &= 0.106 \quad " & z_9 &= 0.3387325\ "
\end{aligned}
\qquad (5.7)
$$

The attenuation of the filter after this adjustment is shown by the solid curve in Fig. 5.1.

5.4 Construction

The filter having the modified design was constructed in strip lines. A few details which might be of interest are given here. The

frequency and impedance normalizations were with respect to 145 MHz and 25 ohm respectively. The velocity of propagation in air was assumed $v = 10^9 \times 11.80283$ in/sec and dielectric constant of circuit board material $\epsilon = 2.32$. Using double stubs at each junction, the characteristic impedances and the effective lengths of the transmission line elements were computed to be

ℓ_1 =	10.121424 inch	Z_1 =	46.865 ohm
ℓ_2 =	2.130322 "	Z_2 =	90.245 "
ℓ_3 =	8.905152 "	Z_3 =	20.201 "
ℓ_4 =	1.584953 "	Z_4 =	88.624 "
ℓ_5 =	6.591684 "	Z_5 =	17.394 "
ℓ_6 =	1.123271 "	Z_6 =	87.927 "
ℓ_7 =	4.112360 "	Z_7 =	18.778 "
ℓ_8 =	0.850540 "	Z_8 =	49.420 "
ℓ_9 =	0.901572 "	Z_9 =	16.936 "

The centre-to-centre physical length of a connecting line between two stubs differs from its electrically effective length. Corrections to be added to the effective lengths to determine the physical lengths of the connecting lines were found from curves for T-junctions in [55]. These corrections were also verified from mathematical expressions for the parameters of the equivalent circuit of a T-junction given by Altschuler and Oliner [56]. The

centre-to-centre physical length of the connecting lines were thus found to be

$$\ell_2 = 2.512 \text{ inch}$$
$$\ell_4 = 2.190 \text{ "}$$
$$\ell_6 = 1.749 \text{ "}$$
$$\ell_8 = 1.407 \text{ "}$$

The physical dimensions of the filter are shown in Fig. 5.3, which has not been drawn to scale. The circuit was etched on 1/8-inch polyguide circuit board deposited with 2 oz. copper.

The measured attenuation of the filter is indicated by crosses in Fig. 5.1, along with the computed attenuation presented by the solid curve.

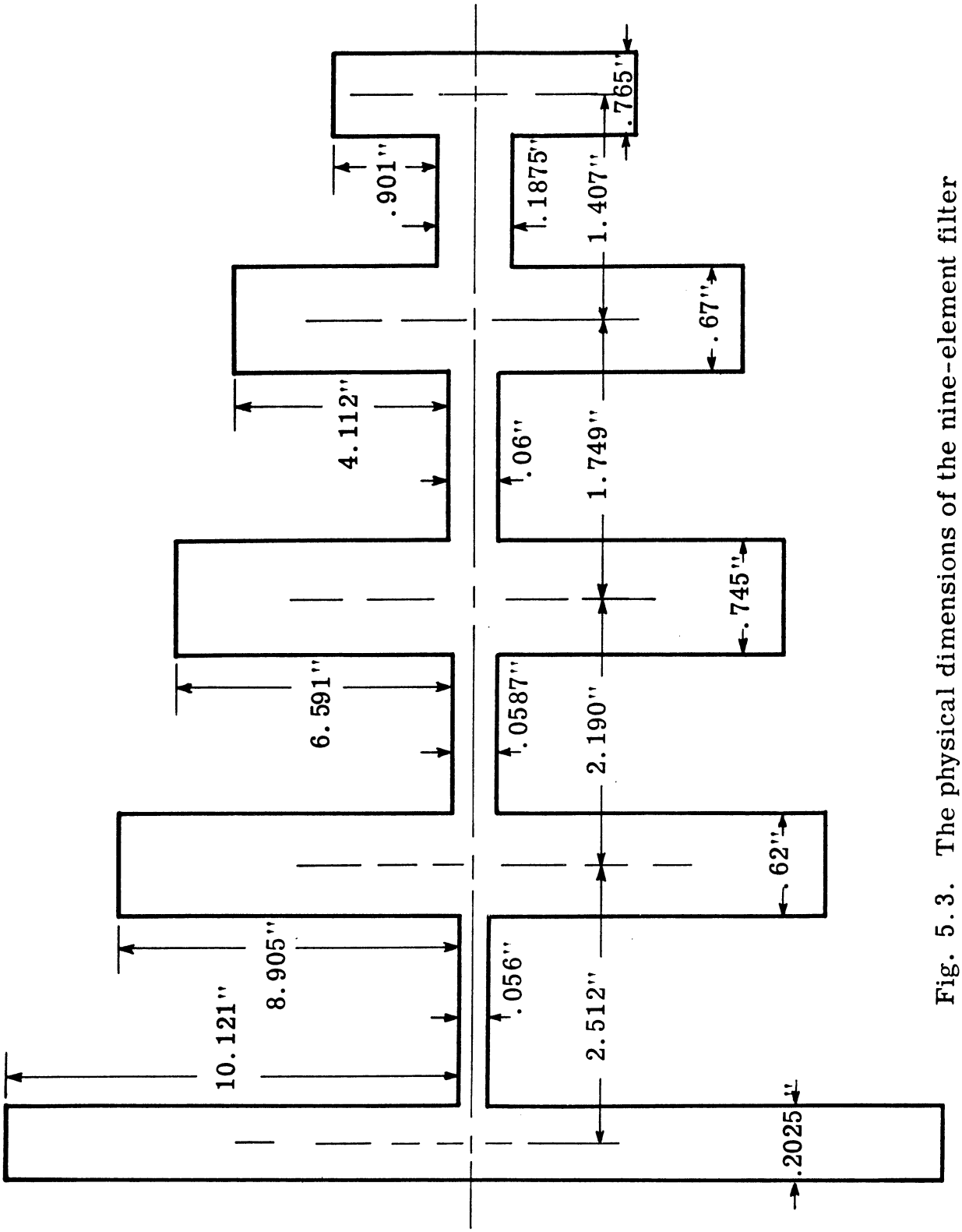

Fig. 5.3. The physical dimensions of the nine-element filter

Chapter 6

Nondominant Poles

It has been found in the last chapter that for a distributed circuit

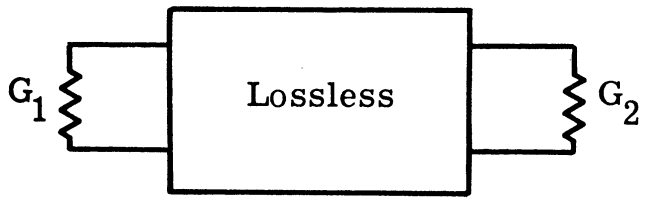

Fig. 6.1. A doubly-terminated lossless 2-port

It then follows that

$$\begin{bmatrix} A_T & B_T \\ C_T & D_T \end{bmatrix} = \begin{bmatrix} 1 & 0 \\ G_1 & 1 \end{bmatrix} \begin{bmatrix} A_t & B_t \\ C_t & D_t \end{bmatrix} \begin{bmatrix} 1 & 0 \\ G_2 & 1 \end{bmatrix}, \qquad (6.1)$$

where

$$\begin{bmatrix} A_t & B_t \\ C_t & D_t \end{bmatrix}$$

represents the general circuit parameter matrix of the lossless part of the network in Fig. 6.1. When the lossless network is composed of open shunt stubs alternating with connecting lines, this matrix as established in Section 3.1 is given by

$$\begin{bmatrix} A_t & B_t \\ C_t & D_t \end{bmatrix} = \frac{1}{\prod_{i=1}^{n} (z_i) \prod_{j} \cosh \Phi_j} \begin{bmatrix} A_m & B_m \\ C_m & D_m \end{bmatrix}, \qquad (6.2)$$

where

$$\Phi_j = \frac{s\ell_j}{v},$$

n = number of transmission line elements,

$\prod_j$ = indicates that the product is taken over the elements which are stubs

and

$$\begin{bmatrix} A_m & B_m \\ C_m & D_m \end{bmatrix} = \begin{bmatrix} \sum_{i=1}^{2^{n-1}} a_i \cosh(\theta_i^n s) & \sum_{i=1}^{2^{n-1}} b_i \sinh(\theta_i^n s) \\ \sum_{i=1}^{2^{n-1}} c_i \sinh(\theta_i^n s) & \sum_{i=1}^{2^{n-1}} d_i \cosh(\theta_i^n s) \end{bmatrix} \tag{6.3}$$

is a modified, all-zero GCP matrix (sometimes abbreviated MGCP matrix) having exactly the same zeros as

$$\begin{bmatrix} A_t & B_t \\ C_t & D_t \end{bmatrix}$$

and, as an examination of Eq. 6.2 and Eq. 3.3 reveals, can be directly found as the product of a chain of matrices. In this chain each connecting line is represented by

$$\begin{bmatrix} z_j \cosh \Phi_j & z_j^2 \sinh \Phi_j \\ \sinh \Phi_j & z_j \cosh \Phi_j \end{bmatrix}, \quad j = 2, 4, \ldots \tag{6.4}$$

and each open stub, by

$$\begin{bmatrix} z_j \cosh \Phi_j & 0 \\ \sinh \Phi_j & z_j \cosh \Phi_j \end{bmatrix}, \quad j = 1, 3, 5, \ldots \quad . \tag{6.5}$$

Now, from Eq. 6.1 C_T is given by

$$C_T = G_1 A_t + G_2 D_t + G_1 G_2 B_t + C_t \quad .$$

The transfer impedance, $z_{12} = \frac{1}{C_T}$, can be expressed, due to Eq. 6.2, as

$$z_{12} = \frac{\prod_{i=1}^{n} (z_i) \prod_{j} \cosh (\Phi_j)}{G_1 A_m + G_2 D_m + G_1 G_2 B_m + C_m} \quad . \tag{6.6}$$

Transmission Zeros. Transmission zeros are zeros of the numerator of Eq. 6.6 and thus satisfy

$$\cosh \frac{s\ell_j}{v} = 0 \quad , \tag{6.7}$$

i.e., $$s = \pm \sqrt{-1}\,(2k - 1)\frac{\pi v}{2\ell_j} \quad , \tag{6.8}$$

where ℓ_j designates the length of any open shunt stub and k is an integer. Expression (6.8) accounts for all the transmission zeros, since the denominator of Eq. 6.6 contains only sums and products of sinh and cosh terms and therefore is finite throughout the finite complex frequency plane. Equation 6.8 establishes that the transmission zeros are all on the $j\omega$-axis and are due to the stubs alone.

Each stub creates an infinite number of equally spaced zeros on the $j\omega$-axis at those frequencies at which the length of the stub is one quarterwave long or odd multiples thereof.

6.2 Transmission Poles and the Zeros of Modified GCP

Expression (6.6) shows that the transmission poles are the roots of

$$(G_1 A_m + G_2 D_m) + K(G_1 G_2 + C_m) = 0 \ , \tag{6.9}$$

for $K = 1$. Each of the roots of Eq. 6.9 starts at a zero of $G_1 A_m + G_2 D_m$ when $K = 0$, moves as K increases, and finally coincides with a zero of $G_1 G_2 B_m + C_m$ when $K = \infty$. Study of the zeros of $G_1 A_m + G_2 D_m$ and $G_1 G_2 B_m + C_m$ is thus at the heart of the study of the transmission poles. Separation of $G_1 A_m + G_2 D_m + G_1 G_2 B_m + C_m$ into two parts, as indicated by the parenthesis in Eq. 6.9 is deliberate, since, as will be shown later in this section, the two parts $G_1 A_m + G_2 D_m$ and $G_1 G_2 B_m + C_m$ have their zeros all on the real frequency axis and the zeros of $G_1 A_m + G_2 D_m$ alternate with those of $G_1 G_2 B_m + C_m$. We begin this section with an investigation into the location and distribution of the zeros of $G_1 G_2 B_m + C_m$ and $G_1 A_m + G_2 D_m$ and their locations.

Observe that A_m/C_m, D_m/C_m, D_m/B_m, A_m/B_m are all reactance functions. An important property of the reactance functions

is that their poles and zeros alternate on the real frequency axis. This fact alone results in the following conclusions regarding the relative distribution of the zeros of A_m, B_m, C_m and D_m.

(1) The zeros of A_m and D_m alternate with the zeros of B_m and C_m.

(2) Of the two consecutive zeros of A_m and D_m either may appear before the other.

(3) Of the two consecutive zeros of B_m and C_m either may appear before the other.

Let $A_m(j\omega) = A_m(\omega)$, $D_m(j\omega) = D_m(\omega)$, $C_m(j\omega) = jC_m(\omega)$, $B_m(j\omega) = jB_m(\omega)$. Direct substitution of $s = 0$ in Eqs. 3.1 and 3.2 shows that GCP matrices for both a connecting line and an open shunt stub are unity matrices at the origin of the complex-frequency plain. This together with Eq. 6.2 gives

$$A_m(\omega)\Big|_{\omega = 0} = \prod_{i=1}^{n} z_i \ , \tag{6.10}$$

and

$$D_m(\omega)\Big|_{\omega = 0} = \prod_{i=1}^{n} z_i \ . \tag{6.11}$$

Since $A_m(\omega)$ and $D_m(\omega)$ are cosine series, their slopes at $\omega = 0$ are zero, i. e.,

$$\frac{d}{d\omega} A_m(\omega)\Big|_{\omega = 0} = 0 \qquad (6.12)$$

$$\frac{d}{d\omega} D_m(\omega)\Big|_{\omega = 0} = 0 \quad . \qquad (6.13)$$

$B_m(\omega)$ and $C_m(\omega)$ are sine series and, therefore have zero magnitude at dc. $B_m(\omega)/A_m(\omega)$ being a reactance function, its derivative,

$$\frac{d}{d\omega}\frac{B_m(\omega)}{A_m(\omega)} = \frac{A_m(\omega)\cdot\frac{d}{d\omega}B_m(\omega) - B_m(\omega)\cdot\frac{d}{d\omega}A_m(\omega)}{[A_m(\omega)]^2}$$

is always positive. This together with Eqs. 6.12 and 6.10 forces $\frac{d}{d\omega} B_m(\omega)$ to be positive at $\omega = 0$. Similarly, $\frac{dC(\omega)}{d\omega}\Big|_{\omega = 0}$ is positive. Typically, therefore, $A_m(\omega)$, $B_m(\omega)$, $C_m(\omega)$ and $D_m(\omega)$ have graphical representation as illustrated in Fig. 6.2(a).

6.2.1 $j\omega$-Axis Zeros of $G_1 A_m + G_2 D_m$. Since G_1 and G_2 are positive, at a frequency where $G_1 A_m + G_2 D_m = 0$, A_m and D_m have opposite signs. Examination of the graphs of A_m and D_m in Fig. 6.2(a) reveals that this can only happen between two consecutive zeros of A_m and D_m, not separated by any zeros of B_m or C_m. Therefore only one zero of $G_1 A_m + G_2 D_m$ will lie on the portion of $j\omega$-axis bounded by one zero of A_m and one zero of D_m, which are not separated by any zeros of B_m and C_m.

6.2.2 jω-Axis Zeros of $G_1G_2B_m + C_m$. Proceeding exactly as in the case of the jω-axis zeros of $G_1A_m + G_2D_m$, it can be concluded that one zero of $G_1G_2B_m + C_m$ occurs on the portion of the jω-axis bounded by two consecutive zeros of B_m and C_m, not separated by any zeros of A_m or D_m.

For the typical curves of Fig. 6.2(a), the intervals on the jω-axis where the zeros of $G_1A_m + G_2D_m$ and $G_1G_2B_m + C_m$ may lie, are shown in Fig. 6.2(b). Since the zeros A_m and D_m alternate with those of B_m and C_m, the zeros of $G_1A_m + G_2D_m$ alternate with those of $G_1G_2B_m + C_m$.

6.2.3 jω-Axis Zeros of $G_1A_m + G_2D_m$ and $G_1G_2B_m + C_m$ Are Their Only Zeros. Consider the function

$$\frac{G_1A_m + G_2D_m}{G_1G_2B_m + C_m} \tag{6.14}$$

which, with a little manipulation, can be written as

$$\frac{G_1A_m + G_2D_m}{G_1G_2B_m + C_m} = \frac{1}{\dfrac{1}{\dfrac{A_m}{G_2B_m} + \dfrac{D_m}{G_1B_m}} + \dfrac{1}{\dfrac{G_1A_m}{C_m} + \dfrac{G_2D_m}{C_m}}} \quad . \tag{6.15}$$

Since A_m/B_m, D_m/B_m, A_m/C_m are all reactance functions, it follows from Eq. 6.15 that so is $(G_1A_m + G_2D_m)/(G_1G_2B_m + C_m)$. Therefore, its zeros must all lie on the jω-axis.

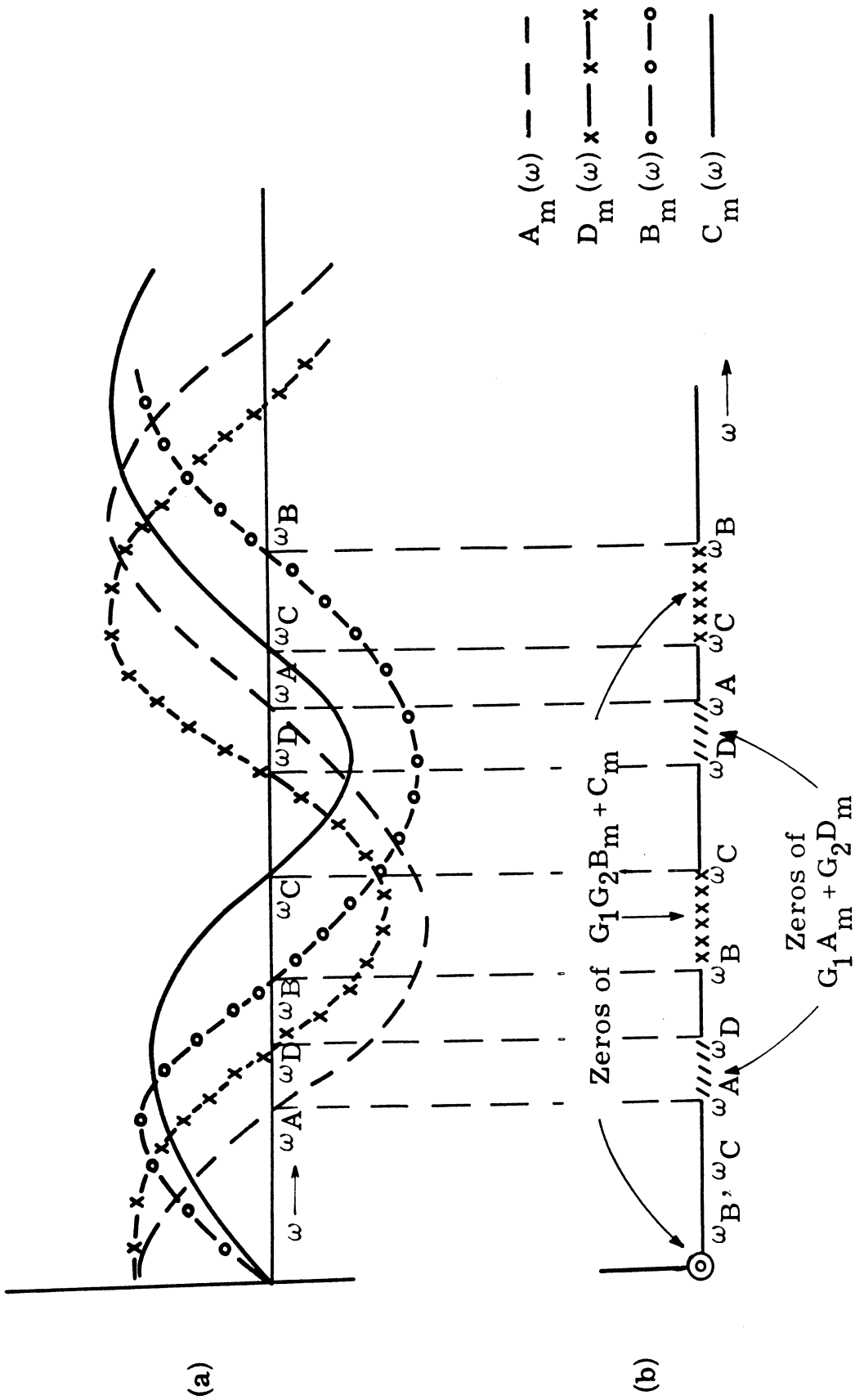

Fig. 6.2. (a) Typical curves of modified general circuit parameters A_m, B_m, C_m and D_m. Their zeros are designated ω_A, ω_B, ω_C and ω_D
(b) Indicates the sections of $j\omega$-axis where the zeros of $G_1A_m + G_2D_m$ and $G_1G_2B_m + C_m$ occur for the curves in (a)

We have already seen that a transmission pole can be associated with one zero of $G_1G_2B_m + C_m$ and one of $G_1A_m + G_2D_m$, each of which, in turn, is produced by two zeros: one each from B_m and C_m for $G_1G_2B_m + C_m$, and one each from A_m and D_m for $G_1A_m + G_2D_m$. Thus, each transmission pole is created by four zeros, one each from A_m, B_m, C_m and D_m.

6.3 No Repetition Interval is Free of Zeros of A_m, B_m, C_m, D_m

Let ω_r be the smallest radian frequency where $\cos \ell\omega_r/v = 0$, ℓ being the length of a component transmission line. Let a repetition interval of this line be defined as the portion of real frequency axis bounded by two consecutive frequencies which are odd multiples of ω_r or $-\omega_r$. The interval between $-\omega_r$ and ω_r will be called principal interval of this line. Figure 6.3 illustrates the repetition intervals of a transmission line element of length ℓ. The purpose of this section is to prove that in each repetition interval of every transmission line that makes up the network in Fig. 3.1, at least one zero of each modified general circuit parameter will appear.

Consider the network in Fig. 6.4 where a connecting line of length ℓ ($\Phi \equiv \frac{s\ell}{v}$) joins two lossless networks each enclosed in a box and mathematically described by their respective MGCP matrices,

$$\begin{bmatrix} A_{m_1} & B_{m_1} \\ C_{m_1} & D_{m_1} \end{bmatrix}$$

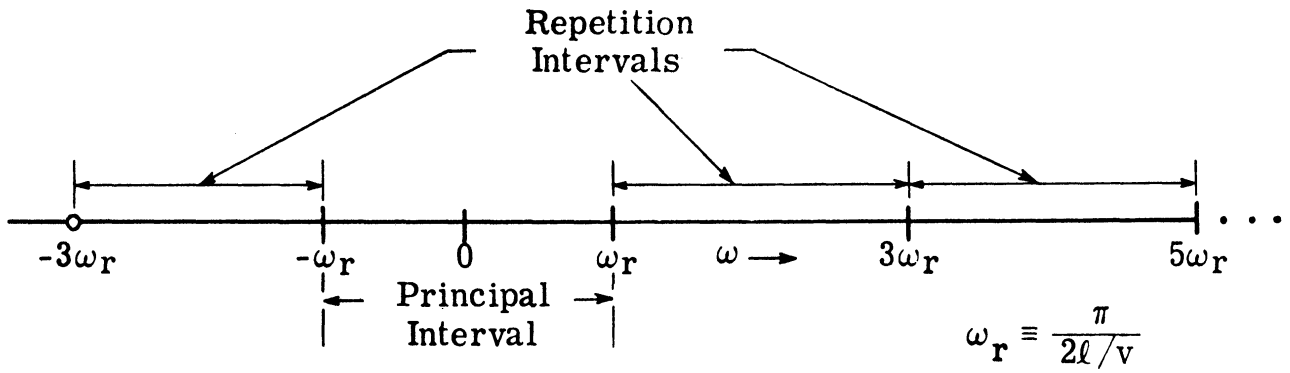

Fig. 6.3. Repetition intervals and principal interval of a transmission line of length ℓ , $\omega_r \equiv \frac{\pi}{2\ell/v}$

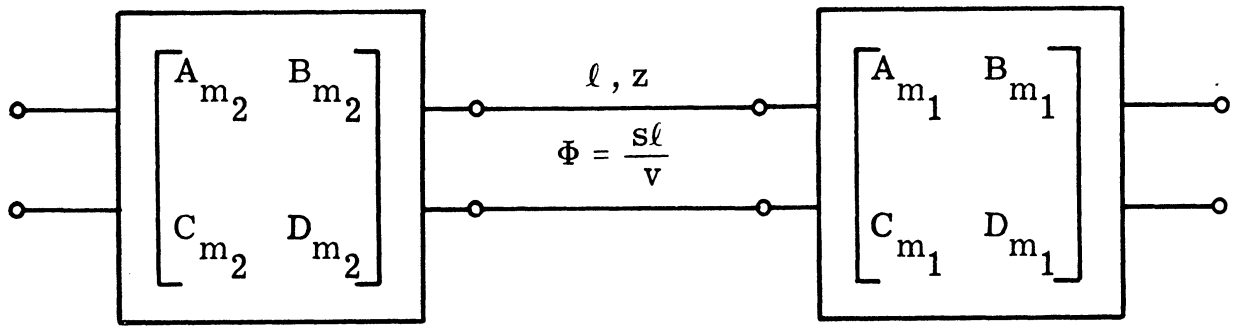

Fig. 6.4. Two lossless transmission line 2-ports joined by a connecting line

and

$$\begin{bmatrix} A_{m_2} & B_{m_2} \\ C_{m_2} & D_{m_2} \end{bmatrix}.$$

The MGCP matrix,

$$\begin{bmatrix} A_m & B_m \\ C_m & D_m \end{bmatrix}$$

of the total configuration is then

$$\begin{bmatrix} A_m & B_m \\ C_m & D_m \end{bmatrix} = \begin{bmatrix} A_{m_2} & B_{m_2} \\ C_{m_2} & D_{m_2} \end{bmatrix} \begin{bmatrix} z\cosh\Phi & z^2\sinh\Phi \\ \sinh\Phi & z\cosh\Phi \end{bmatrix} \begin{bmatrix} A_{m_1} & B_{m_1} \\ C_{m_1} & D_{m_1} \end{bmatrix}. \tag{6.16}$$

Multiplication of the right hand side of Eq. 6.16 gives

$$\begin{aligned} A_m &= z(A_{m_1}A_{m_2} + B_{m_2}C_{m_1})\cosh\Phi \\ &\quad + (z^2 A_{m_2}C_{m_1} + B_{m_2}A_{m_1})\sinh\Phi \end{aligned} \tag{6.17}$$

$$\begin{aligned} B_m &= z(A_{m_2}B_{m_1} + B_{m_2}D_{m_1})\cosh\Phi \\ &\quad + (z^2 A_{m_2}D_{m_1} + B_{m_1}B_{m_2})\sinh\Phi \end{aligned} \tag{6.18}$$

$$C_m = z(A_{m_1} C_{m_2} + C_{m_1} D_{m_2}) \cosh \Phi + (z^2 C_{m_1} C_{m_2} + A_{m_1} D_{m_2}) \sinh \Phi \tag{6.19}$$

$$D_m = z(B_{m_1} C_{m_2} + D_{m_1} D_{m_2}) \cosh \Phi + (z^2 D_{m_1} C_{m_2} + B_{m_1} D_{m_2}) \sinh \Phi \quad . \tag{6.20}$$

From Eq. 6.17, it is seen that the zeros of A_m are given by the roots of

$$\frac{z(A_{m_1} A_{m_2} + B_{m_2} C_{m_1})}{z^2 A_{m_2} C_{m_1} + B_{m_2} A_{m_1}} + \tanh \Phi = 0 \quad . \tag{6.21}$$

Let

$$x(s) \equiv \frac{A_{m_1} A_{m_2} + B_{m_2} C_{m_1}}{z A_{m_2} C_{m_1} + \frac{1}{z}(A_{m_1} B_{m_2})} \quad . \tag{6.22}$$

Now

$$\frac{A_{m_1} A_{m_2} + B_{m_2} C_{m_1}}{z A_{m_2} C_{m_1} + \frac{1}{z}(A_{m_1} B_{m_2})}$$

$$= \frac{1}{\dfrac{z A_{m_2} C_{m_1}}{A_{m_1} A_{m_2} + B_{m_2} C_{m_1}} + \dfrac{\frac{1}{z}(A_{m_1} B_{m_2})}{A_{m_1} A_{m_2} + B_{m_2} C_{m_1}}} \qquad (6.23)$$

$$= \frac{1}{\dfrac{z}{\dfrac{A_{m_1}}{C_{m_1}} + \dfrac{B_{m_2}}{A_{m_2}}} + \dfrac{1/z}{\dfrac{A_{m_2}}{B_{m_2}} + \dfrac{C_{m_1}}{A_{m_1}}}} \quad .$$

Since A_{m_1}/C_{m_1}, B_{m_2}/A_{m_2} and their reciprocals are reactance functions, the form of Eq. 6.23 demonstrates that $x(s)$ is a reactance function. Thus Eq. 6.21 becomes

$$x(s) + \tanh \Phi = 0 \ , \qquad (6.24)$$

$x(s)$ being a reactance function.

Similarly, Eqs. 6.18, 6.19 and 6.20, the expressions for B_m, C_m and D_m respectively, can be manipulated to show that their zeros also are given by an equation having the form of Eq. 6.24, where $x(s)$, in these cases, will have expressions similar to Eq. 6.22 and can be proved to be reactance functions. The zeros of B_m, C_m and D_m will not be considered in detail because the proof for the zeros of A_m will be directly applicable to the other cases as well. The only property of $x(s)$ used in the proof is that it is a reactance function.

All the zeros of A_m are on the $j\omega$-axis. Therefore replacing s by $j\omega$ in Eq. 6.24, the zeros of A_m are found from

$$x(\omega) + \tan \frac{\ell\omega}{v} = 0 \qquad (6.25)$$

i. e.,

$$\tan \frac{\ell\omega}{v} = -x(\omega) \ , \qquad (6.26)$$

where

$$x(\omega) = x(j\omega)/j \ .$$

Equation 6.26 is graphically presented in Fig. 6.5 for one repetition interval of the connecting line. In this interval the function $\tan \ell\omega/v$ varies all the way from $-\infty$ to $+\infty$, is continuous and has positive slope. Since the negative slope of $-x(\omega)$ is guaranteed by its being the negative of a reactance function, there must be at least one intersection of the curves $\tan \ell\omega/v$ and $-x(\omega)$ in this interval, as indicated in Fig. 6.5. Thus the occurrence of at least one zero of A_m (and also of B_m, C_m and D_m) is ensured in each repetition of a connecting line.

Zeros occurring in the repetition intervals of an open shunt stub will now be investigated. A shunt stub, as indicated in Fig. 6.6, connects two lossless networks having MGCP matrices,

$$\begin{bmatrix} A_{m_2} & B_{m_2} \\ C_{m_2} & D_{m_2} \end{bmatrix} \quad \text{and} \quad \begin{bmatrix} A_{m_1} & B_{m_1} \\ C_{m_1} & D_{m_1} \end{bmatrix} \ .$$

The MGCP matrix,

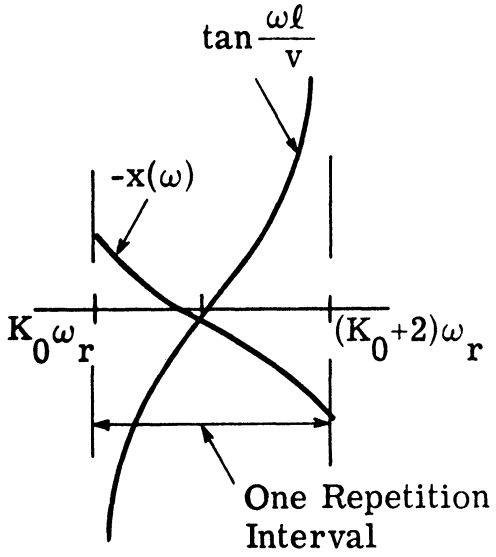

Fig. 6.5. $-x(\omega)$ in Eq. 6.26 and $\tan \frac{\ell\omega}{v}$ for one repetition interval of the connecting line in Fig. 6.4. K_0 is an odd integer and $\omega_r = \frac{\pi}{2} \frac{1}{\ell/v}$

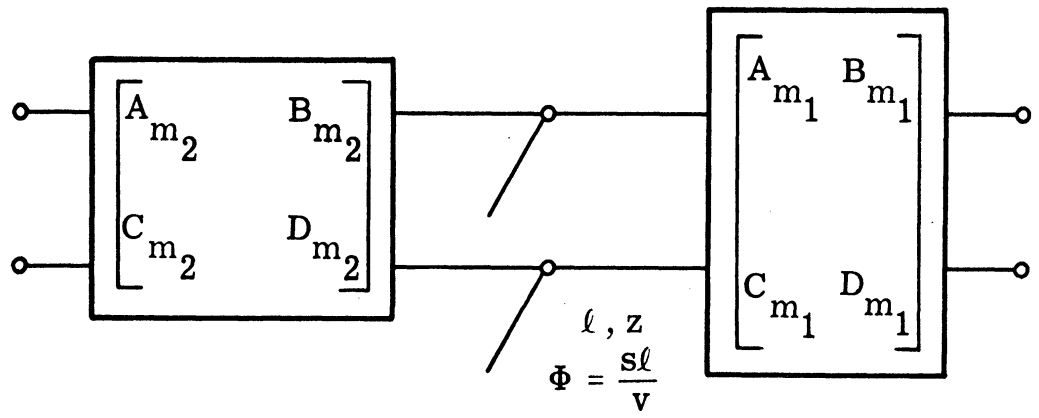

Fig. 6.6. Two lossless transmission line 2-ports having an open shunt stub at their junction

$$\begin{bmatrix} A_m & B_m \\ C_m & D_m \end{bmatrix},$$

of the total network is given by

$$\begin{bmatrix} A_{m_2} & B_{m_2} \\ C_{m_2} & D_{m_2} \end{bmatrix} \begin{bmatrix} z\cosh\Phi & 0 \\ \sinh\Phi & z\cosh\Phi \end{bmatrix} \begin{bmatrix} A_{m_1} & B_{m_1} \\ C_{m_1} & D_{m_1} \end{bmatrix} . \quad (6.27)$$

Multiplication of the matrices in Eq. 6.27 results in

$$A_m = z(A_{m_1} A_{m_2} + B_{m_2} C_{m_1}) \cosh\Phi + A_{m_1} B_{m_2} \sinh\Phi \quad (6.28)$$

$$B_m = z(A_{m_2} B_{m_1} + B_{m_2} D_{m_1}) \cosh\Phi + B_{m_1} B_{m_2} \sinh\Phi \quad (6.29)$$

$$C_m = z(A_{m_1} C_{m_2} + C_{m_1} D_{m_1}) \cosh\Phi + A_{m_1} D_{m_2} \sinh\Phi \quad (6.30)$$

$$D_m = z(B_{m_1} C_{m_2} + D_{m_1} D_{m_2}) \cosh\Phi + B_{m_1} D_{m_2} \sinh\Phi . \quad (6.31)$$

The zeros of only A_m will be studied, since conclusions regarding the zeros of B_m, C_m and D_m can be arrived at exactly in a similar fashion. From Eq. 6.28 it is found that the zeros of A_m are the roots of

$$\frac{z(A_{m_1} A_{m_2} + B_{m_2} C_{m_1})}{A_{m_1} B_{m_2}} + \tanh \Phi = 0 . \qquad (6.32)$$

Let

$$x(s) \equiv \frac{z(A_{m_1} A_{m_2} + B_{m_2} C_{m_1})}{A_{m_1} B_{m_2}} . \qquad (6.33)$$

Observe $x(s)$ can be expressed as

$$z\left(\frac{A_{m_2}}{B_{m_2}} + \frac{C_{m_1}}{A_{m_1}}\right) ,$$

where A_{m_2} / B_{m_2} and C_{m_1} / A_{m_1} are reactance functions.

Therefore the zeros under investigation are found from

$$x(s) + \tanh \frac{s\ell}{v} = 0 , \qquad (6.34)$$

where $x(s)$ is a reactance function. Now compare Eq. 6.34 with Eq. 6.24. It is clear that arguments used to prove our assertion for connecting lines are directly applicable to the present case, and thus lead to the conclusion that there must be at least one zero of A_m in each repetition interval of a stub.

6.4 Exactly One Zero of Each GCP in Each Repetition Interval

It has just been shown that in each section of the real frequency axis bounded by two consecutive zeros of $\cosh(s\ell/v)$, where ℓ is the length of a stub or connecting line in the circuit, at least one zero of each of the general circuit parameters A_m, B_m, C_m and D_m appears. In situations where more than one such interval due to as many lines overlap partially or wholly, just as many zeros will appear in the overlapping intervals. In this section we prove the following.

Theorem I. Exactly one zero of each modified general circuit parameter of the lossless part of the network in Fig. 3.1 occurs within each repetition interval of every transmission line element that the network consists of.

Assuming this theorem to be true for the hypothetical case of a lossless network represented by the box in Fig. 6.7(a), it will first be established that the theorem continues to be true with the addition of a connecting line or a stub to this circuit. Consider the circuits in Figs. 6.7(b) and (c) which are obtained when a connecting line and an open stub respectively are added to the circuit in Fig. 6.7(a), characterized by the modified GCP matrix

$$\begin{bmatrix} A_m & B_m \\ C_m & D_m \end{bmatrix}.$$

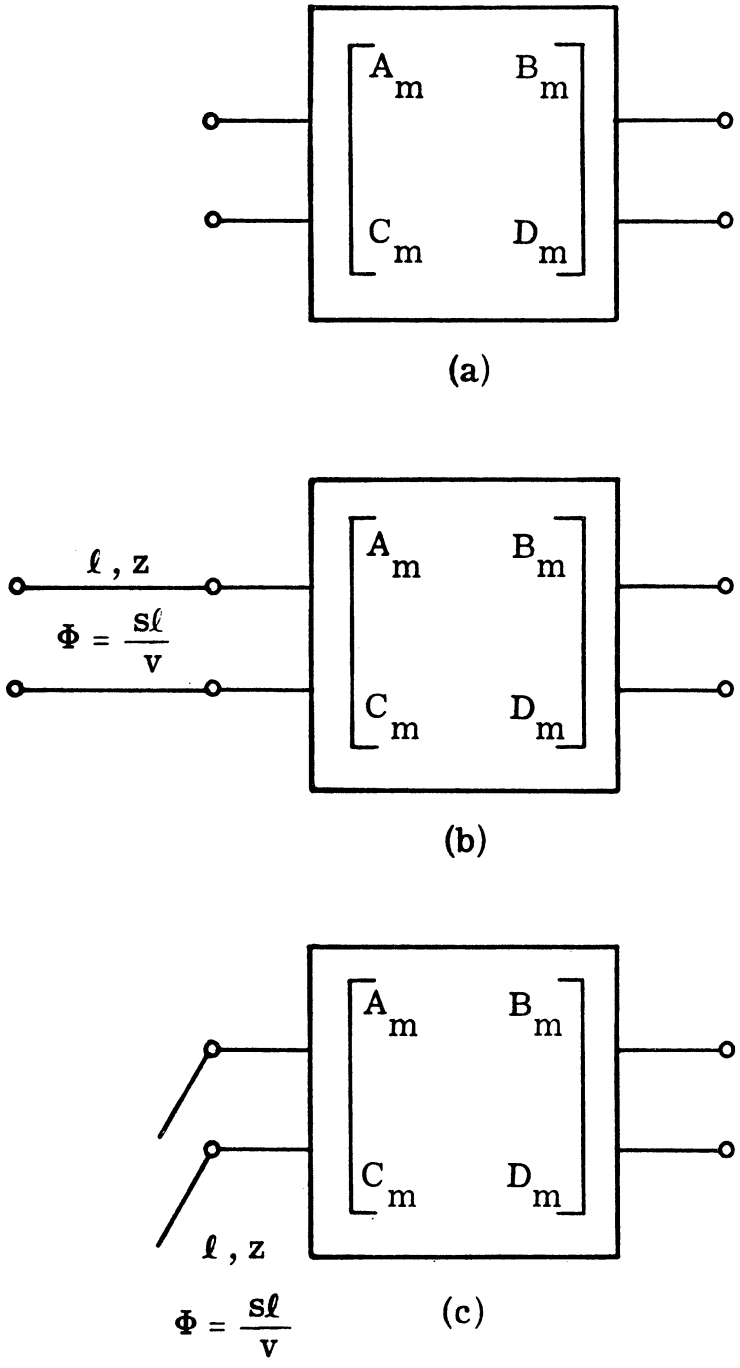

Fig. 6.7. (a) A lossless 2-port satisfying the theorem I in Section 6.4
(b) A connecting line terminated by the lossless 2-port in (a)
(c) An open shunt stub in parallel with the 2-port in (a)

The modified GCP, $A^b_{m_N}$, $B^b_{m_N}$, $C^b_{m_N}$ and $D^b_{m_N}$ of the complete network in Fig. 6.7(b) are given by

$$A^b_{m_N} = A_m z \cosh \frac{s\ell}{v} + C_m z^2 \sinh \frac{s\ell}{v} , \tag{6.46}$$

$$B^b_{m_N} = B_m z \cosh \frac{s\ell}{v} + D_m z^2 \sinh \frac{s\ell}{v} , \tag{6.47}$$

$$C^b_{m_N} = A_m \sinh \frac{s\ell}{v} + C_m z \cosh \frac{s\ell}{v} , \tag{6.48}$$

$$D^b_{m_N} = B_m \sinh \frac{s\ell}{v} + D_m z \cosh \frac{s\ell}{v} , \tag{6.49}$$

and those of the complete network in Fig. 6.7(c) are

$$A^c_{m_N} = A_m z \cosh \frac{s\ell}{v} , \tag{6.50}$$

$$B^c_{m_N} = B_m z \cosh \frac{s\ell}{v} , \tag{6.51}$$

$$C^c_{m_N} = A_m \sinh \frac{s\ell}{v} + C_m z \cosh \frac{s\ell}{v} , \tag{6.52}$$

$$D^c_{m_N} = B_m \sinh \frac{s\ell}{v} + D_m z \cosh \frac{s\ell}{v} . \tag{6.53}$$

Because $\cosh s\ell/v$ possesses exactly one zero in each repetition

interval the theorem is true for the zeros of $A^c_{m_N}$ and $B^c_{m_N}$. If any of the matrix elements A_m, B_m, C_m or D_m is zero as, for example, would be the case for C_m if the circuit in Fig. 6.7(a) were a single open shunt stub, some of the expressions (Eqs. 6.46 through 6.49, 6.52, and 6.53) will have the form of Eq. 6.50. In such cases, the arguments used above for the zeros of Eq. 6.50 can be repeated. Assuming, however, that none of A_m, B_m, C_m or D_m is zero, it is readily seen that all the zeros of each of the modified general circuit parameters $A^b_{m_N}$, $B^b_{m_N}$, $C^b_{m_N}$, $D^b_{m_N}$, $C^c_{m_N}$ and $D^c_{m_N}$ are the roots of an equation having the form

$$x'(s) + \tanh \frac{s\ell}{v} = 0 \ , \tag{6.54}$$

where $x'(s)$, though different in each case, is a reactance function. The expression $x'(s)$ has another important property also; notice that $x'(s)$ is either formed dividing A_m or D_m by B_m or C_m, or obtained from the reciprocal of the expression thus formed. For example, for $A^b_{m_N}$ in Eq. 6.46

$$x'(s) = \frac{1}{z} \frac{A_m}{C_m} \ . \tag{6.55}$$

Since according to the assumption the theorem is true for circuit in Fig. 6.7(a), $x'(s)$ has exactly one pole and one zero in each repetition

interval of every transmission line present in the circuit. Putting $s = j\omega$ in Eq. 6.54, one gets

$$x'(\omega) + \tan\frac{\omega\ell}{v} = 0 \ , \tag{6.56}$$

where

$$x'(\omega) = \frac{x'(j\omega)}{j} \ . \tag{6.57}$$

Equation 6.56 will now be graphically examined. In Fig. 6.8 $-x'(\omega)$ is drawn for the portion $I_1 - I_2$ of a repetition interval that contains the pole and zero of $x'(\omega)$ appearing in this repetition interval.

The expression $\tan \ell\omega/v$, due to the augmenting line, can have three distinct positions relative to $-x'(\omega)$. It can completely straddle a pole of $-x'(\omega)$ as in Fig. 6.9(a), producing two zeros, one for the existing repetition interval and the other for its own repetition interval. Secondly, one repetition interval of $\tan \ell\omega/v$ may be completely contained in a section of real frequency axis where no pole of $x'(\omega)$ occurs. This is shown in Fig. 6.9(b). In such a case, $\tan \ell\omega/v$ produces a zero for its own repetition interval. Finally a pole of $\tan \ell\omega/v$ may coincide with that of $x'(\omega)$, as indicated in Fig. 6.9(c), producing a zero at a pole of $x'(\omega)$, thus giving the required zero within the existing repetition interval of $x'(\omega)$.

We have thus established that a network for which the theorem is true, continues to satisfy the theorem even after it is augmented

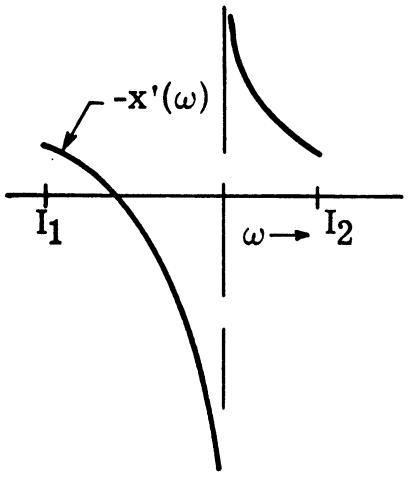

Fig. 6.8. $-x'(\omega)$ in (6.56) for the part $I_1 - I_2$ of a repetition interval of the 2-port in Fig. 6.7(a)

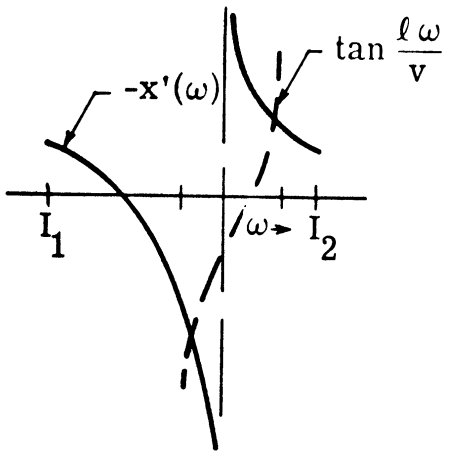

(a)

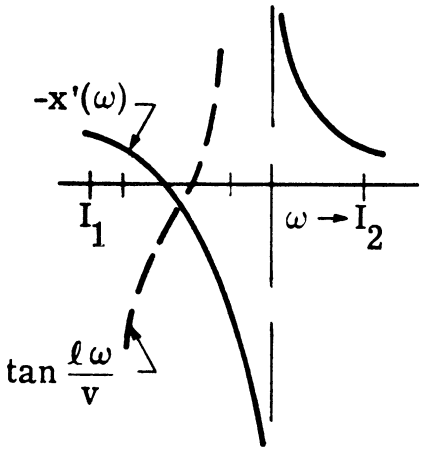

(b)

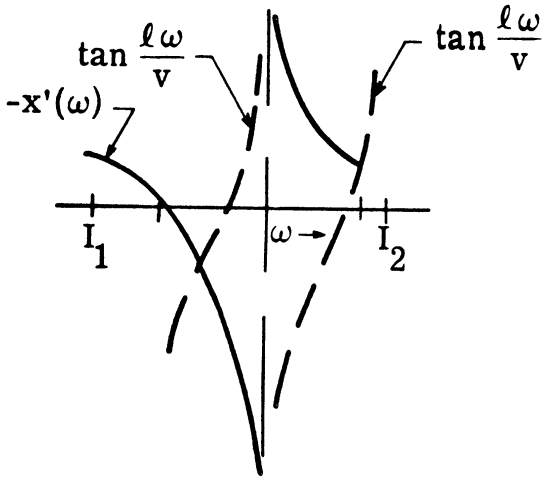

(c)

Fig. 6.9. Graphical representations of $x'(\omega) + \tan \omega\ell/v = 0$ illustrating the three distinct relative positions of $-x'(\omega)$ and $\tan \omega\ell/v$

by adding a connecting line or a stub. The proof of the theorem will be completed by demonstrating that a single connecting line or a stub satisfies the theorem. For such single elements, the zeros of the modified general circuit parameters (Eqs. 6.4 and 6.5) are shown in Fig. 6.10. It is verified that the theorem is true, though this case is degenerate in that the zeros of the terms A_m and D_m lie at the end of the repetition intervals.

Though it has been our purpose above to prove the existence of one and only one zero of each general circuit parameter in each repetition interval of a network in which connecting lines and open shunt stubs alternate, the proof given applies also to circuits consisting of m ($\geqq 0$) connecting lines in cascade alternating with n ($\geqq 0$) shunt open stubs in parallel.

Transmission Poles

We have proved in Section 6.4.1 the existence of exactly one zero for each general circuit parameter in each repetition interval. As a new line having length ℓ is added to a circuit, zeros of $\cos \omega\ell/v$ repeat at regular intervals creating in their wake new zeros of A_m, B_m, C_m and D_m, one to each interval. The zeros existing prior to the addition of this line will in general undergo rearrangement due to the addition of the new line. However, the relocation will be such that exactly one zero of each general circuit parameter of the new circuit is now assignable to and occurs within

each repetition interval. From Section 6.2 it therefore follows that each repetition interval contains exactly one zero of $G_1A_m + G_2D_m$ and of $G_1G_2B_m + C_m$. Since each transmission pole is associated with one zero of $G_1A + G_2D_m$ and one zero of $G_2G_1B + C$, as indicated in Section 6.2, it is reasonable to expect one nondominant pole to each repetition interval occurring, in general, in the region (henceforth referred to as repetition strip) of the left half plane bounded by two straight lines drawn parallel to the imaginary frequency axis through the two extremities of this repetition interval as shown in Fig. 6.11.

6.5 Numerical Evaluation of Transmission Poles

Transmission poles are found from the zeros of

$$(G_1A_m + G_2D_m) + K(G_1G_2B_m + C_m), \tag{6.58}$$

for $K = 1$ (or alternatively, from the zeros of

$$K'(G_1A_m + G_2D_m) + (G_1G_2B_m + C_m) \tag{6.59}$$

for $K' = 1$). The numerical technique used for the determination of a transmission pole is initiated by finding a zero of Eq. 6.58 for $K = 0$ (or at zero of Eq. 6.59 for $K' = 0$). The locus of this zero is then followed off the $j\omega$-axis as K increases, until finally, for $K = 1$, a transmission pole is reached. First it will be established that the

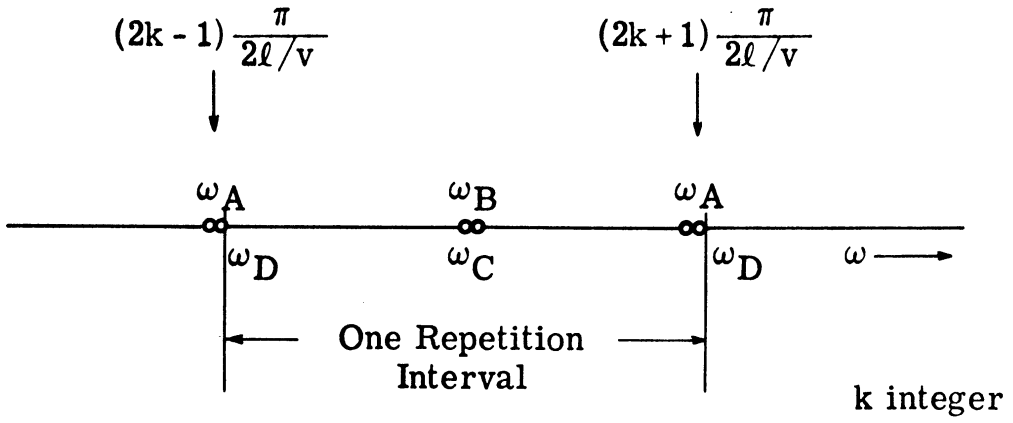

Fig. 6.10. Zeros ω_A, ω_B, ω_C, ω_D of modified general circuit parameters of either a stub or a connecting line of length ℓ in one of its repetition intervals, verifying the occurrence of exactly one zero of each general circuit parameter in such an interval

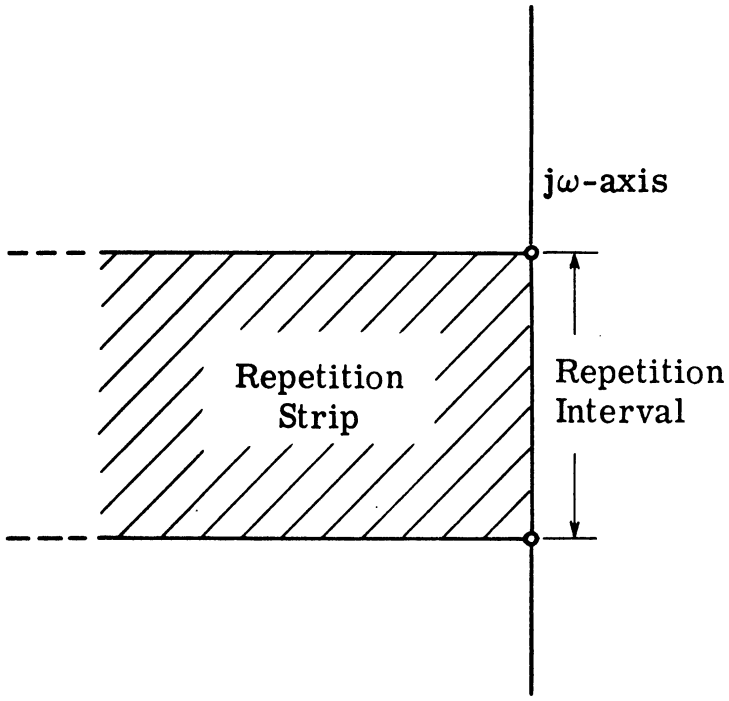

Fig. 6.11. A repetition interval and the associated repetition strip. A nondominant pole will, in general, occur in each repetition strip

root locus of Eq. 6.58 as K varies, which originates at a zero of $G_1 A_m + G_2 D_m$ and terminates at a zero of $G_1 G_2 B_m + C_m$, is perpendicular to the $j\omega$-axis at both these points.

6.5.1 Derivatives of the Zeros of (6.58) with Respect to K.

On any point, ξ, on the root-locus of Eq. 6.58, $\{G_1 A_m(\xi) + G_2 D_m(\xi) + K[G_1 G_2 B_m(\xi) + C_m(\xi)]\} = 0$.

Taking total differentials,

$$\frac{d}{d\xi}[G_1 A_m(\xi) + G_2 D_m(\xi)] \cdot d\xi + K\frac{d}{d\xi}[G_2 G_1 B_m(\xi) + D_m(\xi)] \cdot d\xi + [G_1 G_2 B_m(\xi) + C_m(\xi)] \cdot dK = 0 \quad . \tag{6.60}$$

Let $j\omega_{AD}$ be any zero of $G_1 A_m + G_2 D_m = 0$. At this point $K = 0$. Thus Eq. 6.60 gives

$$\frac{d\xi}{dK} = - \left. \frac{G_1 G_1 B_m(\xi) + C_m(\xi)}{G_1 \frac{d}{d\xi} A_m(\xi) + G_2 \frac{d}{d\xi} D_m(\xi)} \right|_{\xi = j\omega_{AD}} \tag{6.61}$$

as the value of $d\xi / dK$ at $j\omega_{AD}$.

Recall from Section 6.2 that

$$B_m(j\omega_{AD}) = jB_m(\omega_{AD})$$

$$C_m(j\omega_{AD}) = jC_m(\omega_{AD})$$

Also notice that

$$\frac{d}{ds} A_m(s)\Big|_{s = j\omega} = - j \frac{d}{d\omega} A_m(\omega) \tag{6.62}$$

and

$$\frac{d}{ds} D_m(s)\Big|_{s = j\omega} = - j \frac{d}{d\omega} D_m(\omega) \ . \tag{6.63}$$

Therefore,

$$\frac{d\xi}{dK}\Bigg|_{\xi = j\omega_{AD}} = \frac{G_1 G_2 B_m(\omega_{AD}) + C_m(\omega_{AD})}{\frac{d}{d\omega}\left[G_1 A_m(\omega) + G_2 D_m(\omega)\right]\Big|_{\omega = \omega_{AD}}} \ . \tag{6.64}$$

This quantity is real and, as an examination of typical curves of $G_1 A_m(\omega) + G_2 D_m(\omega)$ and $G_1 G_2 B_m(\omega) + C_m(\omega)$, shown in Fig. 6.12 reveals, is also negative since the slope of $G_1 A_m + G_2 D_m$ and $G_1 G_2 B_m + C_m$ always have opposite signs at a zero of the former function.

Studying

$$K'[G_1 A_m(\xi) + G_2 D_m(\xi)] + [G_1 G_2 B_m(\xi) + C_m(\xi)] = 0 \tag{6.65}$$

exactly in the same way, one finds that

$$\frac{d\xi}{dK'} = - \left. \frac{G_1 A_m(\xi) + G_2 D_m(\xi)}{G_1 G_2 \frac{d}{d\xi} B_m(\xi) + \frac{d}{d\xi} C_m(\xi)} \right|_{\xi = j\omega_{BC}} \tag{6.66}$$

at any zero, $j\omega_{BC}$, of $G_1 G_2 B_m + C_m$. Or

$$\left. \frac{d\xi}{dK'} \right|_{\xi = j\omega_{BC}} = - \frac{G_1 A_m(\omega_{AB}) + G_2 D_m(\omega_{AB})}{\left. \frac{d}{d\omega} [G_1 G_2 B_m(\omega) + C_m(\omega)] \right|_{\omega = \omega_{BC}}} \tag{6.67}$$

which is real, and as the curves in Fig. 6.12 show, is always negative. The realness of $d\xi/dK$ and $d\xi/dK'$ indicate that the locus is perpendicular to the $j\omega$-axis at ω_{AD} and ω_{BC}.

6.5.2 Determination of ω_{AD} or ω_{BC}. The zeros $G_1 G_2 B_m + C_m$, designated ω_{BC} and the zeros of $G_1 A_m + G_2 D_m$, called ω_{AD} are all on the $j\omega$-axis. This makes them relatively easy to locate, since only one line, the $j\omega$-axis, has to be examined, instead of the entire complex frequency plane. To compute the approximate location of zeros in the interval $0 \leqq \omega \leqq W$, perhaps the simplest technique is to divide this interval into n subintervals (not necessarily equal), $0 \leqq \omega \leqq \omega_1$, $\omega_1 \leqq \omega \leqq \omega_2, \ldots, \omega_{n-1} \leqq \omega \leqq W$ by points ω_1, ω_2, $\ldots$, ω_{n-1}, W. The value of the function (for example, $G_1 A_m + G_2 D_m$) is evaluated at the points $\omega = 0, \omega_1, \ldots, \omega_{n-1}$, W. The presence of a zero in the interval $\omega_{i-1} \leqq \omega \leqq \omega_i$ is indicated if the value of the function at ω_{i-1} and that at ω_i have opposite signs. Using this

technique a computer program has been written to find the approximate locations for the zeros $G_1 A_m + G_2 D_m$ and $G_1 G_2 D_m + C_m$. This program is listed in Appendix III together with a note on its use.

6.5.3 Transmission Poles. With the approximate value of ω_{AD} thus known, the approximate location for a zero of $G_1 A_m + G_2 D_m + K(G_1 G_2 B+C)$, for K small (for example, 0.1) can be written as

$$\sigma \pm j\omega_{AD} , \tag{6.68}$$

where, from Eq. 6.64,

$$\sigma = K \frac{d\xi}{dK} \Bigg|_{\xi = j\omega_{AD}} . \tag{6.69}$$

A transmission pole is now evaluated in the following way.

Start with a small value of K (for example, 0.1 or 0.2) and an estimate $\sigma + j\omega_{AD}$ for a zero of $G_1 G_2 B_m + C_m + K(G_1 A_m + G_2 D_m)$. Refine this estimate to a desired degree of accuracy by the Newton-Raphson method. Gradually increase K to unity and every time K is changed the zero is refined by the Newton-Raphson iteration with the zero for the previous value of K being used as an estimate.

A listing may be found in Appendix IV, of the computer program written to evaluate the transmission poles following the technique just outlined.

6.6 An Example

The computer technique delineated above is illustrated here with an example. In this example the nondominant poles of the five-element transmission line network indicated in Fig. 6.13 have been found. The elements of this network chosen for dominant Butterworth transmission poles were

$\ell_1/v = 1.52761$ Secs $\quad z_1 = 0.3$ Ohms
$\ell_2/v = 0.1789117$ " $\quad z_2 = 3.333$ "
$\ell_3/v = 0.712483$ " $\quad z_3 = 0.3$ "
$\ell_4/v = 0.1233977$ " $\quad z_4 = 3.333$ "
$\ell_5/v = 0.1940887$ " $\quad z_5 = 0.3$ " .

The approximate locations of ω_{AD} and ω_{BC}, which are the zeros of $G_1 A_m + G_2 D_m$ and $G_1 G_2 B_m + C_m$ respectively, were

ω_{AD}(rdn/sec)	ω_{BC}(rdn/sec)
0.5	0
1.2	0.9
2.2	1.7
4.0	2.6
4.8	4.3
5.8	4.8
7.4	6.3
8.9	8.3
9.1	8.9

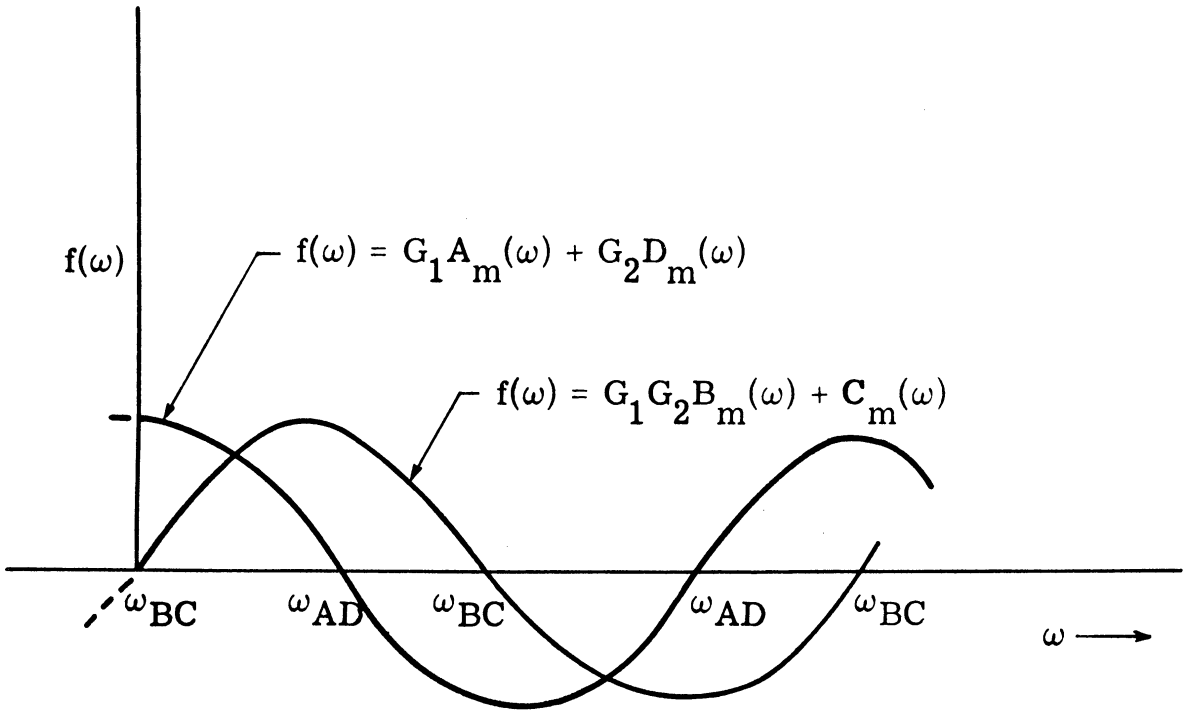

Fig. 6.12. Typical graphs of $G_1A_m(\omega) + G_2D_m(\omega)$ and $G_1G_2B_m(\omega) + C_m(\omega)$

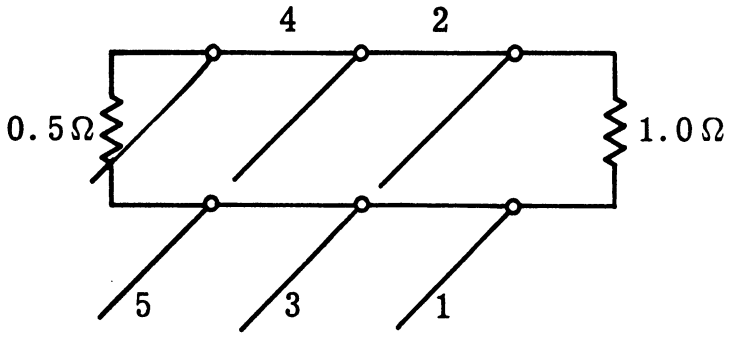

Fig. 6.13. A five element transmission line network

The dominant poles due to the zeros at 0, 0.9, 1.7 of $G_1 G_2 B_m + C_m$ and at 0.5 and 1.2 of $G_1 A_m + G_2 D_m$ were verified to have the fifth order Butterworth locations. The Butterworth pole closest to the $j\omega$-axis, marked BP, together with several non-dominant poles, identified with NP^{I}, NP^{II},..., NP^{VI}, is shown in Fig. 6.14.

To find the nondominant pole, NP^{I}, that resulted from ω_{AD}^{I} = 2.2 rdn (see Fig. 6.14) the starting point for iteration with K = 0.2 was calculated from Eq. 6.68. The point -0.0292 + j2.2 thus obtained was used to initiate the iteration which converged to exact zero at -0.032 + j2.16 for K = 0.2. Changing K several times, the required transmission pole (K = 1) was located at

$$-0.175 \pm j2.204 \ .$$

Starting from ω_{BC}^{I} = 2.6, the iteration found the transmission pole at the same location

$$-0.175 \pm j2.204 \ .$$

Initiating the iteration at the other zeros, ω_{AD}, or ω_{BC} and proceeding in the same manner, several other nondominant transmission poles near the origin were computed to be

$$NP^{II}: \ -0.191 \pm j4.157$$

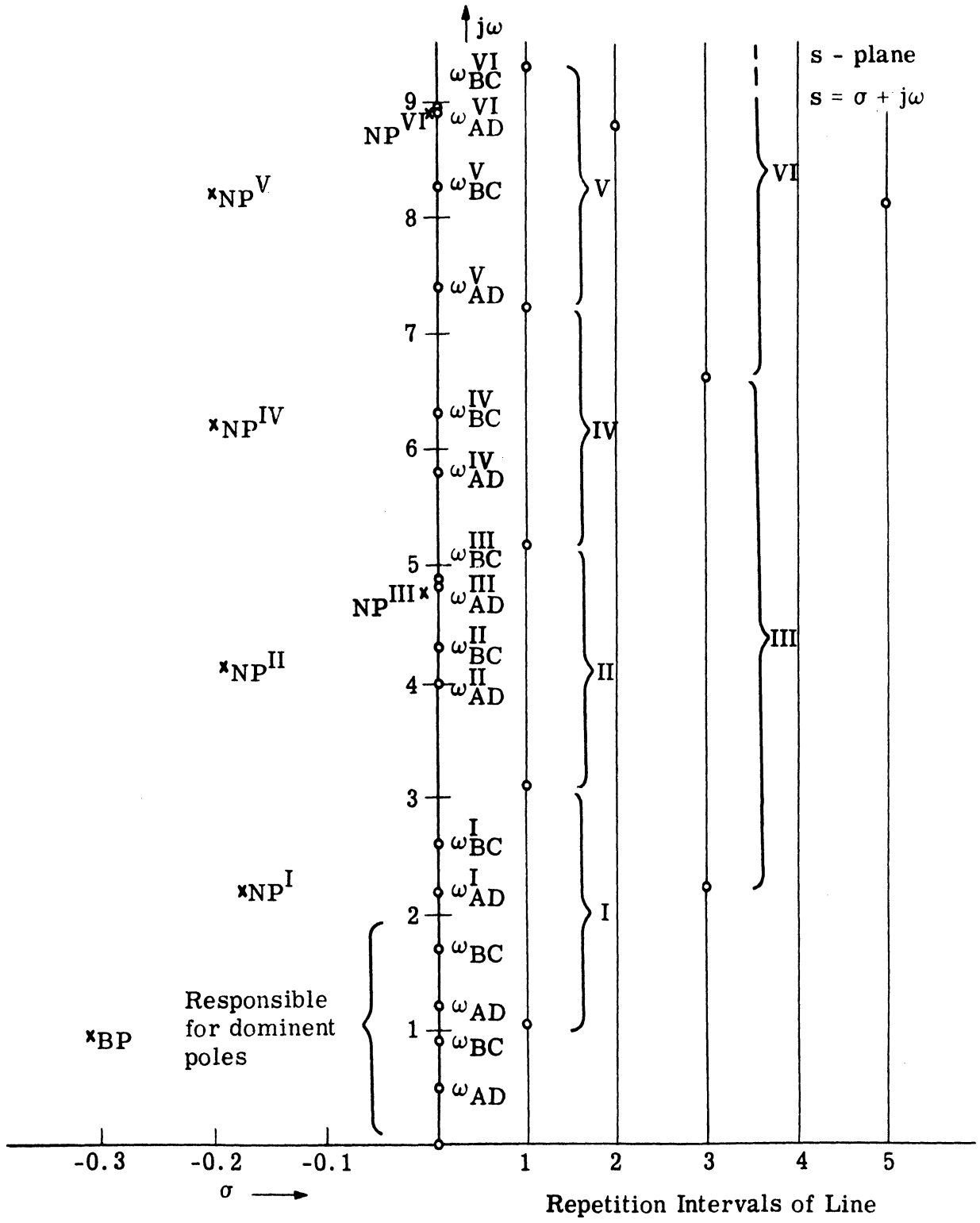

Fig. 6.14. The zeros of $G_1A_m + G_2D_m$ and $G_1G_2B_m + C_m$ are identified by ω_{AD} and ω_{BC} respectively and the nondominant poles of the 5-element network in Fig. 6.13 are identified by NP's, together with the repetition interval of each line. Each repetition interval, ω_{AD} and ω_{BC} occurring in it, and the nondominant pole in its repetition strip are marked with identical Roman numerals

$$NP^{III}: \; -0.013 \pm j4.744$$

$$NP^{IV}: \; -0.198 \pm j6.204$$

$$NP^{V}: \; -0.197 \pm j8.222$$

$$NP^{VI}: \; -0.00142 \pm j8.886 \quad .$$

Figure 6.14 displays these nondominant poles on the s-plane together with the zeros of $G_1 A_m + G_1 D_m$ and $G_1 G_2 B_m + C_m$. The repetition intervals for all the five transmission lines are also shown in this figure. Our earlier assertion that there is exactly one zero of $G_1 A_m + G_2 D_m$ and $G_1 G_2 B_m + C_m$ in each repetition interval can be verified from the figure where each such interval and the zeros associated with it are marked with identical Roman numerals. Notice also that the nondominant poles occur, as expected, one in each repetition strip.

The presence of the nondominant poles of the network in Fig. 6.13 can also be detected from the attenuation versus frequency plot presented in Fig. 6.15.

6.7 Sensitivity of the Zeros of A_m, B_m, C_m and D_m with the Variation of Line Lengths

It has been established in Sections 6.2 and 6.3 that for the network configurations in Figs. 6.4 and 6.6, the zeros of A_m, B_m, C_m and D_m, which are all on the real frequency axis, are obtainable from the roots of

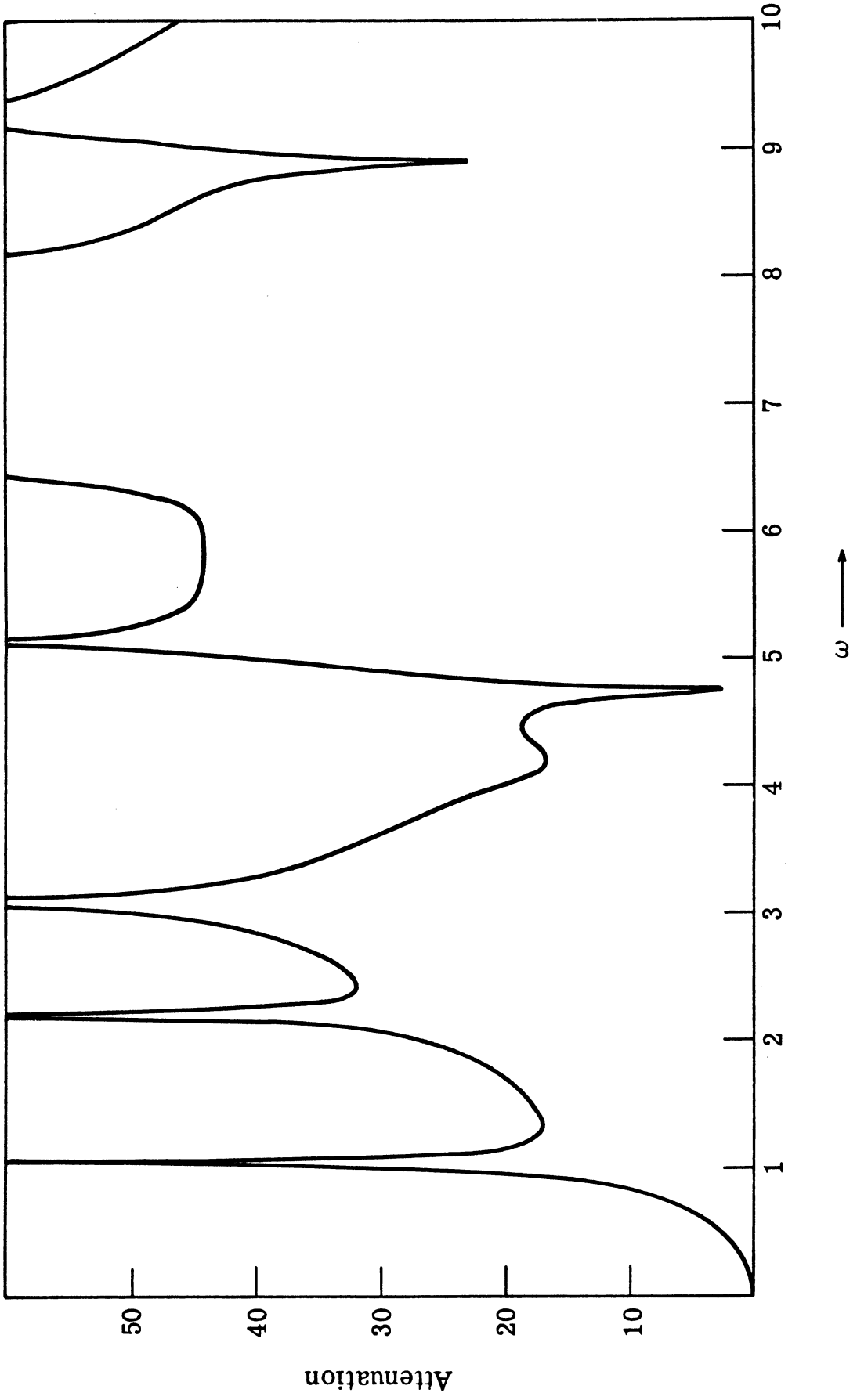

Fig. 6.15. The computed attenuation of the 5-element network in Fig. 6.13

$$x(\omega) + \tan\frac{\ell\omega}{v} = 0 \ , \tag{6.70}$$

where $x(\omega)$ is a reactance function and ℓ is the length of either the stub, as indicated in Fig. 6.6, or of the connecting line as indicated in Fig. 6.4. In this section we determine the sensitivity of a zero designated ζ of Eq. 6.70 with respect to ℓ.

Since ζ is a zero of Eq. 6.70, one can write

$$x(\zeta) + \tan\frac{\zeta\ell}{v} = 0 \ , \tag{6.71}$$

which implicitly relates ζ and ℓ. We want to find $d\zeta/d\ell$. Taking total differential of Eq. 6.71, one gets

$$\frac{dx(\zeta)}{d\zeta}\,d\zeta + \frac{\ell}{v}\sec^2\left(\frac{\zeta\ell}{v}\right)\cdot d\zeta + \frac{\zeta}{v}\sec^2\left(\frac{\zeta\ell}{v}\right)\cdot d\ell = 0 \tag{6.72}$$

which yields

$$\frac{d\zeta}{d\ell} = -\frac{\frac{\zeta}{v}\sec^2\left(\frac{\zeta\ell}{v}\right)}{\frac{dx(\zeta)}{d\zeta} + \frac{\ell}{v}\sec^2\left(\frac{\zeta\ell}{v}\right)} \ . \tag{6.73}$$

Since $dx(\zeta)/d\zeta$ is always positive, $d\zeta/d\ell$ is positive for ζ negative and $d\zeta/d\ell$ is negative for ζ positive. This means that with the increase in ℓ, any zero of A_m, B_m, C_m or D_m moves toward the origin. This result is not different from what one would

anticipate judging from the fact that any repetition interval due to either a stub or a connecting line which contains these zeros slides down the real frequency axis toward the origin when the length is increased. Since nondominant poles result from these zeros, it would be logical to expect the nondominant poles to move toward the origin with the increases in the lengths of the component line elements.

Chapter 7

Optimization

It has been pointed out in Chapter 5 that the undesirable effect of a particular nondominant pole may be eliminated, to an extent, by placing a transmission zero on the real frequency axis opposite the pole. In this chapter a strategy is devised to accomplish this without violating other requirements that the network must satisfy.

7.1 Mathematical Formulation

A transmission zero, in general, will not naturally occur opposite a nondominant pole. Positioning a zero opposite a pole may be viewed as minimizing the projection on the real frequency axis of the straight line that joins a specified nondominant pole and a selected transmission zero. As this minimization progresses, the locations of the specified dominant poles must be maintained and the characteristic impedances have to be held within the prescribed bounds. Such minimization of a function under nonlinear constraints is termed a nonlinear programming problem [46].

Let μ_j be the imaginary part of the j^{th} nondominant pole, and let the transmission zero being utilized to nullify the effect of this pole be designated $\sqrt{-1}\ \nu_j$. The function to be minimized,

also called the cost function, can be expressed as the weighted sum

$$\sum_{j=1}^{J} k_j |\mu_j - \nu_j| \ , \tag{7.1}$$

where

J = the number of nondominant poles being considered,

k_j = nonnegative weights.

These weights k_j are necessary since the importance of a nondominant pole being nullified increases as it approaches the passband.

There are two constraints. (1) The n dominant poles must be preserved at the prescribed locations. Thus, the characteristic impedances z_i and the delays $\tau_i (\equiv \ell_i / v)$ of the component transmission lines must always be so chosen as to satisfy Eq. 3.17, i. e.,

$$f_i(\tau_1, \ldots, \tau_n; z_1, \ldots, z_n) = 0 \ , \quad i = 1, 2, \ldots, n \ . \tag{7.2}$$

(2) The characteristic impedances z_j must be kept within a prescribed bound, i. e.,

$$z_{M_j} \geq z_j \geq z_{m_j} \ , \quad j = 1, 2, \ldots, n \ , \tag{7.3}$$

where

z_j = the characteristic impedance of the j^{th} transmission line,

and z_{M_j} and z_{m_j} are respectively the upper and lower bounds within which z_j must lie. Since the system of Eqs. 7.2 can be solved for z_j in terms of $\tau_1, \tau_2, \ldots, \tau_n$, constraints expressed in Eqs. 7.2 and 7.3 can be combined as

$$z_{M_j} \geqq z_j(\tau_1, \ldots, \tau_n) \geqq z_{m_j}, \quad j = 1, 2, \ldots, n . \tag{7.4}$$

Therefore the nonlinear programming problem can be formalized as

$$\min \sum_{j=1}^{J} k_j |\mu_j - \nu_j| , \tag{7.5}$$

subject to

$$z_{M_j} \geqq z_j(\tau_1, \ldots, \tau_n) \geqq z_{m_j}, \quad j = 1, 2, \ldots, n \tag{7.6}$$

where it is understood that $z_j(\tau_1, \ldots, \tau_n)$ are the solution to the system of Eqs. 7.2 with $\tau_1, \ldots, \tau_n$ given. For computational convenience, the cost function (Eq. 7.5) can be replaced by the following

$$\min \sum_{j=1}^{J} k_j x_j , \tag{7.7}$$

subject to

$$x_j \geqq 0 \qquad j = 1, 2, \ldots, J \ , \tag{7.8}$$

$$x_j \geqq -(\mu_j - \nu_j) \qquad j = 1, 2, \ldots, J \ , \tag{7.9}$$

$$x_j \geqq (\mu_j - \nu_j) \qquad j = 1, 2, \ldots, J \ . \tag{7.10}$$

7.2 Solution

A number of methods are available for the solution of nonlinear programming problems, a survey of which may be found in [47]. Some of these techniques, for instance, the cutting plane method [48] and the small step gradient method [49] are direct extensions of linear programming problem [50, 51]. Large step gradient methods [47], also known as methods of feasible directions [52], work with linear subproblems and make use of procedures developed for unconstrained minimization. Fiacco and McCormick [53] have developed a method that transforms a minimization problem with constraints into an unconstrained one. The solution that is being delineated here for the nonlinear problem posed in Section 7.1 is a small step method where complete linearization takes place at each step and no old information is retained. This, together with predetermined step size make this suitable for application to both convex and nonconvex problems.

The constraints denoted by Eq. 7.6 can be expressed by two inequality constraints

$$z_{M_j} \geqq z_j(\tau_1, \tau_2, \ldots, \tau_n) , \quad j = 1, 2, \ldots, n \tag{7.11}$$

and

$$z_{m_j} \leqq z_j(\tau_1, \tau_2, \ldots, \tau_n) , \quad j = 1, 2, \ldots, n . \tag{7.12}$$

Expand $z_j(\tau_1, \tau_2, \ldots, \tau_n)$ in the Taylor series about the point $(\tau_1^i, \tau_2^i, \ldots, \tau_n^i)$ to get

$$z_j = z_j^i + \sum_{k=1}^{n} \frac{\partial z_j^i}{\partial \tau_k^i} \Delta\tau_k^i , \quad j = 1, 2, \ldots, n , \tag{7.13}$$

where

$$z_j^i = z_j(\tau_1^i, \ldots, \tau_n^i) , \tag{7.14}$$

$$\frac{\partial z_j^i}{\partial \tau_k^i} = \frac{\partial}{\partial \tau_k} [z_j(\tau_1^i, \ldots, \tau_n^i)] , \tag{7.15}$$

$$\Delta\tau_k^i = \tau_k^{i+1} - \tau_k^i . \tag{7.16}$$

Here superscript i indicates that the linearization is being carried out at the solution $(\tau_k^i, z_k^i, k = 1, 2, \ldots, n)$ reached at the conclusion of the i^{th} iteration.

Substituting this Taylor's series in Eqs. 7. 11 and 7. 12 results in

$$\sum_{k=1}^{n} \frac{\partial z_j^i}{\partial \tau_k^i} \Delta \tau_k^i \leqq z_{M_j} - z_j^i \ , \quad j = 1, 2, \ldots, n \tag{7.17}$$

$$- \sum_{k=1}^{n} \frac{\partial z_j^i}{\partial \tau_k^i} \Delta \tau_k^i \leqq - z_{m_j} + z_j^i \ , \quad j = 1, 2, \ldots, n \ . \tag{7.18}$$

Similar substitution of the Taylor's Series expansions of μ_j and ν_j in Eqs. 7. 9 and 7. 10 gives

$$-x_j - \sum_{k=1}^{n} \left(\frac{\partial \mu_j^i}{\partial \tau_k^i} - \frac{\partial \nu_j^i}{\partial \tau_k^i} \right) \Delta \tau_k^i \leqq (\mu_j^i - \nu_j^i) \ , \quad j = 1, 2, \ldots, J \ , \tag{7.19}$$

$$-x_j + \sum_{k=1}^{n} \left(\frac{\partial \mu_j^i}{\partial \tau_k^i} - \frac{\partial \nu_j^i}{\partial \tau_k^i} \right) \Delta \tau_k^i \leqq - (\mu_j^i - \nu_j^i) \ , \quad j = 1, 2, \ldots, J \ . \tag{7.20}$$

For the Taylor Series expansions to be accurate, differential increments $\Delta \tau_k^i$ must be small. This consideration leads to the further constraints where δ is small:

$$-\delta \leqq \Delta \tau_k^i \leqq \delta \ , \quad k = 1, \ldots, n \ . \tag{7.21}$$

Putting

$$\Delta\tau_k^i = x_{J+2k-1} - x_{J+2k} \ , \quad k = 1, \ldots, n \ , \tag{7.22}$$

Eq. 7.21 can be expressed as

$$\begin{aligned} x_{J+2k-1} &\geqq 0 \\ x_{J+2k} &\geqq 0 \\ x_{J+2k-1} + x_{J+2k} &\leqq \delta \ , \quad k = 1, 2, \ldots, n \ . \end{aligned} \tag{7.23}$$

Substitution of Eq. 7.22 in Eqs. 7.17, 7.18, 7.19 and 7.20 and combining them with Eqs. 7.7 and 7.23 finally gives the following linear programming problem:

$$\min \sum_{j=1}^{J} k_j x_j \tag{7.24}$$

Subject to

$$-x_j' - \sum_{k=1}^{n} \left(\frac{\partial \mu_j^i}{\partial \tau_k^i} - \frac{\partial \nu_j^i}{\partial \tau_k^i} \right) (x_{J+2k-1} - x_{J+2k}) \leqq (\mu_j^i - \nu_j^i) \ , \tag{7.25}$$

$$j = 1, 2, \ldots, J$$

$$-x_j + \sum_{k=1}^{n} \left(\frac{\partial \mu_j^i}{\partial \tau_k^i} - \frac{\partial \nu_j^i}{\partial \tau_k^i} \right) (x_{J+2k-1} - x_{J+2k}) \leqq -(\mu_j^i - \nu_j^i) ,$$

$$j = 1, 2, \ldots, J \tag{7.26}$$

$$\sum_{k=1}^{n} \frac{\partial z_j^i}{\partial \tau_k^i} (x_{J+2k-1} - x_{J+2k}) \leqq z_{M_j} - z_j^i , \quad j = 1, 2, \ldots, n , \tag{7.27}$$

$$-\sum_{k=1}^{n} \frac{\partial z_j^i}{\partial \tau_k^i} (x_{J+2k-1} - x_{J+2k}) \leqq -z_{m_j} + z_j^i , \quad j = 1, 2, \ldots, n , \tag{7.28}$$

$$x_{J+2k-1} + x_{J+2k} \leqq \delta , \quad k = 1, 2, \ldots, n \tag{7.29}$$

$$x_j \geqq 0 , \quad j = 1, 2, \ldots, J + 2n . \tag{7.30}$$

This linear programming problem is amenable to solution by one of the several established methods [50, 51]. This linear problem is now solved repeatedly. After each solution the increments $\Delta \tau_k^i$ are added to τ_k^i to get τ_k^{i+1}, and the nonlinear problem is linearized again at this point. This is continued until the increments become so small that no further improvement in cost function results.

7.3 Calculation of Derivatives

(i) $\partial z_j / \partial \tau_k$ ($j = 1, \ldots, n$; $k = 1, \ldots, n$) can be expressed in terms of two Jacobian determinants as

$$\frac{\partial z_j}{\partial \tau_k} = - \frac{\dfrac{\partial(f_1, f_2, \ldots, f_n)}{\partial(z_1, z_2, \ldots, z_{j-1}, \tau_k, z_{j+1}, \ldots, z_n)}}{\dfrac{\partial(f_1, f_2, \ldots, f_n)}{\partial(z_1, z_2, \ldots, z_n)}} \tag{7.31}$$

where

$$\frac{\partial(f_1, f_2, \ldots, f_n)}{\partial(z_1, z_2, \ldots, z_n)} = \begin{vmatrix} \dfrac{\partial f_1}{\partial z_1} & \dfrac{\partial f_1}{\partial z_2} & \cdots & \dfrac{\partial f_1}{\partial z_n} \\ \dfrac{\partial f_2}{\partial z_1} & \dfrac{\partial f_2}{\partial z_2} & \cdots & \dfrac{\partial f_2}{\partial z_n} \\ \vdots & \vdots & & \vdots \\ \dfrac{\partial f_n}{\partial z_1} & \dfrac{\partial f_n}{\partial z_2} & \cdots & \dfrac{\partial f_n}{\partial z_n} \end{vmatrix}$$

and the functions f_i are defined in Eq. 3.17.

An alternative way to find these derivatives is to perturb the delay of the k^{th} transmission line τ_k by a small amount $\Delta\tau_k$ and then solve the system of Eqs. 7.2 to find z_j', $j = 1, 2, \ldots, n$. If z_j, $j = 1, 2, \ldots, n$ was the solution of the system to begin with, the partial derivatives $\partial z_j / \partial \tau_k$ are approximately expressed as

$$\frac{\partial z_j}{\partial \tau_k} \cong \frac{z_j' - z_j}{\Delta \tau_k}, \quad \begin{matrix} j = 1, 2, \ldots, n, \\ k = 1, 2, \ldots, n. \end{matrix} \tag{7.32}$$

This method was used to determine the derivatives in the example given later in this chapter to illustrate the method of solution put forth earlier in Section 7. 2.

(ii) Any transmission pole ξ of the transmission line network satisfies Eq. 3. 12. The j^{th} nondominant pole,

$$\alpha_j \pm j\gamma_j$$

may, therefore, be computed as the solution to

$$\mathrm{Re}[\,C_T'(\tau_1,\ldots,\tau_n; z_1,\ldots,z_n; \alpha_j, \gamma_j)] = 0 \qquad (7.34)$$

$$\mathrm{Im}[\,C_T'(\tau_1,\ldots,\tau_n; z_1,\ldots,z_n; \alpha_j, \gamma_j)] = 0 \quad . \qquad (7.35)$$

γ_j thus determined may be written as

$$\gamma_j(\tau_1,\ldots,\tau_n; z_1,\ldots,z_n) \ .$$

However, since each z_j is a function of $(\tau_j,\ j = 1,\ldots,\ n)$, it is possible to express γ_j as a function of delays alone. Designate this $\mu_j(\tau_1,\ldots,\tau_n)$. Therefore,

$$\mu_j(\tau_1,\ldots,\tau_n) = \gamma_j(\tau_1,\ldots,\tau_n; z_1,\ldots,z_n)\Big|_{\substack{z_1 = z_1(\tau_1,\ldots,\tau_n) \\ \vdots \\ z_n = z_n(\tau_1,\ldots,\tau_n)}} \quad . \qquad (7.36)$$

Equating total differentials on both sides of Eq. 7.36,

$$\sum_{k=1}^{n} \frac{\partial \mu_j}{\partial \tau_k} \Delta \tau_k = \sum_{k=1}^{n} \frac{\partial \gamma_j}{\partial \tau_k} \Delta \tau_k + \sum_{k=1}^{n} \frac{\partial \gamma_j}{\partial z_k} \Delta z_k \quad . \tag{7.37}$$

Thus

$$\frac{\partial \mu_j}{\partial \tau_m} = \frac{\partial \gamma_j}{\partial \tau_m} + \sum_{k=1}^{n} \frac{\partial \gamma_j}{\partial z_k} \frac{\partial z_k}{\partial \tau_m} \quad , \qquad \begin{matrix} j = 1, 2, \ldots, J \ , \\ m = 1, 2, \ldots, n \ . \end{matrix} \tag{7.38}$$

The derivatives $\partial \mu_j / \partial \tau_m$ may be computed making use of either side of Eq. 7.38. In the example given to illustrate the minimization technique we used Eq. 7.38 in the following way.

μ_j was found at $\tau_1, \tau_2, \ldots, \tau_n$ and $z_1, z_2, \ldots, z_n$, where $z_1, z_2, \ldots, z_n$ were the solution of Eq. 7.2 with $\tau_1, \ldots, \tau_n$ given. τ_m was then perturbed by $\Delta \tau_m$. The system of Eqs. 7.2 was solved for $z'_1, z'_2, \ldots, z'_n$ with $\tau_1, \tau_2, \ldots, \tau_m + \Delta \tau_m, \ldots, \tau_n$ specified. Finally the imaginary part, designated μ'_j, of the j^{th} non-dominant pole was again determined from Eqs. 7.34 and 7.35 using $\tau_1, \ldots, \tau_m + \Delta \tau_m, \ldots, \tau_n$ and $z'_1, z'_2, \ldots, z'_n$ for the delays and the characteristic impedances. $\partial \mu_j / \partial \tau_m$ was then evaluated from

$$\frac{\partial \mu_j}{\partial \tau_m} \cong \frac{\mu_j' - \mu_j}{\Delta \tau_m} \quad . \tag{7.39}$$

(iii) If the j^{th} transmission zero, $\pm j\nu_j$, being associated with the j^{th} nondominant pole, is assumed to be produced by the stub whose delay is τ_p, then

$$\cos(\nu_j \tau_p) = 0 \quad . \tag{7.40}$$

This allows the derivative $\partial \nu_j / \partial \tau_p$ to be expressed as

$$\frac{\partial \nu_j}{\partial \tau_p} = \frac{\nu_j}{\tau_p} \quad , \tag{7.41}$$

and all the other derivatives

$$\frac{\partial \nu_j}{\partial \tau_k} = 0 \quad , \quad k \neq p \quad . \tag{7.42}$$

7.4 Example

An example of the optimization procedure outlined above is herein presented. The initial design is a two-element (n = 2) transmission line network in Fig. 7.1. The element values of this network which were selected for dominant Butterworth poles are

$$z_1^o = 0.3 \qquad \tau_1^o = 0.253895$$

$$z_2^o = 3.0 \qquad \tau_2^o = 0.5621879$$

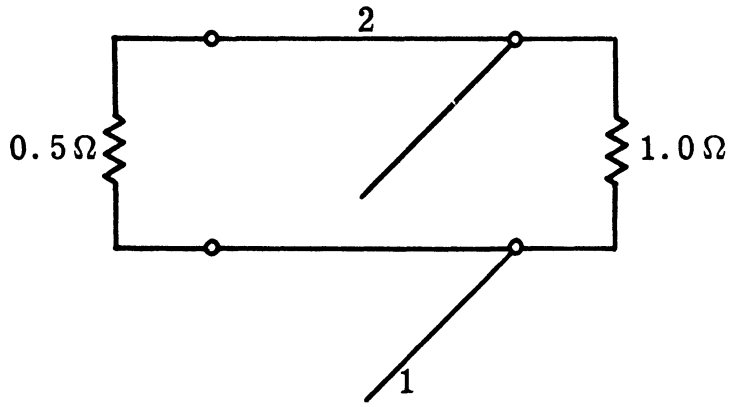

Fig. 7.1. A 2-element transmission line network

The first nondominant pole was found to be $\mu_1^o = 5.615151$ and the transmission zero created by the stub was at $\nu_1^o = 6.18677$. The optimization problem is to minimize the distance between the transmission zero and the nondominant pole (J = 1) without violating the constraints on characteristic impedances

$$0.3 \leqq z_1 \leqq 3.0 \quad \text{and} \quad 0.3 \leqq z_2 \leqq 3.0 \ .$$

It is also necessary to maintain the pole locations at the Butterworth poles. This results in the constraints

$$f_1(\tau_1, \tau_2, z_1, z_2) = 0 \quad \text{and} \quad f_2(\tau_1, \tau_2, z_1, z_2) = 0 \ .$$

These functions f_1 and f_2 are the real and imaginary parts of the denominator of the input impedance looking into either end of the distributed network.

The derivatives needed were

$$\frac{\partial z_1^o}{\partial \tau_1^o} = 1.2082 \ , \quad \frac{\partial z_1^o}{\partial \tau_2^o} = 0.05195 \ , \quad \frac{\partial z_2^o}{\partial \tau_1^o} = 0.5813 \ , \quad \frac{\partial z_2^o}{\partial \tau_2^o} = -5.4208 \ ,$$

$$\frac{\partial \mu_1^o}{\partial \tau_1^o} = -0.94 \ , \quad \frac{\partial \mu_1^o}{\partial \tau_2^o} = -8.3123 \ , \quad \frac{\partial \nu_1^o}{\partial \tau_1^o} = -24.4 \ , \quad \frac{\partial \nu_1^o}{\partial \tau_2^o} = 0 \ .$$

Substituting these derivatives in Eqs. 7.24 through 7.30, (constraints $z_1 \leqq 3.0$ and $z_2 \geqq 0.3$ are not included in the tableau) the linear problem was written as

$$\min x_1$$

Subject to

$$\begin{bmatrix} -1 & 23.46 & -23.46 & -8.3123 & 8.3123 \\ -1 & -23.46 & 23.46 & 8.3123 & -8.3123 \\ 0 & -1.2082 & 1.2082 & -0.05195 & 0.05195 \\ 0 & 0.5813 & -0.5813 & -5.4208 & 5.4208 \\ 0 & 1 & 1 & 0 & 0 \\ 0 & 0 & 0 & 1 & 1 \end{bmatrix} \begin{bmatrix} x_1 \\ x_2 \\ x_3 \\ x_4 \\ x_5 \end{bmatrix} \leqq \begin{bmatrix} 0.575 \\ -0.575 \\ 0 \\ 0 \\ 0.2 \\ 0.2 \end{bmatrix}$$

$$x_i \geqq 0 \quad i = 1, 2, \ldots, 5 .$$

This linear subproblem was solved by LINPG, a program for solving linear programming problems available in MTS [57]. The solution was found to be

$$x_1 = 4.1633 \times 10^{-17}$$

$$x_2 = 2.547784 \times 10^{-2}$$

$$x_3 = 0$$

$$x_4 = 2.732119 \times 10^{-3}$$

$$x_5 = 0$$

The correction to the delays of the lines were found from Eq. 7. 22. They were

$$\Delta\tau_1^o = x_2 - x_3 = 0.025477$$

$$\Delta\tau_2^o = x_4 - x_5 = 0.002732$$

Using Eq. 7. 16, τ_1^1 and τ_2^1 were found to be

$$\tau_1^1 = 0.279372$$

$$\tau_2^1 = 0.5649199$$

For these lengths of the transmission lines, other quantities of interest were

$$z_1^1 = 0.3309906$$

$$z_2^1 = 3.0001984$$

$$\mu_1^1 = 5.5645$$

$$\nu_1^1 = 5.62257$$

The value of the cost function, $|\mu_1 - \nu_1|$, was reduced from $|\mu_1^o - \nu_1^o|$ = 0.57162 to $|\mu_1^1 - \nu_1^1|$ = 0.05807.

Repeating the procedure at τ_1^1, τ_2^1, z_1^1, z_2^1, the cost function was reduced to

$$|\mu_1^2 - \nu_1^2| = 5.5562 - 5.5499 = 0.0063$$

at

$$\tau_1^2 = 0.283028$$

$$\tau_2^2 = 0.5653892$$

$$z_1^2 = 0.3354596$$

$$z_2^2 = 2.9999294$$

The attenuation of the two element network before and after optimization is indicated in Fig. 7.2.

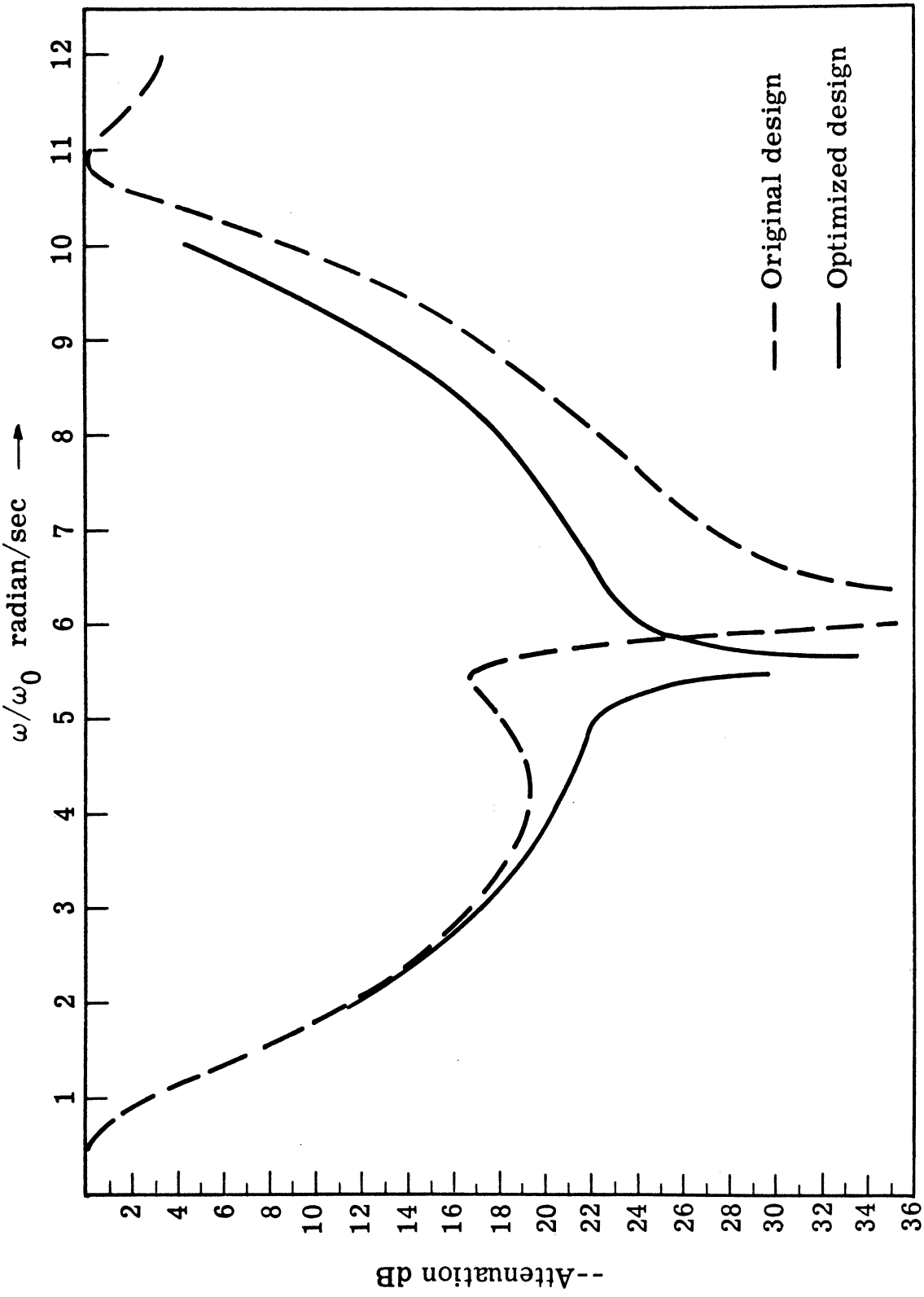

Fig. 7.2 Attenuation of a two-element distributed filter

Chapter 8

Existence Consideration For The Solution Of The Two-Element Transmission Line Networks

The element values of the network configuration that realizes a prescribed set of dominant transmission poles are the solution of the system of equations

$$f_i(\ell_1, \ldots, \ell_n; z_1, \ldots, z_n) = 0 \ , \quad i = 1, 2, \ldots, n \ , \qquad (8.1)$$

where n is the number of the elements in the network. It has been shown that under special conditions of very high impedance connecting lines and very low impedance stubs and all the lengths being electrically short, the solution of the system (Eq. 8.1) can be approximately determined and this can then be refined by an iterative procedure. However, as the characteristic impedances are perturbed toward a desired range of values, solution of the system (Eq. 8.1) for real $\ell_1, \ldots, \ell_n$ and $z_1, \ldots, z_n$ is not analytically guaranteed, though solutions did exist in every one of the limited number of cases tried by the author.

For the relatively simple case of $n = 2$, two questions will be answered here. In the circuit given in Fig. 8.1, if R_c, R_s, z_c, z_s are specified, are there values of τ_c and τ_s that will

realize a prescribed set of dominant poles $s_{1,2} = x \pm jy$? If there are, what approximately are their values?

It is known that at a pole of the network in Fig. 8.2, $y_1 + y_2 = 0$, where y_1 and y_2 are admittances as indicated in the figure. The network in Fig. 8.1 may be divided along 1 - 1'. At a specified pole $s = x \pm jy$

$$y_c + y_s = 0 \ . \tag{8.2}$$

As defined in Fig. 8.1,

$$y_c = \frac{1}{z_c} \frac{e^{2s\tau_c} - a}{e^{2s\tau_c} + a} \ , \tag{8.3}$$

and

$$y_s = \frac{1}{R_s} + \frac{1}{z_s} \frac{e^{2s\tau_s} - 1}{e^{2s\tau_s} + 1} \ , \tag{8.4}$$

where

$$a = \frac{R_c - z_c}{R_c + z_c} \ . \tag{8.5}$$

The transformation $w = e^{2s\tau}$ maps each of the infinite strips

$(2k - 1)\frac{\pi}{2} < \mathrm{Im}(s\tau) < (2k + 1)\frac{\pi}{2}$, $k = \ldots, -2, -1, 0, 1, 2, \ldots$

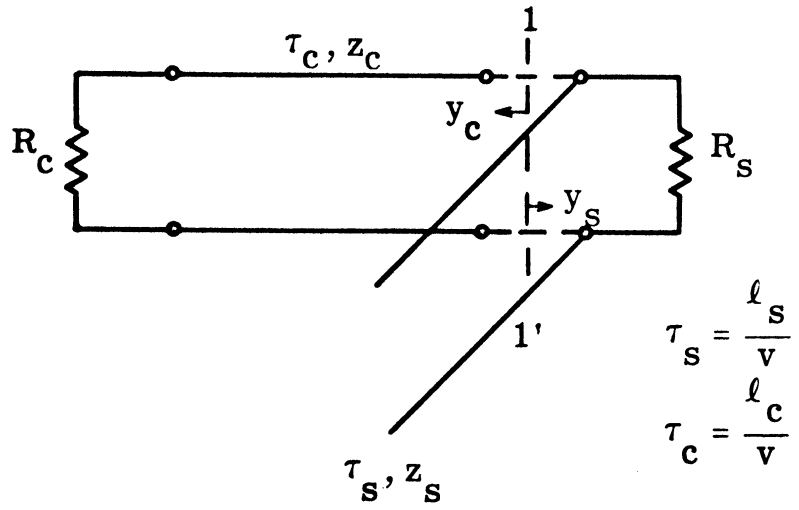

Fig. 8.1. A doubly terminated 2-element transmission line network. ℓ_c, ℓ_s are the lengths, and z_c, z_s are the characteristic impedances of the connecting line and the stub respectively

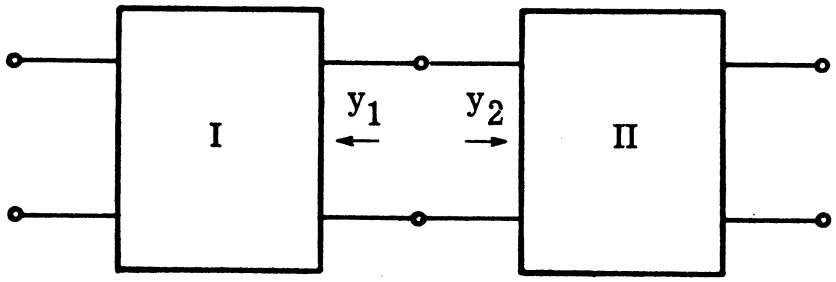

Fig. 8.2. A 2-port network shown bisected into two 2-ports, I and II

into the whole of the w plane. For the pole s to be in the principal strip of $e^{2s\tau_c}$ and $e^{2s\tau_s}$, the maximum value of τ_s and τ_c cannot exceed τ_m, where τ_m is given by

$$2y\tau_m = \pi \ . \tag{8.6}$$

(Here the principal strip is defined as the strip that contains the origin.) If the admittances $-y_c$ and y_s are plotted as functions of τ_c and τ_s respectively for $0 \leqq \tau_c \leqq \pi/2y$ and $0 \leqq \tau_s \leqq \pi/2y$, the points of intersection of the two curves will satisfy Eq. 8.2. Thus, intersection of the curves $-y_c$ and y_s drawn with τ_c and τ_s as parameters will indicate the existence of the solution of the system of Eqs. 8.1. Also approximate values of τ_c and τ_s at the solution can be read off at the intersection.

8.1 Variation of the Input Admittance of A Resistance-Terminated Transmission Line

This section deals with the general shape of the admittance y_c drawn with τ_c as parameter. Since

$$e^{2s\tau_c} = e^{2(x+jy)\tau_c}$$

$$= e^{2x\tau_c} e^{j2y\tau_c} \ ,$$

this represents, in the complex-plane, a vector that starts, at

$\tau_c = 0$, on the real axis with a magnitude of unity, rotates counter-clockwise decreasing in magnitude as τ_c increases and finally lines up with negative real axis at $\tau_c = \pi/2y$, the magnitude at this value of τ_c being given by $-e^{x(\pi/y)}$. The locus of the extremity of $e^{2s\tau_c}$ with τ_c as parameter for $0 < \tau_c < \pi/2y$ is shown in Fig. 8.3.

Case I: $a > 0$.

Since $a = (R_c - z_c / R_c + z_c)$, the condition of a being positive means that the connecting line is terminated in a resistance greater than its characteristic impedance.

(a) $a < e^{x(\pi/y)}$. In Fig. 8.4(a), the position of a is shown on a plot of $e^{2s\tau_c}$. The vectors $e^{2s\tau_c} - a$ and $e^{2s\tau_c} + a$, and their associated angles α and β are also indicated. The angle $(\alpha-\beta)$ is the angle associated with

$$y_c = \frac{1}{z_c} \frac{e^{2s\tau_c} - a}{e^{2s\tau_c} + a} .$$

Now as the point D moves from E to F on the curve $e^{2s\tau_c}$ corresponding to the increase in τ_c, $\alpha - \beta$ starts at zero, increases and comes back to zero. Typically, y_c can therefore be represented as in Fig. 8.4(b).

(b) $a > e^{\pi(x/y)}$. However, if a is greater than $e^{\pi(x/y)}$ as indicated in Fig. 8.5(a), it can be concluded $(\alpha-\beta)$ now ranges from

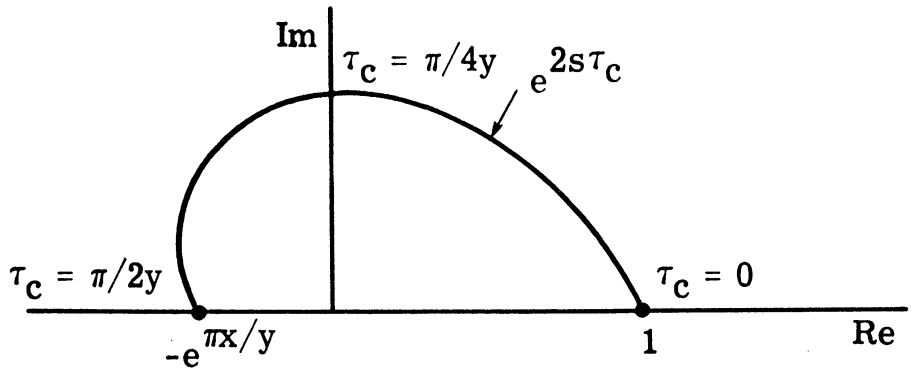

Fig. 8.3. The locus of the extremity of $e^{2s\tau_c}$ for $0 \leq \tau_c \leq \pi/2y$

(a)

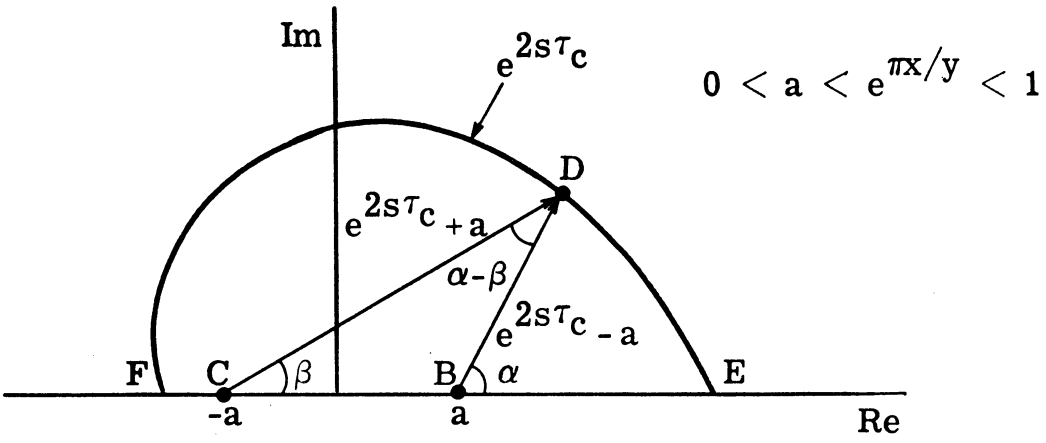

(b)

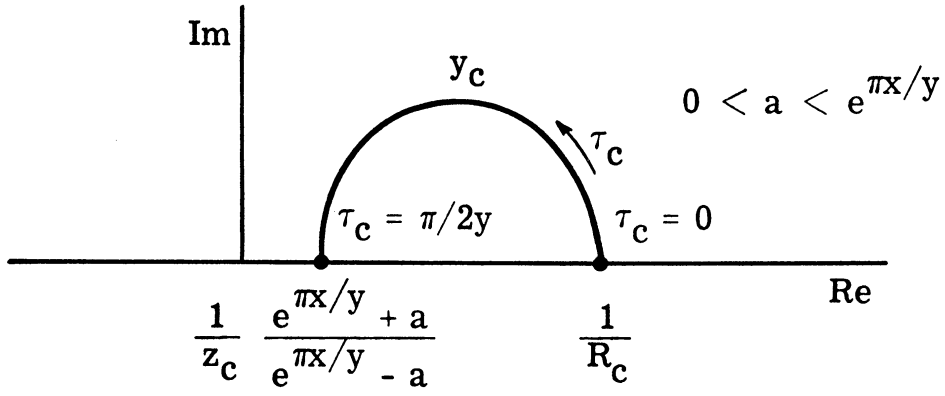

Fig. 8.4. (a) Vectors $e^{2s\tau_c} + a$ and $e^{2s\tau_c} - a$ with $0 < a < e^{\pi x/y}$ and their associated angles β and α
(b) Typical representation of y_c with $0 < a < e^{\pi x/y}$

(a)

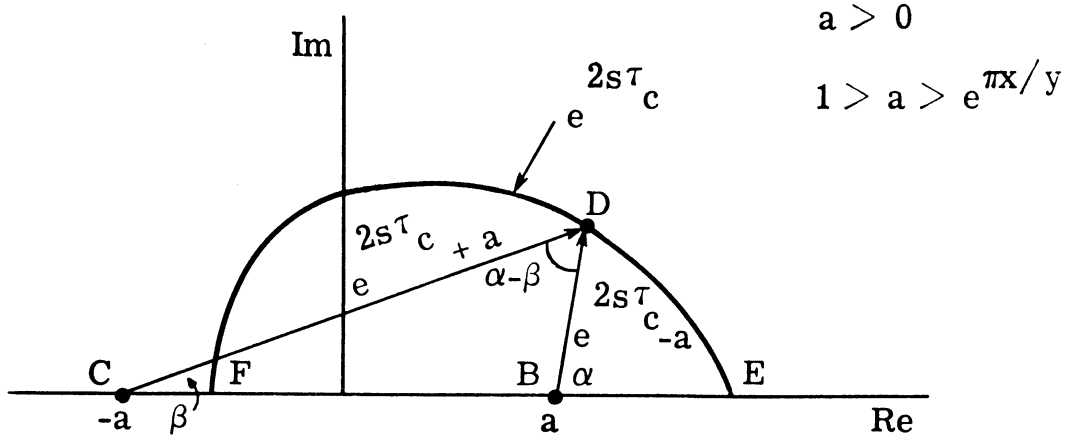

(b)

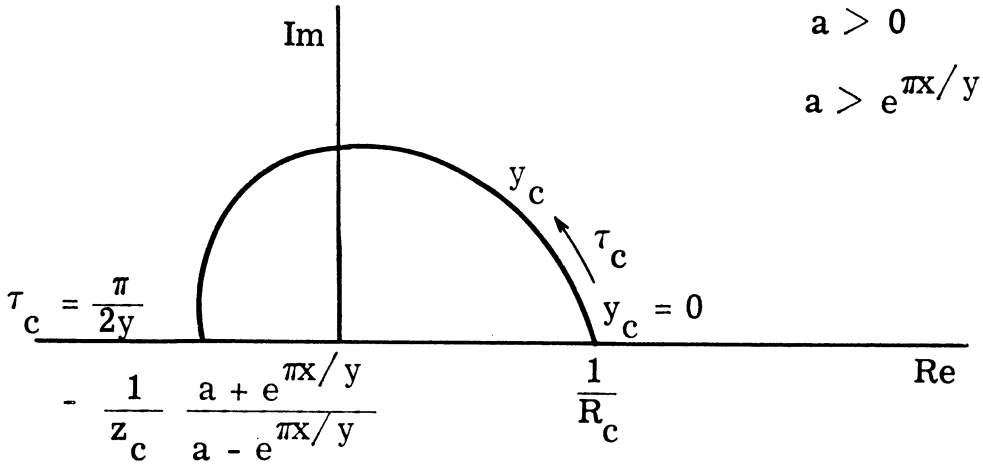

Fig. 8.5. (a) Vectors $e^{2s\tau_c} + a$ and $e^{2s\tau_c} - a$ with $0 < e^{\pi x/y} < a < 1$ and their associated angles β and α

(b) Typical representation of y_c with $e^{\pi x/y} < a$

zero to 180 degrees. Typical representation y_c for this case is shown in Fig. 8.5(b).

Case II: $a < 0$

This means that the resistance that terminates the connecting line is less than the characteristic impedance of the line.

(a) $0 > a > -e^{\pi(x/y)}$. The positions of a, $-a$ and of the vectors $e^{2s\tau_c} - a$ and $e^{2s\tau_c} + a$ are shown in Fig. 8.6(a). The angle β, it is seen from the figure, is greater than α except at E and F where they are equal. Thus $(\alpha-\beta)$ starts at zero degrees, decreases and then increases to zero degrees. The variation of y_c with τ_c as parameter can be represented as in Fig. 8.6(b).

(b) $-e^{-\pi(x/y)} > a$. For this case the point B in Fig. 8.6(a) lies beyond F on the negative real axis. Therefore, $(\alpha-\beta)$ ranges from zero to $-\pi$. The corresponding y_c is shown in Fig. 8.7.

8.2 Variation of the Admittance of an Open Shunt Stub in Shunt With A Resistor

The admittance y_s is given by

$$\frac{1}{R_s} + \frac{1}{z_s} \frac{e^{2s\tau_s} - 1}{e^{2s\tau_s} + 1} .$$

Fig. 8.8(a) shows the vectors $e^{2s\tau_s} - 1$ and $e^{2s\tau_s} + 1$ on a plot of $e^{2s\tau_s}$. It is deduced from the figure that $\alpha - \beta$ ranges from

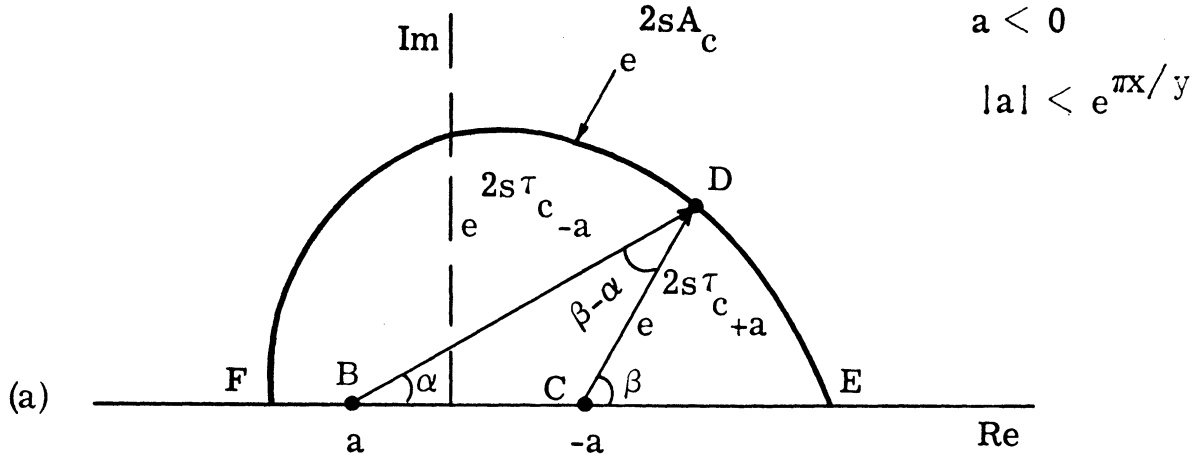

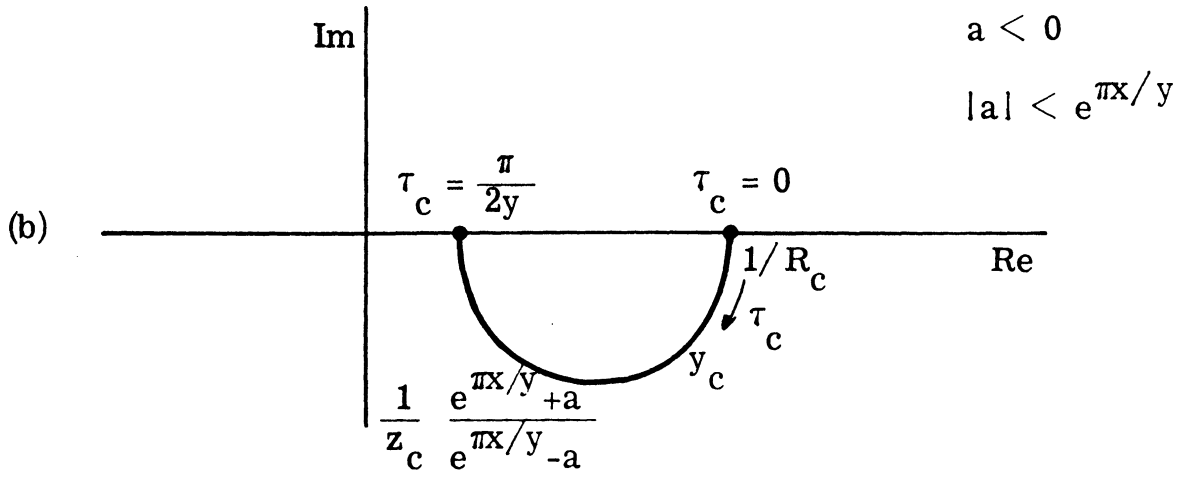

Fig. 8.6. (a) Vectors $e^{2s\tau_c} - a$ and $e^{2s\tau_c} + a$ with $0 < -a < e^{\pi x/y}$
(b) Typical representation of y_c with $0 < -a < e^{\pi x/y}$ for $0 \leq \tau_c \leq \pi/2y$

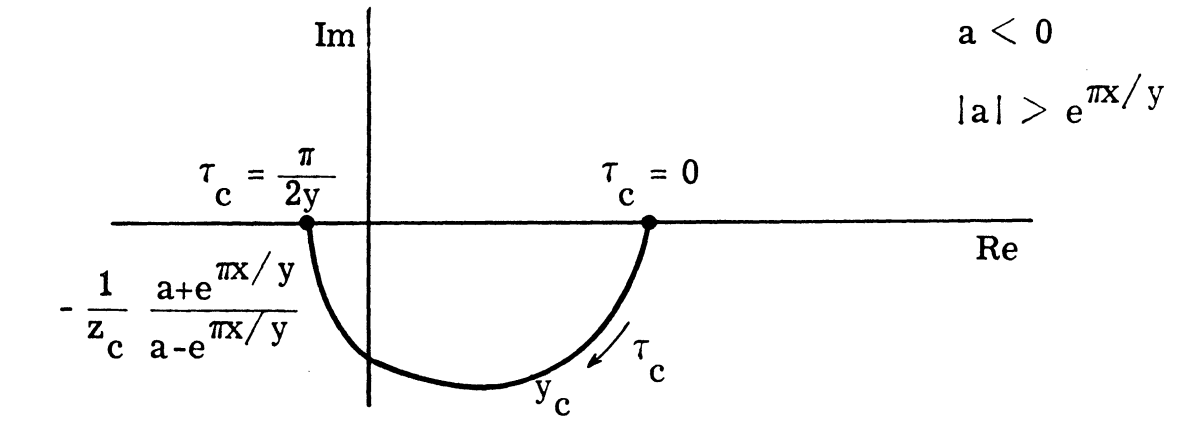

Fig. 8.7. Typical representation of y_c with $0 < e^{\pi x/y} < -a$ for $0 \leq \tau_c \leq \pi/2y$

$\pi/2$ to π. Therefore typically

$$\frac{1}{z_s}\,\frac{e^{2s\tau_s}-1}{e^{2s\tau_s}+1}$$

and y_s can be represented as in Fig. 8.8(b).

8.3 Condition for Existence of Solution

Typical shapes of the curves y_c and y_s as the lengths of the connecting line and the stub varies are now known. Since the existence of the solution is indicated by the intersection of $-y_c$ and y_s, examine $-y_c$ in Figs. 8.4(b), 8.5(b), 8.6(b) and 8.7 and y_s in Fig. 8.8(b). Since y_s occupies the first and second quadrants and $-y_c$ lies in the third and fourth quadrants when $a > 0$, no intersection is possible. Therefore no solution in the range $0 \leqq \tau_s \leqq \tau_m$ and $0 \leqq \tau_c \leqq \tau_m$ can exist when R_c is greater than z_c. For $a < 0$, $-y_c$ is capacitive and thus $-y_c$ may intersect with y_s. If either of the extremeties of $-y_c$ (y_s) lies in the interval defined by the extremeties of y_s ($-y_c$) and the other outside this interval, the solution is guaranteed; since the two curves have to intersect under this condition. If, however, this condition is not met by the element values of the network, the question of existence is decided by drawing the curves $-y_c$ and y_s and determining if they intersect or not.

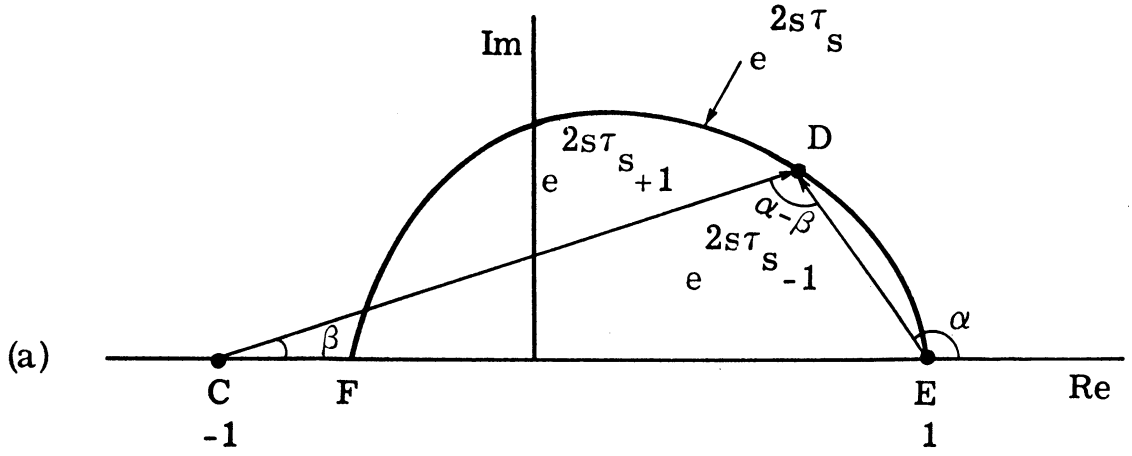

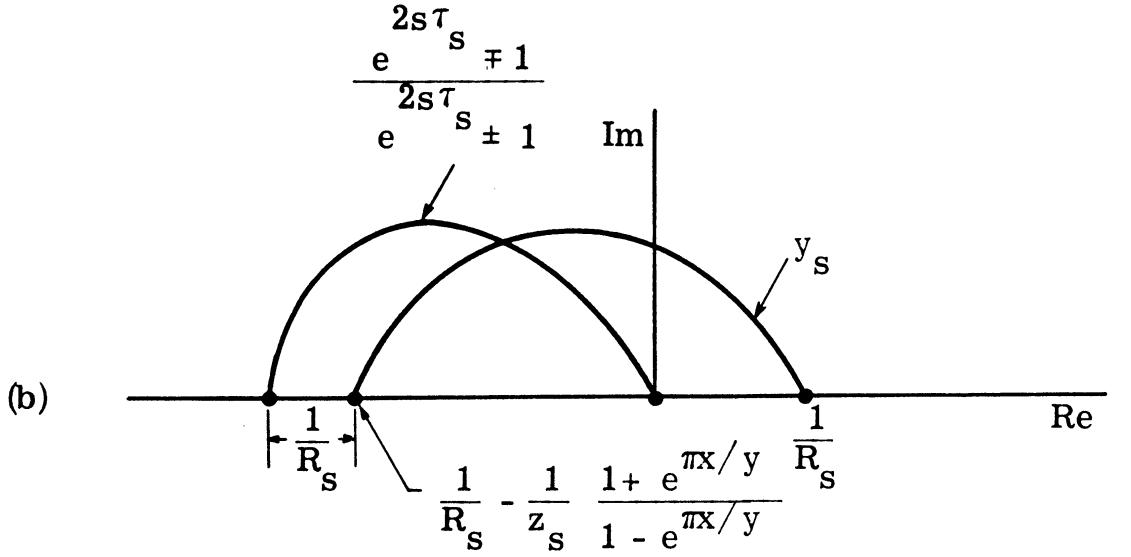

Fig. 8.8. (a) Vectors $e^{2s\tau_s}+1$ and $e^{2s\tau_s}-1$ and the locus of $e^{2s\tau_s}$ for $0 \leq \tau_s \leq \pi/2y$

(b) Typical representation of y_s for $0 \leq \tau_s \leq \pi/2y$

It is also observed that when the condition is not satisfied, the two curves, if they intersect, will intersect at two points, thus giving two solutions.

8.4 Example

In Fig. 8.1, let

$$R_s = 0.5 \ , \quad R_c = 0.5 \ ,$$

$$z_s = 0.3 \ , \quad z_c = 3.0 \ ,$$

and

$$s = -0.707 \pm j\, 0.707$$

For $\tau_s = 0$,

$$y_s = \frac{1}{R_s} = 2 \ .$$

For $\tau_s = \pi / 2y$,

$$y_s = \frac{1}{R_s} + \frac{1}{z_s} \frac{e^{2s\tau_s} - 1}{e^{2s\tau_s} + 1}$$

$$= \frac{1}{R_s} + \frac{1}{z_s} \frac{e^{2x\tau_s} e^{2jy\tau_s} - 1}{e^{2x\tau_s} e^{2jy\tau_s} + 1}$$

$$= \frac{1}{R_s} + \frac{1}{z_s} \frac{-e^{x\pi/y} - 1}{-e^{x\pi/y} + 1}$$

$$= \frac{1}{R_s} - \frac{1}{z_s} \frac{1 + e^{\pi x/y}}{1 - e^{\pi x/y}}$$

$$= -1.639 \ .$$

For $\tau_c = 0$,

$$-y_c = -\frac{1}{z_c} \frac{e^{2s\tau_c} - a}{e^{2s\tau_c} + a}$$

$$= -\frac{1}{z_c} \frac{1 - a}{1 + a}$$

$$= -\frac{1}{z_c} \frac{2z_c}{2R_c}$$

$$= -\frac{1}{R_c} = -2 \ .$$

For $\tau_c = \pi/2y$,

$$-y_c = -\frac{1}{z_c} \frac{-e^{\pi(x/y)} - a}{-e^{\pi(x/y)} + a}$$

$$= 0.295 \ .$$

The two extremities of $-y_c$ are

$$-2 \text{ and } 0.295$$

and those for y_s are

$$2 \text{ and } -1.639 \ .$$

Since 0.295 lies between -1.639 and 2, and -2 is outside this range, the existence of τ_c and τ_s that will realize the dominant poles $-0.707 \pm j\,0.707$ is assured. $-y_c$ and y_s are plotted in solid line in Fig. 8.9 with τ_c and τ_s as parameters. The two curves intersect, as predicted from the positions of their extremities.

It is possible that for the specified values of R_s, R_c, z_s and z_c the desired condition will not be satisfied. For example, in the above example if R_s is specified to be 1.0 instead of 0.5, the other quantities being left unchanged, the two extremities of y_s are

$$1.0 \text{ and } -2.639$$

and the condition is not satisfied. For this case, y_s is shown by the dashed curve in Fig. 8.9. Since y_c and y_s now intersect at two positions, there are two solutions.

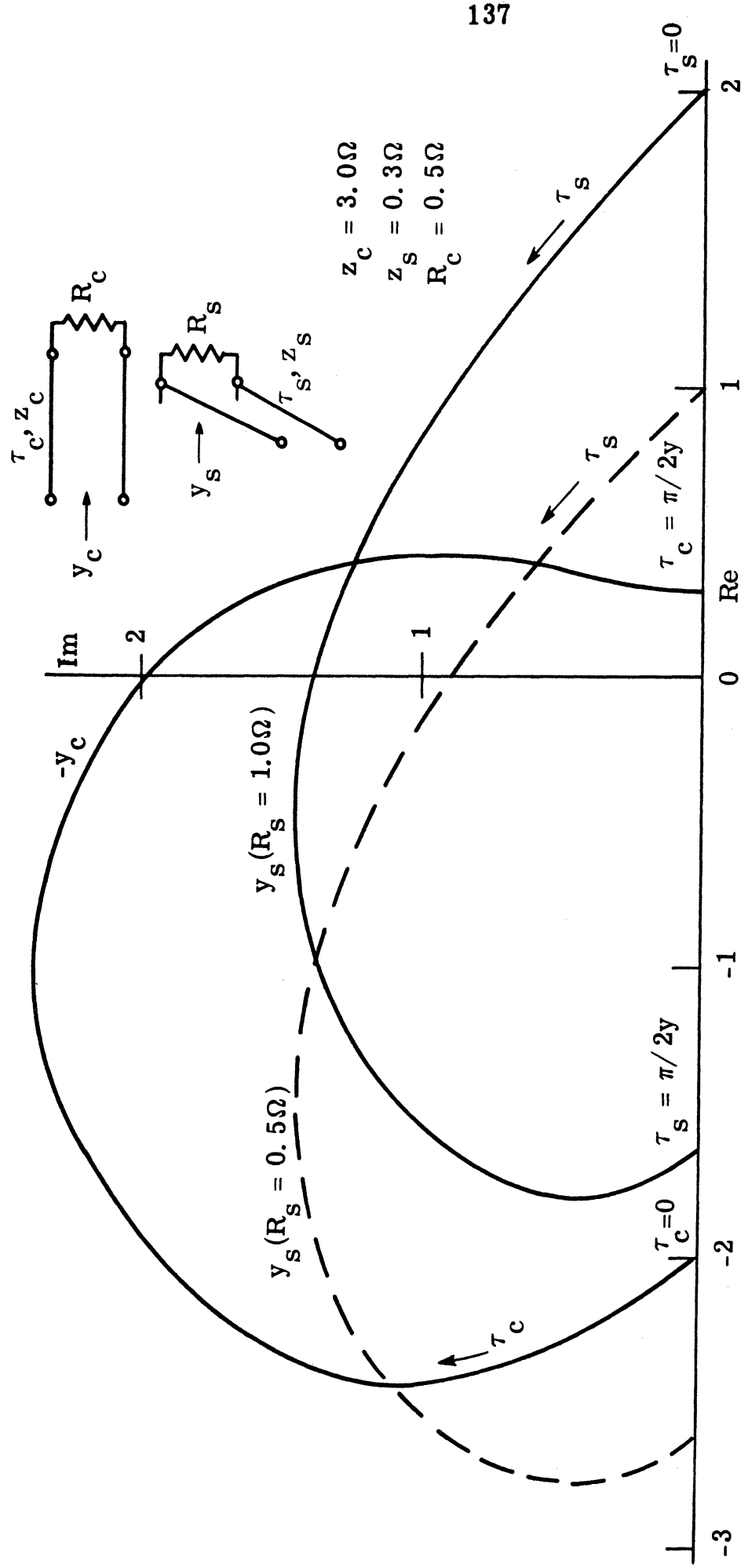

Fig. 8.9. Plots of $-y_c$ for $0 \leq \tau_c \leq \pi/2y$, and y_s for $0 \leq \tau_s \leq \pi/2y$

Chapter 9

Summary

An iterative numerical technique has been presented for the synthesis of noncommensurate transmission line networks to realize a prescribed set of dominant transmission poles and zeros. It has been shown in Chapter 3 that the synthesis is accomplished when a system of nonlinear equations is solved. In Chapter 4, a Newton-Raphson iteration has been outlined which solves the system of nonlinear equations obtained when the distributed networks have a particular structure: open shunt stubs alternating with connecting lines in cascade. The initial solution which is required to start the Newton-Raphson iteration has been derived.

In Chapter 5, the method has been illustrated with the example of a nine-element transmission line network for which nine dominant transmission poles and four pairs of real frequency axis zeros are specified. The transmission characteristics of the realized distributed filter differ from those of a lumped element prototype because of the nondominant poles and zeros which appear. For the nine-element low-pass example the principal effect is a sharp drop in the stopband attenuation at about 1.5 octaves above the passband cutoff frequency. This design was then modified by shifting a transmission zero along

the $j\omega$-axis to a position opposite the nondominant pole closest to the passband. The modified design maintains the stopband attenuation to about two octaves beyond the passband edge. This design was fabricated; its measured response verifies the theoretically predicted response.

The periodic nature of network functions that are characteristic of distributed parameter networks gives rise to nondominant poles. In Chapter 6, it has been proved that one and only one nondominant pole is present in each repetition strip of every transmission line of a network that is made up of alternating open shunt stubs and connecting lines. A numerical technique has been delineated to compute the nondominant pole positions and illustrated with an example, which verifies the occurrence of exactly one nondominant pole in each repetition strip.

The example of Chapter 5 demonstrates that the undesirable effect of a nondominant pole on the response of a network in the frequency range of interest can be nullified, to an extent, by aligning a nondominant transmission zero opposite the pole. In Chapter 7, a nonlinear programming problem has been formulated for this purpose and a method for its solution by successive linearizations has been given. An example has been added to illustrate this method.

Finally in Chapter 8, the existence of solutions for the system of equations (Eq. 3. 17) developed in Chapter 3 has been analytically investigated for $n = 2$.

Appendix I

Proof of The Expressions Given in Eqs. 3. 4 Through 3. 7

An expression for the general circuit paramater matrix for the lossless part of the network in Fig. 3. 1 is derived here. We want to prove that

> the general circuit parameters A_t, B_t, C_t and D_t of a circuit consisting of stubs and connecting lines in cascade can be expressed respectively by Eqs. 3. 4 through 3. 7.

Proof: An examination of Eq. 3. 3 and Eqs. 3. 4 through 3. 7 shows that the denominators of A_t, B_t, C_t and D_t which are all identical are formed when factors $1/z_j \cosh \Phi_j$ from the stubs (j=1, 3,..., n) (see Eq. 3. 1) and factors $1/z_j$ from the connecting lines (j=2, 4,..., n-1) (see Eq. 3. 2) are multiplied. Thus it only remains to be proved that the numerators of Eqs. 3. 4 through 3. 7, that is, the modified GCP matrix as defined in Eq. 6. 3 is the product of a chain of matrices that is obtained when each stub in Fig. 3. 1 is represented by Eq. 6. 5 and each connecting line, by Eq. 6. 4. This will be demonstrated by induction.

Let us assume that the lossless network in Fig. I. 1(a) which is made up of n - 1 transmission line elements in cascade satisfy the

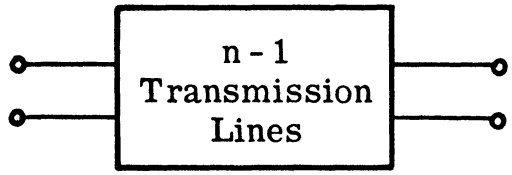

(a)

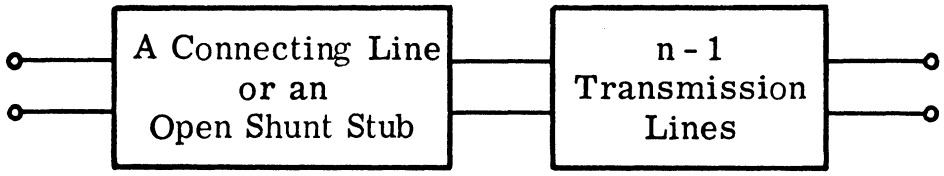

(b)

Fig. I.1. (a) A lossless 2-port having n - 1 transmission line elements in cascade
(b) The network in (a) augmented

theorem. The modified GCP matrix of this network can, therefore, be written as

$$\begin{bmatrix} A'_m & B'_m \\ C'_m & D'_m \end{bmatrix} \triangleq \begin{bmatrix} \sum_{i=1}^{2^{n-2}} a'_i \cosh(\theta_i^{n-1} s) & \sum_{i=1}^{2^{n-2}} b'_i \sinh(\theta_i^{n-1} s) \\ \sum_{i=1}^{2^{n-1}} c'_i \sinh(\theta_i^{n-1} s) & \sum_{i=1}^{2^{n-2}} d'_i \cosh(\theta_i^{n-1} s) \end{bmatrix} . \quad \text{(I. 1)}$$

We now prove that adding a stub or a connecting line to the circuit in Fig. I. 1(a) results in an augmented circuit [Fig. I. 1(b)] whose modified GCP matrix can be expressed as Eq. 6. 3. The modified GCP matrix of the augmented circuit can be written as

$$\begin{bmatrix} A_m & B_m \\ C_m & D_m \end{bmatrix} = \begin{bmatrix} z_n \cosh \Phi_n & F z_n^2 \sinh \Phi_n \\ \sinh \Phi_n & z_n \cosh \Phi_n \end{bmatrix} \begin{bmatrix} A'_m & B'_m \\ C'_m & D'_m \end{bmatrix} \quad \text{(I. 2)}$$

where

$\Phi_n = \frac{s l_n}{v}$, l_n being the length of the augmenting line,

z_n = the characteristic impedance of the augmenting line,

F = 0, if the augmenting line is a stub,

= 1, if the augmenting line is a connecting line.

Therefore, one can write

$$A_m = A'_m z_n \cosh \Phi_n + C'_m z_n^2 F \sinh \Phi_n \tag{I. 3}$$

$$B_m = B'_m z_n \cosh \Phi_n + D'_m z_n^2 F \sinh \Phi_n \tag{I. 4}$$

$$C_m = A'_m \sinh \Phi_n + C'_m z_n \cosh \Phi_n \tag{I. 5}$$

$$D_m = B'_m \sinh \Phi_n + D'_m z_n \cosh \Phi_n \tag{I. 6}$$

A_m can now be manipulated in the following way. Substituting for A'_m and C'_m from Eq. I. 1 in Eq. I. 3,

$$\begin{aligned} A_m &= \sum_{i=1}^{2^{n-2}} a'_i z_n \cosh \Phi_n \cosh (\theta_i^{n-1} s) + \sum_{i=1}^{2^{n-2}} F z_n^2 c'_i \sinh \Phi_n \sinh (\theta_i^{n-1} s) \\ &= \sum_{i=1}^{2^{n-2}} \frac{1}{2} a'_i z_n [\cosh (\theta_i^{n-1} s + \Phi_n) + \cosh (\theta_i^{n-1} s - \Phi_n)] \\ &+ \sum_{i=1}^{2^{n-2}} \frac{1}{2} F c'_i z'^2_n [\cosh (\theta_i^{n-1} s + \Phi_n) - \cosh (\theta_i^{n-1} s - \Phi_n)] \\ &= \sum_{i=1}^{2^{n-2}} \frac{1}{2} (a'_i + F c'_i z_n) z_n \cosh (\theta_i^{n-1} s + \Phi_n) \end{aligned} \tag{I. 7}$$

$$+ \sum_{i=1}^{2^{n-2}} \frac{z_n}{2}(a_i' - Fc_i' z_n') \cosh(\theta_i^{n-1} s - \Phi_n)$$

(I. 7 Cont.)

$$= \sum_{i=1}^{2^{n-1}} a_i \cosh(\theta_i^n s)$$

where

$$a_i = \frac{1}{2}(a_i' z_n + Fc_i' z_n^2) \quad , \quad i = 1, 2, \ldots, 2^{n-2}$$

$$a_{2^{n-2}+i} = \frac{1}{2}(a_i' z_n - Fc_i' z_n^2) \quad , \quad i = 1, 2, \ldots, 2^{n-2} \quad .$$

The expressions for B_m, C_m and D_m in Eqs. I. 4, I. 5 and I. 6 can also be manipulated in the same manner into the forms given in Eq. 6. 3.

The proof will be completed by pointing out that a circuit having a single stub or a connecting line satisfies the theorem. This is verified when matrix (Eq. 6. 3) for $n = 1$ is compared with Eqs. 6. 4 or 6. 5.

Appendix II

A Program to Solve The System of Eqs. 3. 17 And To Decrease $z_{\text{Connecting Line}}/z_{\text{Stub}}$ Automatically

It has been shown in Section 3. 2 that for the network in Fig. 3. 1 to have a prescribed set of transmission poles, the lengths and the characteristic impedances of the transmission lines in the network must be selected to satisfy Eqs. 3. 17. The generation of this system of equations and its solution by the Newton-Raphson method has been presented in Sections 4. 1 through 4. 4. A part (subroutines FITER, ZCAS, ZPAR and the main program with DMF = 1) of the program listed here solves Eq. 3. 17 following the techniques outlined in Sections 4. 1 through 4. 4. The rest of the main program (when DMF > 1 and none of the variable parameters is an impedance) uses subroutines FITER, ZCAS, ZPAR and MULFAC to bring down the ratio $z_{\text{connecting line}}/z_{\text{stub}}$ automatically. The block diagram in Fig. II. 1 explains the operation of the program. For the successful convergence of iterations terminations of the network in Fig. 3. 1 must be unequal.

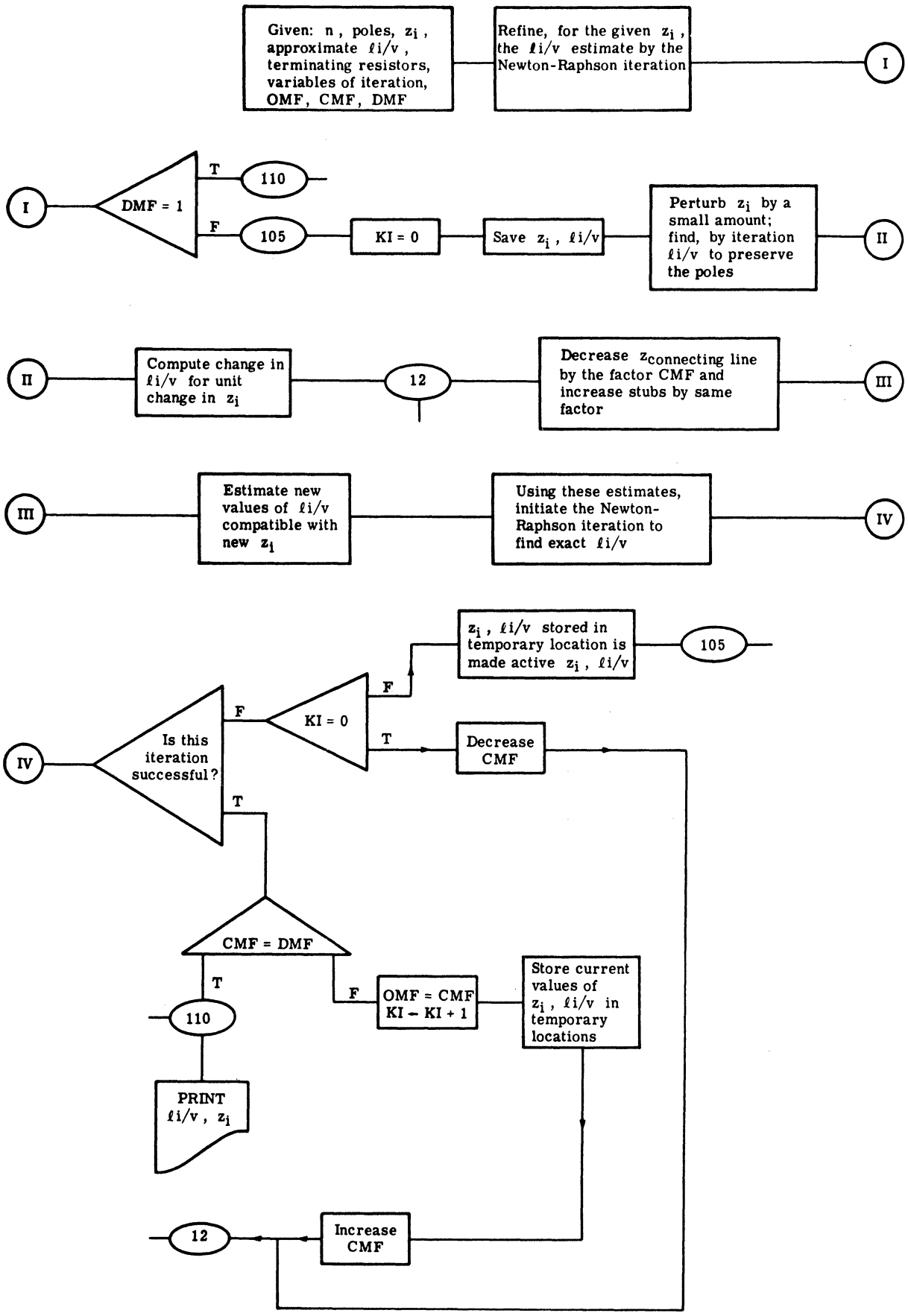

Fig. II.1. The block-diagram of the program

```
FORTRAN IV G COMPILER          MAIN          10-09-69          14:09.05

0001                DIMENSION ASAVE(15),ZSAVE(15),ATEMP(15),ZTEMP(15),ACHANG(15),
                   1ZINIT(15)
0002                COMMON X(15),Y(15),A(15),Z(15),LINE(15),IMP(15)
                C***    N=NO. OF LINES
                C***    R2 = RESISTANCE ON LINE(1) END
0003                READ(5,500)N,R1,R2
0004          500   FORMAT(I2,2F10.0)
                C***    Z(I),  I=1,N  ARE CHARACTERISTIC IMPEDANCES OF LINES;
                C***    LINE 1  IS A STUB.
                C***    A(I) ARE DELAYS ( LINE LENGTH/VELOCITY OF PROPAGATION. )
0005                READ(5,505)(A(I),I=1,N),(Z(I),I=1,N)
0006          505   FORMAT(8F10.0)
                C***    SPECIFIED POLES  S(I)=X(I)+J*Y(I) , I=1,3,...,N
                C***    IF N IS ODD, LAST POLE IS REAL.
0007                READ(5,505)(X(I),I=1,N,2),(Y(I),I=1,N,2)
                C***    LINE(I) AND IMP(I) SPECIFY PARAMETERS AS
                C***    FIXED(=1) OR ADJUSTABLE(=0).
0008                READ(5,510)(LINE(I),I=1,N),(IMP(I),I=1,N)
0009          510   FORMAT(30I2)
                C***    DMF, CMF, DMF CONTROL AUTOMATIC REDUCTION OF
                C***    Z RATIO TO (ZHI/ZLO)/(DMF*DMF).  INITIAL
                C***    STEP OF REDUCTION IS 1/(CMF*CMF); DMF=1.0.
                C***    WHEN ANY IMP(I)=0; MUST SET DMF=1.0 .
0010                READ(5,600)CMF,CMF,DMF
0011          600   FORMAT(3F10.0)
0012                DO 100 I=1,N
0013          100   ZINIT(I)=Z(I)
0014          10    CALL FITER(R1,R2,N,&125)
                C***    IF DMF=1., WRITE RESULTS AND STOP.
                C***    REST OF PROGRAM IMPLEMENTS ZHI/ZLO REDUCTION.
```

```
0015            IF(CMF.EQ.1.) GO TO 110
0016      105   KI=0
0017            DO 1 I=1,N
0018            ASAVE(I)=A(I)
0019      1     ZSAVE(I)=Z(I)
0020            WRITE(6,300)
0021      300   FORMAT(15X,'THE IMPEDANCE VECTOR')
0022            WRITE(6,305)(Z(I),I=1,N)
0023      305   FORMAT(4(5X,F15.7))
0024            WRITE(6,310)
0025      310   FORMAT(15X,'THE LENGTH VECTOR')
0026            WRITE(6,315)(A(I),I=1,N)
0027      315   FORMAT(4(5X,F15.7))
0028            WRITE(6,320)CMF
0029      320   FORMAT(F15.7)
0030            DO 2 I=1,N,2
0031      2     Z(I)=1.1*ZSAVE(I)
0032            DO 3 I=2,N,2
0033      3     Z(I)=.9*ZSAVE(I)
0034            DO 4 I=1,N
0035      4     A(I)=1.1*ASAVE(I)
0036            WRITE(6,300)
0037            WRITE(6,305)(Z(I),I=1,N)
0038            WRITE(6,310)
0039            WRITE(6,315)(A(I),I=1,N)
0040            WRITE(6,320)CMF
0041            CALL FITER(R1,R2,N,&125)
0042            WRITE(6,300)
0043            WRITE(6,305)(Z(I),I=1,N)
0044            WRITE(6,310)
0045            WRITE(6,315)(A(I),I=1,N)
0046            WRITE(6,320)CMF
0047            DO 5 I=1,N
0048      5     ACHANG(I)=(A(I)-ASAVE(I))/(Z(I)-ZSAVE(I))
0049      12    DO 6 I=1,N,2
0050      6     Z(I)=CMF*ZINIT(I)
```

```
0051                    DO 7 I=2,N,2
0052          7         Z(I)=ZINIT(I)/CMF
0053                    DO 8 I=1,N
0054          8         A(I)=ASAVE(I)+ACHANG(I)*(Z(I)-ZSAVE(I))
0055                    WRITE(6,300)
0056                    WRITE(6,305)(Z(I),I=1,N)
0057                    WRITE(6,310)
0058                    WRITE(6,315)(A(I),I=1,N)
0059                    WRITE(6,320)CMF
0060                    CALL FITER(R1,R2,N,&9)
0061                    IF(CMF .LT.(DMF+.01) .AND. CMF .GT. (DMF-.01)) GO TO 110
0062                    DMF=CMF
0063                    KEY=1
0064                    KI=KI+1
0065                    DO 11 I=1,N
0066                    ATEMP(I)=A(I)
0067         11         ZTEMP(I)=Z(I)
0068                    CALL MULFAC(KEY,DMF,CMF,OMF)
0069                    GO TO 12
0070          9         IF(KI.EQ.0) GO TO 120
0071                    DO 115 I=1,N
0072                    A(I)=ATEMP(I)
0073        115         Z(I)=ZTEMP(I)
0074                    GO TO 105
0075        120         KEY=2
0076                    CALL MULFAC(KEY,DMF,CMF,OMF)
0077                    GO TO 12
0078        110         WRITE(6,300)
0079                    WRITE(6,305)(Z(I),I=1,N)
0080                    WRITE(6,310)
0081                    WRITE(6,315)(A(I),I=1,N)
0082                    WRITE(6,320)CMF
0083        125         CALL SYSTEM
0084                    END
```

```
FORTRAN IV G COMPILER        MULFAC          10-09-69        14:09.12

0001                SUBROUTINE MULFAC(KEY,DMF,CMF,OMF)
0002                GO TO (5,7), KEY
0003          5     IF((DMF-CMF).GT..4) GO TO 9
0004                CMF=DMF
0005                RETURN
0006          9     CMF=OMF+(DMF-CMF)/2.
0007                RETURN
0008          7     UMF=CMF-(CMF-CMF)/2.
0009                CMF=UMF
0010                RETURN
0011                END
```

```
FORTRAN IV G COMPILER        MAIN            10-09-69        14:09.13

                    C***      SUBROUTINE FITER PERFORMS NEWTON-RAPHSON ITERATIONS
                    C***      TO SATISFY FF(A(I),...,A(N);Z(1),...,Z(N);S(J))=0, J=1,3,...
                    C***      IT RETURNS NECESSARY NEW PARAMETERS.
0001                SUBROUTINE FITER(R1,R2,N,*)
0002                COMMON X(15),Y(15),A(15),Z(15),LINF(15),IMP(15)
0003                DIMENSION B(15),BSUB(15),RHS(15),DERIV(9,9),S(81)
0004          20    K=0
0005          30    CALL DENCM(R1,R2,X,Y,A,Z,B,N)
                    C***      RHS IS RIGHT HAND  SIDE OF RE(FF)+J*IM(FF) SYSTEM .
0006                DO 1 I=1,N
0007          1     RHS(I)=-B(I)
0008                WRITE(6,200)
0009          200   FORMAT( 'THE RHS VECTOR' )
0010                WRITE(6,110)(RHS(I),I=1,N)
0011          110   FORMAT(6(E18.7,2X))
0012                INK=0
                    C***      DO 2 CALCULATES DERIVATIVES OF B'S WITH RESPECT TO
                    C***      VARIABLE LENGTH PARAMETERS.
```

```
0013                    DO 2 I=1,N
0014                    IF(1 .EQ. LINE(I)) GO TO 2
0015                    PERT=.0001*A(I)
0016                    ASAVE=A(I)
0017                    A(I)=ASAVE+PERT
0018                    INK=INK+1
0019                    CALL DENOM(R1,R2,X,Y,A,Z,BSUB,N)
0020                    DO 3 J=1,N
0021            3       DERIV(J,INK)=(BSUB(J)-B(J))/PERT
0022                    A(I)=ASAVE
0023            2       CONTINUE
                C***        DO 7 SAME AS DO 2 FOR VARIABLE Z PARAMETERS
0024                    DO 7 I=1,N
0025                    IF(1 .EQ. IMP(I)) GO TO 7
0026                    PERT=.0001*Z(I)
0027                    ZSAVE=Z(I)
0028                    Z(I)=ZSAVE+PERT
0029                    INK=INK+1
0030                    CALL DENOM(R1,R2,X,Y,A,Z,BSUB,N)
0031                    DO 8 J=1,N
0032            8       DERIV(J,INK)=(BSUB(J)-B(J))/PERT
0033                    Z(I)=ZSAVE
0034            7       CONTINUE
                C***        INK IS NO. OF VARIABLE PARAMETERS PROGRAM
                C***        HAS CALCULATED DERIVATIVES FOR.
0035                    WRITE(6,115)INK
0036            115     FORMAT(5X,4HINK=,I2)
0037                    DO 210 I=1,N
0038            210     WRITE(6,110)(DERIV(I,J),J=1,N)
0039                    CAL=0.
0040                    DO 4 I=1,N
0041            4       CAL=CAL+ABS(B(I))
0042                    IF(K.EQ.0) CALSAV=CAL
                C***        ARRAY(    ) AND SIMQ(    ) ARE IN *SSP;
                C***        SIMQ RETURNS CHANGES IN A'S AND Z'S FOUND BY ITERATION .
0043                    CALL ARRAY(2,N,N,9,9,S,DERIV)
```

```
0044                CALL SIMQ(S,RHS,N,0)
0045                INK=0
                C***    DO 5 AND DO 9 CHANGE VARIABLE PARAMETERS.
0046                DO 5 I=1,N
0047                IF(1 .EQ. LINE(I)) GO TO 5
0048                INK=INK+1
0049                A(I)=A(I)+RHS(INK)
0050          5     CONTINUE
0051                DO 9 I=1,N
0052                IF(1 .EQ. IMP(I)) GO TO 9
0053                INK=INK+1
0054                Z(I)=Z(I)+RHS(INK)
0055          9     CONTINUE
0056                ERR=0.
0057                DO 6 I=1,N
0058           6    ERR=ERR+ABS(RHS(I))
0059                WRITE(6,230)
0060          230   FORMAT( 'THE INCREMENTS' )
0061                WRITE(6,110)(RHS(I),I=1,N)
0062                WRITE(6,240)
0063          240   FORMAT( 'THE LENGTH VECTOR' )
0064                WRITE(6,110)(A(I),I=1,N)
0065                WRITE(6,250)
0066          250   FORMAT( 'THE IMPEDANCE VECTOR' )
0067                WRITE(6,110)(Z(I),I=1,N)
0068                WRITE(6,110)CAL
                C***    K= TOTAL NO. OF ITERATIONS.
0069                WRITE(6,130)K,INK
0070          130   FORMAT(5X,2HK=,I2,5X,4HINK=,I2)
0071                IF(K-1)70,75,75
0072           70   K=K+1
0073                GO TO 30
                C***    CAL.GT.2*CALSAV MEANS ITERATION IS DIVERGING
0074           75   IF(CAL.GT.2.*CALSAV) GO TO 80
0075                CALSAV=CAL
                C***    IF CAL IS SMALL OR PARAMETER CHANGES SMALL, RETURN.
```

```
0076          10    IF(CAL.LT.1.E-05 .OR. ERR.LT.1.E-07) GO TO 90
0077                K=K+1
0078                GO TO 30
0079          90    RETURN
0080          80    RETURN 1
0081                END
```

```
FORTRAN IV G COMPILER        MAIN          10-09-69        14:09.18

                C***    SUBROUTINE DENOM TAKES R1,R2,X(J),Y(J),A(I),Z(I), AND N
                C***    AND CALCULATES REAL AND IMAGINARY PARTS OF FF AS
                C***    RE(FF(S(1))) + J*IM(FF(S(1))) = B(1) +J*B(2), ETC.
0001                SUBROUTINE DENOM(R1,R2,X,Y,A,Z,B,N)
0002                DIMENSION X(15),Y(15),A(15),Z(15),B(15)
0003                DO 2 J=1,N,2
0004                E=R2
0005                F=0.
0006                G=1.
0007                H=0.
0008                I=1
0009              3 CALL ZPAR(E,F,G,H,X(J),Y(J),A(I),Z(I))
0010                I=I+1
0011                IF(I.GT.N) GO TO 1
0012                CALL ZCAS(E,F,G,H,X(J),Y(J),A(I),Z(I))
0013                I=I+1
0014                IF(I.LE.N) GO TO 3
0015              1 B(J)=E+R1*G
0016              2 B(J+1)=F+R1*H
0017                RETURN
0018                END
```

```
FORTRAN IV G COMPILER        MAIN          10-09-69        14:09.19

C***    SUBROUTINE ZPAR CALCULATES INPUT IMPEDANCE OF A
C***    TRANSMISSION LINE WITH A=V, Z=CHI IN PARALLEL
C***    WITH  IMP. (E+J*F)/(G+J*H) AT XX+J*YY.
C***    IMPEDANCE THUS FOUND REPLACES IMP. .
0001        SUBROUTINE ZPAR(E,F,G,H,XX,YY,V,CHI)
0002        R=COS(V*YY)*(EXP(V*XX)+EXP(-V*XX))/2.
0003        S=SIN(V*YY)*(EXP(V*XX)-EXP(-V*XX))/2.
0004        P=COS(V*YY)*(EXP(V*XX)-EXP(-V*XX))/2.
0005        Q=SIN(V*YY)*(EXP(V*XX)+EXP(-V*XX))/2.
0006        ESAVE=CHI*(E*R-F*S)
0007        FSAVE=CHI*(F*R+E*S)
0008        GSAVE=E*P-F*Q+CHI*(R*G-H*S)
0009        HSAVE=F*P+E*Q+CHI*(G*S+R*H)
0010        E=ESAVE
0011        F=FSAVE
0012        G=GSAVE
0013        H=HSAVE
0014        RETURN
0015        END
```

```
FORTRAN IV G COMPILER        MAIN          10-09-69        14:09.21

C***    SUBROUTINE ZCAS  IS SAME AS ZPAR FOR CASCADE LINE
C***    TERMINATED IN IMP. .
0001        SUBROUTINE ZCAS(E,F,G,H,XX,YY,V,CHI)
0002        R=COS(V*YY)*(EXP(V*XX)+EXP(-V*XX))/2.
0003        S=SIN(V*YY)*(EXP(V*XX)-EXP(-V*XX))/2.
0004        P=COS(V*YY)*(EXP(V*XX)-EXP(-V*XX))/2.
0005        Q=SIN(V*YY)*(EXP(V*XX)+EXP(-V*XX))/2.
0006        ESAVE=(E*R-F*S)+CHI*(P*G-Q*H)
0007        FSAVE=(F*R+E*S)+CHI*(Q*G+P*H)
0008        GSAVE=CHI*(P*G-S*H)+(E*P-F*Q)
```

```
0009          HSAVE=CHI*(G*S+R*H)+(F*P+E*Q)
0010          E=ESAVE*CHI
0011          F=FSAVE*CHI.
0012          G=GSAVE
0013          H=HSAVE
0014          RETURN
0015          END
```

Appendix III

A Program For The Numerical Evaluation of ω_{AD} and ω_{BC}

A numerical technique has been presented in Section 6. 5. 2 for the evaluation of ω_{AD} and ω_{BC}. The Fortran-coded program developed to determine these zeros for the circuit in Fig. 3. 1 is listed here. The flow-sheet of the program is given in Fig. III. 1.

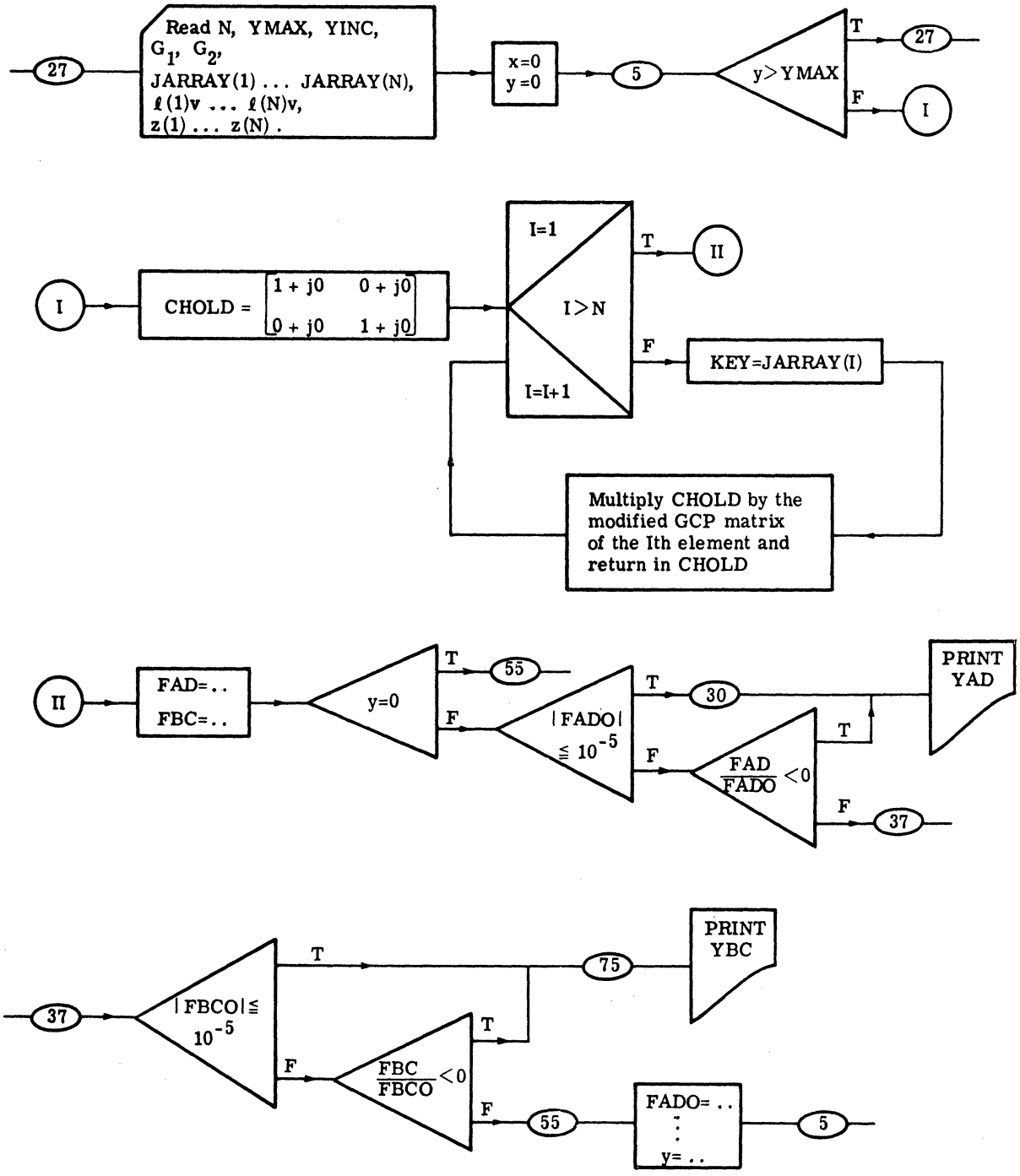

Fig. III.1. The flow-sheet of the program RTAPR

```
FORTRAN IV G COMPILER        MAIN              10-09-69        14:16.50

C***     PROGRAM RTAPR FINDS APPROXIMATE ZEROS FOR
C***     G1*A+G2*D AND G1*G2*B+C
0001        DIMENSION JARRAY(15),FLENG(15),FIMP(15),CHNEW(8),CHOLD(8)
C***          INPUTS:
C***          N=NUMBER OF LINES
C***          YMAX=MAXIMUM VALUE ON JW-AXIS
C***          YINCR=SEARCH INCREMENT ON JW-AXIS
C***          G1=TERMINATION AT LINE N END
C***          G2=TERMINATION AT LINE 1  END
C***          VECTOR JARRAY DEFINES NETWORK TOPOLOGY
C***           JARRAY(I)=0 MEANS ITH LINE IS A STUB
C***          JARRAY(I)=1 MEANS ITH LINE IS A CONNECTING LINE
C***          FLENG(I)=LENGTH ( L/V ) OF THE ITH LINE
C***          FIMP(I)= IMPEDANCE OF THE ITH LINE
0002        27  READ(5,1,END=29)N,YMAX,YINCR,G1,G2
0003            1 FORMAT(I2,4F10.0)
0004              READ(5,2)(JARRAY(I),I=1,N)
0005            2 FORMAT(15I2)
0006              READ(5,3)(FLENG(I),I=1,N),(FIMP(I),I=1,N)
0007            3 FORMAT(8F10.0)
0008              X=0.
0009              Y=0.
C***       Y IS LOCATION OF ZEROS
0010            5 IF(Y.GT.YMAX) GO TO 25
C***       CHOLD VECTOR DEFINES A UNITY COMPLEX MATRIX:
C***            CHOLD(1)+J*CHOLD(2)    CHOLD(3)+J*CHOLD(4)
C***            CHOLD(5)+J*CHOLD(6)    CHOLD(7)+J*CHOLD(8)
0011        CHOLD(1)=1.
0012        CHOLD(2)=0.
0013        CHOLD(3)=0.
0014        CHOLD(4)=0.
```

```
0015                CHOLD(5)=0.
0016                CHOLD(6)=0.
0017                CHOLD(7)=1.
0018                CHOLD(8)=0.
              C***     DO 7 COMPUTES MODIFIED ABCD MATRIX FOR THE  LOSSLESS
              C***     PART OF A TRANSMISSION LINE NETWORK.
0019                DO 7 I=1,N
0020                KEY=JARRAY(I)
0021                CALL GENCH(X,Y,CHNEW,KEY,FIMP(I),FLENG(I))
0022                CALL PRODUC(CHNEW,CHOLD)
0023              7 CONTINUE
0024                FAD=G1*CHOLD(1)+G2*CHOLD(7)
0025                FBC=G1*G2*CHOLD(4)+CHOLD(6)
0026                IF(Y.EQ.0.) GO TO 55
0027                IF(ABS(FADO).LE.1.E-05) GO TO 30
0028                IF(FAD/FADO)30,37,37
0029           30   WRITE(6,38)Y
0030           38   FORMAT(3X,4HYAD=,F12.5)
0031           37   IF(ABS(FBCO).LE.1.E-05) GO TO 75
0032                IF(FBC/FBCO)75,55,55
0033           75   WRITE(6,77)Y
0034           77   FORMAT(3X,4HYBC=,F12.5)
0035           55   FADO=FAD
0036                FBCO=FBC
0037                Y=Y+YINCR
0038                GO TO 5
0039           25   GO TO 27
0040           29   CALL SYSTEM
0041                END
```

```
0001            SUBROUTINE GENCH(X,Y,CHNEW,KEY,Z,W)
          C***    GENCH(X,Y,CHNEW,FIMP(I),FLENG(I)) CALCULATES
          C***    MODIFIED ABCD MATRIX ( THAT IS, WITHOUT COSH FACTOR )
          C***    OF STUB OR CONNECTING LINE AT S=X+J*Y. THIS MATRIX
          C***    IS RETURNED IN
          C***         CHNEW(1)+J*CHNEW(2)    CHNEW(3)+J*CHNEW(4)
          C***         CHNEW(5)+J*CHNEW(6)    CHNEW(7)+J*CHNEW(8)
0002            DIMENSION CHNEW(8)
0003            WX=W*X
0004            WY=W*Y
0005            A=COSH(WX)*COS(WY)
0006            B=SINH(WX)*SIN(WY)
0007            C=SINH(WX)*COS(WY)
0008            D=COSH(WX)*SIN(WY)
0009            IF(KEY)1,2,1
0010          1 CHNEW(1)=A
0011            CHNEW(2)=B
0012            CHNEW(3)=C*Z
0013            CHNEW(4)=D*Z
0014            CHNEW(5)=C/Z
0015            CHNEW(6)=D/Z
0016            CHNEW(7)=A
0017            CHNEW(8)=B
0018            RETURN
0019          2 CHNEW(1)=A
0020            CHNEW(2)=B
0021            CHNEW(3)=0.
0022            CHNEW(4)=0.
0023            CHNEW(5)=C/Z
0024            CHNEW(6)=D/Z
0025            CHNEW(7)=A
0026            CHNEW(8)=B
0027            RETURN
0028            END
```

```
0001                  SUBROUTINE PRODUC(CHNEW,CHOLD)
                C***     PRODUC(CHNEW,CHOLD) MULTIPLIES THE MATRICES
                C***     CHNEW AND CHOLD, AND RETURNS THE PRODUCT IN CHOLD.
0002                  DIMENSION CHNEW(8),CHOLD(8),SAVE(8)
0003                  SAVE(1)=CHNEW(1)*CHOLD(1)-CHNEW(2)*CHOLD(2)
                     1+CHNEW(3)*CHOLD(5)-CHNEW(4)*CHOLD(6)
0004                  SAVE(2)=CHNEW(1)*CHOLD(2)+CHNEW(2)*CHOLD(1)
                     1+CHNEW(3)*CHOLD(6)+CHNEW(4)*CHOLD(5)
0005                  SAVE(3)=CHNEW(1)*CHOLD(3)-CHNEW(2)*CHOLD(4)
                     1+CHNEW(3)*CHOLD(7)-CHNEW(4)*CHOLD(8)
0006                  SAVE(4)=CHNEW(1)*CHOLD(4)+CHNEW(2)*CHOLD(3)
                     1+CHNEW(3)*CHOLD(8)+CHNEW(4)*CHOLD(7)
0007                  SAVE(5)=CHNEW(5)*CHOLD(1)-CHNEW(6)*CHOLD(2)
                     1+CHNEW(7)*CHOLD(5)-CHNEW(8)*CHOLD(6)
0008                  SAVE(6)=CHNEW(5)*CHOLD(2)+CHNEW(6)*CHOLD(1)
                     1+CHNEW(7)*CHOLD(6)+CHNEW(8)*CHOLD(5)
0009                  SAVE(7)=CHNEW(5)*CHOLD(3)-CHNEW(6)*CHOLD(4)
                     1+CHNEW(7)*CHOLD(7)-CHNEW(8)*CHOLD(8)
0010                  SAVE(8)=CHNEW(5)*CHOLD(4)+CHNEW(6)*CHOLD(3)
                     1+CHNEW(7)*CHOLD(8)+CHNEW(8)*CHOLD(7)
0011                  DO 3 I=1,8
0012                3 CHOLD(I)=SAVE(I)
0013                  RETURN
0014                  END
```

Appendix IV

A Program For The Numerical Evaluation of Transmission Poles

An outline of a numerical technique for finding the transmission poles, i. e., the zeros of $(G_1 A + G_2 D) + K(G_1 G_2 B + C)$ has been given in Section 6. 5. 3. The Fortran program to compute the transmission poles for the network in Fig. 3. 1 according to this method is listed here. Fig. IV. 1 shows the flow-sheet of this program.

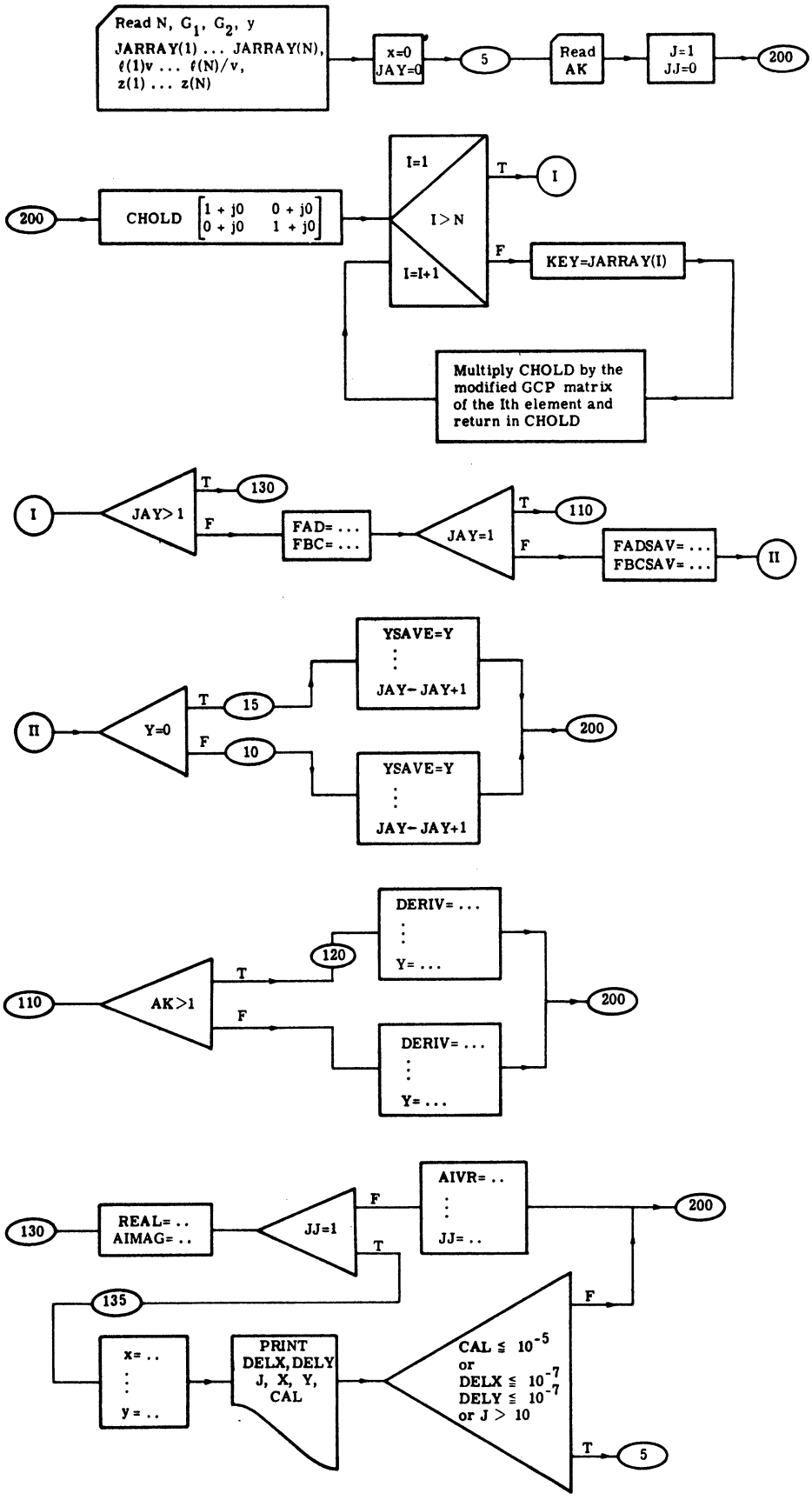

Fig. IV.1. The flow-sheet of the program RTLOC

```
FORTRAN IV G COMPILER        MAIN              10-20-69        13:33.11

            C***     PROGAM RTLOC FINDS A ZERO OF (G1*A+G2*D)+AK*(G1*G2*B+C)=0
0001                DIMENSION JARRAY(15),FLENG(15),FIMP(15),CHNEW(8),CHOLD(8)
            C***              INPUTS:
            C***              N=NUMBER OF LINES
            C***              G1=TERMINATION AT LINE N END
            C***              G2=TERMINATION AT LINE 1  END
            C***              Y=APPROXIMATE ZERO OF (G1*A+G2*D) OR (G1*G2*B+C)
            C***              JARRAY SETS TOPOLOGY OF NETWORK AS IN RTAPP
            C***              FLENG(I) AND FIMP(I) AS IN RTAPR
            C***              AK SHOULD BE SMALL(0.1 OR 0.2) IF Y IS A ZERO G1*A+G2*D ,
            C***              AK SOULD BE LARGE (2. TO 10.) IF Y IS A ZERO OF G1*G2*B+C
            C***        A SERIES OF AK CARDS SERVES  TO STEP ALONG THE ROOT LOCUS
0002                READ(5,1)N,G1,G2,Y
0003                READ(5,2)(JARRAY(I),I=1,N)
0004          1     FORMAT(I2,3F10.0)
0005          2     FORMAT(15I2)
0006                READ(5,3)(FLENG(I),I=1,N),(FIMP(I),I=1,N)
0007          3     FORMAT(8F10.0)
0008                JAY=0
            C***        FIRST PASS FROM 0009 TO 0056 CALCULATES DERIVATIVE
            C***        ON THE ROOT LOCUS AND ESTIMATES INITIAL X.
0009                X=0.
0010          5     READ(5,4,END=69)AK
0011          4     FORMAT(F10.0)
0012                J=1
0013                JJ=0
0014        200     CHOLD(1)=1.
0015                CHOLD(2)=0.
0016                CHOLD(3)=0.
0017                CHOLD(4)=0.
0018                CHOLD(5)=0.
```

```
0019                CHOLD(6)=0.
0020                CHOLD(7)=1.
0021                CHOLD(8)=0.
0022                DO 7 I=1,N
0023                KEY=JARRAY(I)
0024                CALL GENCH(X,Y,CHNEW,KEY,FIMP(I),FLENG(I))
0025                CALL REDUC(CHNEW,CHOLD)
0026          7     CONTINUE
0027                IF(JAY.GT.1) GO TO 130
0028                FAD=G1*CHOLD(1)+G2*CHOLD(7)
0029                FBC=G1*G2*CHOLD(4)+CHOLD(6)
0030                IF(JAY.EQ.1) GO TO 110
0031                FADSAV=FAD
0032                FBCSAV=FBC
0033                IF(Y)10,15,10
0034          15    YSAVE=Y
0035                Y=.001
0036                YPD=.001
0037                JAY=JAY+1
0038                GO TO 200
0039          10    YSAVE=Y
0040                YPD=.001*YSAVE
0041                Y=Y*1.001
0042                JAY=JAY+1
0043                GO TO 200
              C***      110 DECIDES WHICH END OF THE ROOT-LOCUS ONE STARTS FROM.
0044          110   IF(AK.GT.1.) GO TO 120
0045                DERIV=(FAD-FADSAV)/YPD
0046                XSAVE=FBCSAV/DERIV
0047                WRITE(6,500)XSAVE
0048          500   FORMAT(5X,6HXSAVE=,E15.5)
0049                X=AK*YSAVE
              C***      JAY=1 MEANS THIS IS THE FIRST TIME AFTER ESTIMATING X.
0050                JAY=JAY+1
0051                Y=YSAVE
0052                GO TO 200
```

```
0053          120   DERIV=(ERC-ERCSAV)/YPD
0054                XSAVE=EACSAV/DERIV
0055                WRITE(6,500)XSAVE
0056                X=-XSAVE/AK
0057                JAY=JAY+1
0058                Y=YSAVE
0059                GO TO 200
0060          130   REAL=G1*CHOLD(1)+G2*CHOLD(7)+AK*(G1*G2*CHOLD(3)+CHOLD(5))
0061                AIMAG=G1*CHOLD(2)+G2*CHOLD(8)+AK*(G1*G2*CHOLD(4)+CHOLD(6))
              C***     JJ=1 MEANS THE NEW X HAS BEEN INCREMENTED TO ESTIMATE DERIVATIVE
0062                IF(JJ.EQ.1) GO TO 135
0063                AIVR=REAL
0064                AIVI=AIMAG
0065                XSAVE=X
0066                X=XSAVE*1.001
0067                JJ=JJ+1
0068                GO TO 200
0069          135   X=XSAVE
0070                JJ=0
0071                ANVR=REAL
0072                ANVI=AIMAG
0073                RX=(ANVR-AIVR)/(.001*X)
0074                AIX=(ANVI-AIVI)/(.001*X)
              C***     BETWEEN 72 TO 73  CALCULATE DERIVATIVES WITH RESPECT TO
              C***     X AND Y ( USING CAUCHY-RIEMAN CONDITION ).
0075                RY=-AIX
0076                AIY=RX
0077                DEN=RY*AIX-RX*AIY
              C***     BETWEEN 76 TO 77 CALCULATES NEW X AND Y BY NEWTON-RAPHSON.
              C***     J=NUMBER OF PASSES THROUGH NEWTON-RAPHSON.
0078                DELX=(AIVR*AIY-AIVI*RY)/DEN
0079                DELY=(AIVI*RX-AIVR*AIX)/DEN
0080                CAL=ABS(AIVR)+ABS(AIVI)
0081                X=X+DELX
0082                Y=Y+DELY
0083                WRITE(6,100)DELX,DELY,J
```

```
0084          100   FORMAT(5HDELX=,E15.5,5X,5HDELY=,E15.5,5X,2HJ=,I2)
0085                WRITE(6,105)X,Y,CAL
0086          105   FORMAT(2HX=,E15.5,5X,2HY=,E15.5,5X,4HCAL=,E15.5)
0087                IF(CAL.LE.1.E-05 .OR. (ABS(DELX).LE.1.E-07 .AND.
                     1ABS(DELY).LE.1.E-07) .OR. J.GT.10) GO TO 5
0088                J=J+1
0089                GO TO 200
0090          69    CALL SYSTEM
0091                END
```

```
FORTRAN IV G COMPILER          GENCH              10-20-69          13:33.20

0001                SUBROUTINE GENCH(X,Y,CHNEW,KEY,Z,W)
                C***    GENCH(X,Y,CHNEW,FIMP(I),FLENG(I)) CALCULATES
                C***    MODIFIED ABCD MATRIX ( THAT IS, WITHOUT COSH FACTOR )
                C***    OF STUB OR CONNECTING LINE AT S=X+J*Y. THIS MATRIX
                C***    IS RETURNED IN
                C***         CHNEW(1)+J*CHNEW(2)     CHNEW(3)+J*CHNEW(4)
                C***         CHNEW(5)+J*CHNEW(6)     CHNEW(7)+J*CHNEW(8)
0002                DIMENSION CHNEW(8)
0003                WX=W*X
0004                WY=W*Y
0005                A=COSH(WX)*COS(WY)
0006                B=SINH(WX)*SIN(WY)
0007                C=SINH(WX)*COS(WY)
0008                D=COSH(WX)*SIN(WY)
0009                IF(KEY)1,2,1
0010              1 CHNEW(1)=A
0011                CHNEW(2)=B
0012                CHNEW(3)=C*Z
0013                CHNEW(4)=D*Z
0014                CHNEW(5)=C/Z
0015                CHNEW(6)=D/Z
```

```
0016                CHNEW(7)=A
0017                CHNEW(8)=B
0018                RETURN
0019              2 CHNEW(1)=A
0020                CHNEW(2)=B
0021                CHNEW(3)=0.
0022                CHNEW(4)=0.
0023                CHNEW(5)=C/Z
0024                CHNEW(6)=D/Z
0025                CHNEW(7)=A
0026                CHNEW(8)=B
0027                RETURN
0028                END
```



```
0001                SUBROUTINE PRODUC(CHNEW,CHOLD)
                C***    PRODUC(CHNEW,CHOLD) MULTIPLIES THE MATRICES
                C***    CHNEW AND CHOLD, AND RETURNS THE PRODUCT IN CHOLD.
0002                DIMENSION CHNEW(8),CHOLD(8),SAVE(8)
0003                SAVE(1)=CHNEW(1)*CHOLD(1)-CHNEW(2)*CHOLD(2)
                   1+CHNEW(3)*CHOLD(5)-CHNEW(4)*CHOLD(6)
0004                SAVE(2)=CHNEW(1)*CHOLD(2)+CHNEW(2)*CHOLD(1)
                   1+CHNEW(3)*CHOLD(6)+CHNEW(4)*CHOLD(5)
0005                SAVE(3)=CHNEW(1)*CHOLD(3)-CHNEW(2)*CHOLD(4)
                   1+CHNEW(3)*CHOLD(7)-CHNEW(4)*CHOLD(8)
0006                SAVE(4)=CHNEW(1)*CHOLD(4)+CHNEW(2)*CHOLD(3)
                   1+CHNEW(3)*CHOLD(8)+CHNEW(4)*CHOLD(7)
0007                SAVE(5)=CHNEW(5)*CHOLD(1)-CHNEW(6)*CHOLD(2)
                   1+CHNEW(7)*CHOLD(5)-CHNEW(8)*CHOLD(6)
0008                SAVE(6)=CHNEW(5)*CHOLD(2)+CHNEW(6)*CHOLD(1)
                   1+CHNEW(7)*CHOLD(6)+CHNEW(8)*CHOLD(5)
0009                SAVE(7)=CHNEW(5)*CHOLD(3)-CHNEW(6)*CHOLD(4)
                   1+CHNEW(7)*CHOLD(7)-CHNEW(8)*CHOLD(8)
```

```
0010            SAVE(8)=CHNEW(5)*CHOLD(4)+CHNEW(6)*CHOLD(3)
               1+CHNEW(7)*CHOLD(2)+CHNEW(8)*CHOLD(1)
0011            DO 3 I=1,8
0012          3 CHOLD(I)=SAVE(I)
0013            RETURN
0014            END
```

Bibliography

1. P. I. Richards, "Resistor-Transmission-Line Circuits," Proc. IRE, Vol. 36, February 1948, pp. 217-220.

2. H. Ozaki and J. Ishii, "Synthesis of Transmission Line Networks and The Design of UHF Filters," IRE Trans. On Circuit Theory, Vol. CT-2, December 1955, pp. 325-336.

3. M. C. Horton and R. J. Wenzel, "General Theory And Design of Optimum Quarterwave TEM Filters," IEEE Trans. On Microwave Theory and Techniques, Vol. MTT-13, May 1965, pp. 316-327.

4. R. J. Wenzel, "Exact Design of TEM Microwave Networks Using Quarterwave Lines," IEEE Trans. on Microwave Theory and Techniques, Vol. MTT-12, January 1964, pp. 94-111.

5. B. K. Kinariwala, "Theory of Cascaded Transmission Lines," Proceedings of The Symposium on Generalized Networks, Microwave Research Institute Symposia Series, Vol. XVI, Polytechnic Press of The Polytechnic Institute of Brooklyn, New York, 1966.

6. R. M. Fano and A. W. Lawson, "Microwave Filters Using Quarterwave Couplings," Proc. IRE, Vol. 35, November 1947, pp. 1318-1323.

7. W. W. Mumford, "Maximally Flat Filters in Waveguides," Bell System Technical Journal, Vol. 27, October 1948, pp. 684-713.

8. S. B. Cohn, "Direct-Coupled-Resonator Filters," Proc. IRE, Vol. 45, February 1957, pp. 187-196.

9. R. E. Collin, "Theory and Design of Wideband Multisection Quarterwave Transformers," Proc. IRE, Vol. 43, February 1955, pp. 179-185.

Bibliography (Cont.)

10. H. J. Riblet, "General Synthesis of Quarterwave Impedance Transformers," IRE Trans. on Microwave Theory and Techniques, Vol. MTT-5, January 1957, pp. 36-43.

11. R. Levy, "Tables of Element Values for The Distributed Low-Pass Prototype Filter," IEEE Trans. on Microwave Theory and Techniques, Vol. MTT-13, September 1965, pp. 514-536.

12. L. Young, "The Quarterwave Transformer Prototype Circuit," IRE Trans. on Microwave Theory and Techniques, Vol. MTT-8, September 1960, pp. 483-489.

13. L. Young, "Direct Coupled Cavity Filters for Wide and Narrow Bandwidths," IEEE Trans. on Microwave Theory and Techniques, Vol. MTT-11, May 1963. pp. 162-178.

14. L. Young, "Tables for Cascaded Homogeneous Quarterwave Transformers," IRE Trans. on Microwave Theory and Techniques, Vol. MTT-7, April 1959, pp. 233-237 and Vol. MTT-8, March 1960, pp. 243-244.

15. L. Young, "Stepped Impedance Transformers and Filter Prototypes," IRE Trans. on Microwave Theory and Techniques, Vol. MTT-10, September 1962, pp. 339-359.

16. E. M. T. Jones and J. T. Bolljahn, "Coupled Strip Transmission Line Filters and Directional Couplers," IRE Trans. on Microwave Theory and Techniques, Vol. 4, April 1956, pp. 75-81.

17. S. B. Cohn, "Parallel-Coupled Transmission-Line-Resonator Filters," IRE Trans. on Microwave Theory and Techniques, Vol. MTT-6, April 1958, pp. 223-231.

18. G. L. Matthaei, "Design of Wideband (and Narrowband) Bandpass Microwave Filters on The Insertion Loss Basis," IRE Trans. on Microwave Theory and Techniques, Vol. MTT-8, November 1960, pp. 580-593.

Bibliography (Cont.)

19. H. Ozaki and J. Ishii, "Synthesis of A Class of Stripline Filters," IRE Trans. on Circuit Theory, Vol. CT-5, June 1958, pp. 104-109.

20. G. L. Matthaei, "Interdigital Bandpass Filters," IRE Trans. on Microwave Theory and Techniques, Vol. MTT-10, November 1962, pp. 479-491.

21. R. J. Wenzel, "Exact Theory of Interdigital Bandpass Filters And Related Coupled Structures," IEEE Trans. on Microwave Theory and Techniques, Vol. MTT-13, September 1965, pp. 559-575.

22. L. A. Robinson, "Wideband Interdigital Filters with Capacitively Loaded Resonators," G-MTT Symposium Digest, 1965, pp. 33-37

23. G. L. Matthaei, "Combline Bandpass Filters of Narrow Or Moderate Bandwidth," Microwave Journal, Vol. 6, August 1963, pp. 82-91.

24. B. M. Shiffman and G. L. Matthaei, "Exact Design of Bandstop Microwave Filters," IEEE Trans. on Microwave Theory And Techniques, Vol. MTT-12, January 1964, pp. 6-15.

25. B. M. Shiffman, "A Harmonic Rejection Filter Designed By An Exact Method," IEEE Trans. on Microwave Theory And Techniques, Vol. MTT-12, January 1964, pp. 58-60.

26. L. Young, G. L. Matthaei and E. M. T. Jones, "Microwave Bandstop Filters with Narrow Stop Bands," IRE Trans. On Microwave Theory and Techniques, Vol. MTT-10, November 1962, pp. 416-427.

27. B. M. Shiffman, "A Multi-Harmonic Rejection Filter Designed By an Exact Method," IEEE Trans. on Microwave Theory And Techniques, Vol. MTT-12, September 1964, pp. 512-516.

28. H. J. Carlin and W. Kohler, "Direct Synthesis of Bandpass Transmission Line Structures," IEEE Trans. on Microwave Theory and Techniques, Vol. MTT-13, May 1965, pp. 283-297.

Bibliography (Cont.)

29. A. I. Grayzel, "A Synthesis Procedure for Transmission Line Networks," IEEE Trans. on Circuit Theory, Vol. CT-5, September 1958, pp. 172-181.

30. P. I. Richards, "A Special Class of Functions with Positive Real Part in a Half Plane," Duke Mathematical Journal, Vol. 14, September 1947, pp. 777-786.

31. N. Ikeno, "On Distributed Filters," Proc. Joint Conference Of Three Societies Related to Electrical Engineering, May 1952 (Japanese).

32. N. Ikeno, "A Consideration in Coaxial Filters," Journal of The Institute of Electrical Communication Engineers, Japan, Vol. 36, June 1953 (Japanese).

33. N. Ikeno, "Design of Rod-Like Circuits," Proc. Joint Conference of Three Societies Related to Electrical Engineering (Tokyo Chapter), October 1952 (Japanese).

34. K. Kuroda, "A Method to Derive Distributed Filters From Lumped Filters," Proc. Joint Conference of Three Societies Related to Electrical Engineering (Kansai Chapter), October 1952 (Japanese).

35. H. Ozaki, "Synthesis of Unbalanced 4-Pole Consisting Of Distributed Elements," Journal of The Institute of Electrical Communications Engineers, Japan, Vol. 36, December 1953 (Japanese).

36. N. Ikeno, "Design Theory of Distributed Filters," Progress Report of The Institute of Electrical Communications of JTT, Vol. 4, 1957 (Japanese).

37. K. Kuroda, "Exact Design Theory of Distributed Networks," Journal of The Institute of Electrical Communications Engineers, Japan, Vol. 37, May 1954 (Japanese).

38. Y. Kasahara and T. Fujisawa, "Design of Distributed Constant Filters," Journal of The Institute of Electrical Communications Engineers, Japan, Vol. 37, Janaury 1954 (Japanese).

Bibliography (Cont.)

39. Y. Kasahara, H. Ozaki and T. Fujisawa, "Design of Distributed Constant Filters," Technological Reports, Osaka University, Vol. 4, 1954.

40. A. M. Ostrowski, Solution of Equations and Systems of Equations, Academic Press, New York, 1966.

41. V. L. Zaguskin, Handbook of Numerical Methods for The Solution of Algebraic and Transcendental Equations, Pergamon Press, New York, 1961 (Translated from the Russian by G. O. Harding).

42. J. Todd, Survey of Numerical Analysis, McGraw-Hill Book Company, Inc., New York, 1962.

43. P. Henrici, Elements of Numerical Analysis, John Wiley and Sons, Inc., New York, 1964.

44. E. Isaacson and H. B. Keller, Analysis of Numerical Methods, John Wiley and Sons, Inc., New York, 1966.

45. A. S. Householder, Principles of Numerical Analysis, McGraw-Hill Book Company, Inc., New York, 1953.

46. G. Hadley, Nonlinear and Dynamic Programming, Addison-Wesley, Reading, Massachusetts, 1964.

47. G. Zoutendijk, "Nonlinear Programming: A Numerical Survey," SIAM Journal on Control, Vol. 4, February 1966, pp. 194-210.

48. E. W. Cheney and A. A. Goldstein, "Newton's Method For Convex Programming and Tchebycheff Approximation," Numer. Math., Vol. 1, 1959, pp. 253-268.

49. R. E. Griffith and R. A. Stewart, "A Nonlinear Programming Technique for Optimization of Continuous Processing Systems," Management Science, Vol. 7, July 1961, pp. 379-392.

50. G. B. Dantzig, Linear Programming and Extensions, Princeton University Press, Princeton, 1963.

Bibliography (Cont.)

51. G. Hadley, Linear Programming, Addison-Wesley Publishing Co., Massachusetts, 1962.

52. G. Zoutendijk, Methods of Feasible Directions, Elsevier, Amsterdam, 1960.

53. A. V. Fiacco and G. P. McCormick, "The Sequential Unconstrained Minimization Technique for Nonlinear Programming, A Primal Dual Method," Management Science, Vol. 10, January 1964, pp. 360-366.

54. L. Weinberg, Network Analysis and Synthesis, McGraw-Hill Book Company, Inc., New York, 1962.

55. G. L. Matthaei, L. Young and E. M. T. Jones, Microwave Filters, Impedance Matching Networks and Coupling Structures, McGraw-Hill, New York, 1965.

56. H. M. Altschuler and A. A. Oliner, "Discontinuities in The Centre Conductor of Symmetric Strip Transmission Line," IRE Trans. on Microwave Theory and Techniques, Vol. MTT-8, May 1960, pp. 328-339.

57. University of Michigan Terminal System (MTS), Second Edition, December 1967, pp. 171-174, 266.

DISTRIBUTION LIST

No. of copies	
20	National Security Agency Fort George G. Meade, Maryland 20755
1	Technical Library Dir. of Defense Research and Engineering Rm. 3E-1039, The Pentagon Washington, D.C. 20301
1	Defense Intelligence Agency Attn: DIARD Washington, D.C. 20301
2	Director National Security Agency Attn: C31 Fort George G. Meade, Maryland 20755
1	Naval Ships Systems Command Attn: Code 20526 (Technical Library) Main Navy Building, Rm. 1528 Washington, D.C. 20325
1	Naval Ships Systems Command Attn: Code 6179 B Department of the Navy Washington, D.C. 20360
2	Director U.S. Naval Research Laboratory Attn: Code 2027 Washington, D.C. 20390

DISTRIBUTION LIST (Cont.)

No. of copies	
1	Commanding Officer and Director U.S. Navy Electronics Laboratory Attn: Library San Diego, California 92152
1	Commander U.S. Naval Ordnance Laboratory Attn: Technical Library White Oak, Silver Spring, Maryland 20910
1	Dir. Marine Corps Landing Force Dev Ctr Attn: C-E Division Marine Corps Schools Quantico, Virginia 22134
1	Commandant of the Marine Corps (Code AO2F) Headquarters, U.S. Marine Corps Washington, D.C. 20380
1	Rome Air Development Center (EMTLD) Attn: Documents Library Griffiss Air Force Base New York 13440
1	U.S. Army Security Agency Test and Evaluation Center Fort Huachuca, Arizona 85613 Code IAOVT
2	Electronic Systems Division (ESTI) L. G. Hanscom Field Bedford, Massachusetts 01730

DISTRIBUTION LIST (Cont.)

No. of copies	
1	U.S. Air Force Security Service Attn: TSG, VICE Attn: ESD San Antonio, Texas 78241
1	ADTC (ADBRL-2) Eglin Air Force Base, Florida 32542
1	Headquarters, AFSC Attn: SCTSE Bolling AFB, D.C. 20332
1	Air University Library (3T) Maxwell Air Force Base Alabama 36112
1	HQ, USAF Tactical Air Recon Ctr (TAC) Department of the Air Force Shaw Air Force Base, South Carolina 29152
2	Chief of Research and Development Department of the Army Washington, D.C. 20315
2	Commanding General U.S. Army Materiel Command Attn: R&D Directorate Washington, D.C. 20315
3	Redstone Scientific Information Center Attn: Chief, Document Section U.S. Army Missile Command Redstone Arsenal, Alabama 35809
1	Headquarters U.S. Army Weapons Command Attn: AMSWE-RDR Rock Island, Illinois 61201

DISTRIBUTION LIST (Cont.)

No. of copies	
1	Commanding Officer U.S. Foreign Science & Tech Ctr Attn: AMXST-RD-R, Munitions Bldg Washington, D.C. 20315
1	Director, National Security Agency Attn: N-2, Mr. Sherwood Fort George G. Meade, Maryland 20755
2	Commanding Officer Aberdeen Proving Ground Attn: Technical Library, Bldg. 313 Aberdeen Proving Ground, Maryland 21005
2	Headquarters U.S. Army Materiel Command Attn: AMCMA-RM/3 Washington, D.C. 20315
1	Commanding General U.S. Army Combat Developments Command Attn: CDCMR-E Fort Belvoir, Virginia 22060
3	Commanding Officer U.S. Army Combat Developments Command Communications-Electronics Agency Fort Monmouth, New Jersey 07703
1	Commander U.S. Army Research Office (DURHAM) Box CM-DUKE Station Durham, North Carolina 27706

DISTRIBUTION LIST (Cont.)

No. of copies	
1	Commanding Officer U. S. Army Sec Agcy Combat Dev ACTV Arlington Hall Station Arlington, Virginia 22212
1	U. S. Army Security Agency Attn: OACofS, DEV Arlington Hall Station Arlington, Virginia 22212
1	U. S. Army Security Agcy Processing Ctr Attn: IAVAPC-R&D Vint Hill Farms Station Warrenton, Virginia 22186
1	Technical Support Directorate Attn: Technical Library Bldg 3330, Edgewood Arsenal Maryland 21010
2	U. S. Army Research and Dev Command Branch Library, Bldg 5695 Nuclear Effects Laboratory Edgewood Arsenal, Maryland 21010
1	Harry Diamond Laboratories Attn: Library Connecticut Avenue and Van Ness Street Washington, D. C. 20438
1	Commandant U. S. Army Air Defense School Attn: C&S Dept. MSL SCI DIV Fort Bliss, Texas 79916

DISTRIBUTION LIST (Cont.)

No. of copies	
1	Commanding General U.S. Army Electronic Proving Ground Attn: Technical Information Center Fort Huachuca, Arizona 85613
1	Asst. Secretary of the Army (R&D) Department of the Army Attn: Deputy Asst. for Army (R&D) Washington, D.C. 20315
1	Commanding Officer U.S. Army Limited War Laboratory Aberdeen Proving Ground, Maryland 21005
1	CH, Special Techniques Division Unconventional Warfare Department U.S. Army Special Warfare School Fort Bragg, North Carolina 28307
1	USAECOM Liaison Office U.S. Army Electronic Proving Ground Fort Huachuca, Arizona 85613
1	Office, AC of S for Intelligence Department of the Army Attn: ACSI-DSRS Washington, D.C. 20310
1	Chief, Mountain View Office EW Lab USAECOM Attn: AMSEL-WL-RU P.O. Box 205 Mountain View, California 94042
1	Chief, Intelligence Materiel Dev Office Electronic Warfare Lab, USAECOM Fort Holabird, Maryland 21219

DISTRIBUTION LIST (Cont.)

No. of copies	
1	Chief Missile Electronic Warfare Tech Area EW Lab, USA Electronics Command White Sands Missile Range, N. M. 88002
1	Headquarters U. S. Army Combat Developments Command Attn: CDCLN-EL Fort Belvoir, Virginia 22060
1	USAECOM Liaison Officer MIT, Bldg. 26, Rm. 131 77 Massachusetts Avenue Cambridge, Massachusetts 02139
18	Commanding General U. S. Army Electronics Command Fort Monmouth, New Jersey 07703 Attn: 1 AMSEL-EW 1 AMSEL-PP 1 AMSEL-IO-T 1 AMSEL-GG-DD 1 AMSEL-RD-LNJ 1 AMSEL-XL-D 1 AMSEL-NL-D 1 AMSEL-VL-D 1 AMSEL-KL-D 3 AMSEL-HL-CT-D 1 AMSEL-BL-D 3 AMSEL-WL-S 1 AMSEL-WL-S (office of records) 1 AMSEL-SC
1	Dr. T. W. Butler, Jr., Director Cooley Electronics Laboratory The University of Michigan Ann Arbor, Michigan 48105
16	Cooley Electronics Laboratory The University of Michigan Ann Arbor, Michigan 48105

Security Classification

DOCUMENT CONTROL DATA - R & D

(Security classification of title, body of abstract and indexing annotation must be entered when the overall report is classified)

1. ORIGINATING ACTIVITY *(Corporate author)*
Cooley Electronics Laboratory
The University of Michigan
Ann Arbor, Michigan 48105

2a. REPORT SECURITY CLASSIFICATION
Unclassified

2b. GROUP

3. REPORT TITLE

Iterative Synthesis of TEM-Mode Distributed Networks

4. DESCRIPTIVE NOTES *(Type of report and inclusive dates)*
C.E.L. Technical Report No. 199

5. AUTHOR(S) *(First name, middle initial, last name)*

Mahdi, Solaimanul

6. REPORT DATE	7a. TOTAL NO. OF PAGES	7b. NO. OF REFS
November 1970	210	57

8a. CONTRACT OR GRANT NO.	9a. ORIGINATOR'S REPORT NUMBER(S)
DAAB07-68-C-0138	01482-12-T TR 199
b. PROJECT NO. 1 HO 62102 A042 01 02	
c.	9b. OTHER REPORT NO(S) *(Any other numbers that may be assigned this report)*
d.	ECOM-0138-12-T

10. DISTRIBUTION STATEMENT This document is subject to special export controls and each transmittal to foreign governments or foreign nationals may be made only with prior approval of CG, U. S. Army Electronics Command, Fort Monmouth, N. J. Attn: AMSEL-WL-S

11. SUPPLEMENTARY NOTES	12. SPONSORING MILITARY ACTIVITY
	U. S. Army Electronics Command Fort Monmouth, New Jersey 07703 Attn: AMSEL-WL-S

13. ABSTRACT A procedure is described for synthesizing transmission networks which are interconnections of uniform line sections. An iterative, digital computer algorithm is developed which achieves a dominant pole synthesis. The line lengths and the characteristic impedances are controlled individually, which gives design flexibility not found in synthesis procedures based on Richards' transformation. The characteristic impedances may be restricted by upper and lower bounds when there is no restriction on the line lengths. The procedure is detailed for a TEM mode structure of alternating open stubs and connecting lines. The method uses a Newton-Raphson iterative scheme to adjust the characteristic impedances and lengths of the transmission lines for a prescribed set of dominant transmission poles. By controlling the stub line lengths, the dominant pole positions, the principal transmission zeros, and bounded characteristic impedances can be achieved simultaneously. The occurrence of nondominant poles has been analytically investigated. Frequencies at which each transmission line element is a quarterwave long divide the s-plane imaginary axis into halfwave frequency bands. In every semi-infinite s-plane strip which these frequency bands subtend parallel to the imaginary frequency axis, one and only one nondominant pole is present. A numerical technique has been outlined which locates these poles. The approximate cancellation of these poles extends the frequency range over which the network characteristics can be controlled.

14. KEY WORDS	LINK A		LINK B		LINK C	
	ROLE	WT	ROLE	WT	ROLE	WT
Iterative synthesis						
TEM-Mode						
Newton-Raphson iterative scheme						
Synthesizing transmission networks						